PREDICTIVE POTENTIAL OF EAST AFRICAN SEASONAL RAINFALL DERIVED FROM SEA SURFACE TEMPERATURE MODES.

BY

ELIPHAZ BAZIRA

A Thesis submitted in part fulfillment for the Degree of Master of Science in the University of Nairobi.

February, 1997.

This thesis is my original work and has not been presented for a degree in any other University.

Signature: _____

E. BAZIRA

This thesis has been submitted for evaluation with our approval as University Supervisors.

Signature: _____

PROFESSOR L.A. OGALLO

Signature: _____

DR. M.S. RAO

DEPARTMENT OF METEOROLOGY

UNIVERSITY OF NAIROBI

P.O. BOX 30197,

NAIROBI , KENYA.

CONTENTS:

CHAPTER 1

INTRODUCTION AND LITERATURE REVIEW

CHAPTER 2

DATA AND METHODS APPLIED

CHAPTER 3

RESULTS AND DISCUSSIONS

Abstract

The major objective of this study was to determine the predictability of East African seasonal rainfall using sea surface temperatures as the major predictors. Due to the problems associated with timely availability of SST records, the second objective attempted to search for some potential SST proxies which could be used as alternative predictors. Under this concept SST proxies were searched from the surface air temperatures of some coastal/island stations, as well as 200 Hectapascal (Hpa) temperatures. The area of the study namely East African region is located within latitudes 5°N and 12°S and longitudes 29°E and 43°E.

The seasonal SST data which were used in this study were generated from SST grid point data which were obtained from United Kingdom Meteorological Office (UK.Met.office). Point rainfall records were obtained through the respective meteorological departments. The rainfall records were quality controlled before they were used in the study. The SST data sets used had already been subjected to various quality control methods by the UK.Met. office. The quality controlled data were subjected to the various analyses including studies of space-time rainfall anomaly patterns, trends, spectral, correlation, principal component and regression analyses. Both zero and time lagged correlation analyses were used to search for the potential predictors. Principal component analysis was however used first to delineate the complex relationships between various variables and predictors. The final part of the study used step wise regression methods to fit the best regression equations between the predictand (rainfall) and the various predictors.

The period 1940-1975 was used for model building while the period 1976-1990 was used for testing the skill of the developed models. The results from the

CHAPTER 4

SUMMARY, CONCLUSIONS AND RECOMMENDATIONS

study indicated that dry and wet anomaly patterns were recurrent in the seasonal rainfall time series. There were however significant Spatial variations in the observed anomaly patterns with exceptions of some years in which the spatial anomaly patterns were relatively similar. These included some of the El-Niño and la-Nina years. Trend analysis detected no significant changes in the observed inter annual rainfall patterns aaaat most locations.

Spectral analysis however delineated some dominant spectral bands of about 2.2-2.8, 3.0-3.7, 4.9-6.0, and 10-12.5 years. The first three peaks were detectable in all the seasons and at all locations. There were however large spatial variations in the variances accounted for by the various spectral peaks at the individual locations. The 10-12.5 year peak was dominant in the shores of lake Victoria as well as regions of high terrain. The 2.2-2.8 year cycle has been associated with Quasi-biennial oscillation (QBO) while the 3.0-3.7 and 5-6 cycles are common in the El-niño and southern oscillation temporal patterns. Both systems have been observed to be significantly correlated with rainfall over parts of East Africa. The 10-12.5 years cycle has been associated with sunspot cycles by a number of authors.

The results from Principal component analysis (PCA) highlighted the significant differences in the seasonal rainfall characteristics. The number of significant PCA modes and variance accounted for by SST varied significantly from season to season. Maximum and minimum seasonal variances were however accounted for by SST during the September-November and March-May rainfall seasons respectively.

Correlation analysis indicated significant correlation between regional rainfall and SST over some specific ocean regions. These formed the fundamental base for the predictors which were used in this study. The results from the study further

showed that surface temperatures at some coastal/island stations namely , Lamu and Mombasa/Aldabra and Seychelles respectively were closely correlated with some of the SST modes which had correlated significantly with rainfall. This signifies the likely use of some of the coastal/island surface temperatures as proxies of some of the SST predictors. Low correlation was however observed with the 200 Hpa temperature.

Results from regression analysis indicated that although SST had some skill in the prediction of seasonal rainfall during some seasons, seasonal variance accounted by SST were generally less than 50% with exception of June-August and September-November seasons when relatively high percentages of 71.6% and 58.7% respectively were observed. Time coefficients of the SSTs explained a maximum variance of the seasonal rainfall of 59.5%, 54.1%, 57.5%, 49.2% for the seasons of December to February, March to May, June to August and September to November respectively.

In general, higher prediction skills were recorded during the years with larger SST anomaly signals like in the cases of la-Nina and El-niño years. The results from this study indicate that SST modes could be used to give some useful lead time seasonal rainfall information which could help to minimize the severe negative socio-economic impacts of wide spread rainfall anomalies which are common in the region. Such information are not only useful in the planning and management of rain-dependant activities but can also form a crucial component of any early warning system for shortage of food, water, energy, and other basic socio-economic activities.

LIST OF TABLES

LIST OF FIGURES

CHAPTER 1

INTRODUCTION AND LITERATURE REVIEW

1.0 INTRODUCTION

Rain fed agriculture in East Africa provides the major source of foreign exchange and it is also the largest employing economic sector. In addition to cash crops, the agriculture sector further provides food resources for the community. The agriculture systems in East Africa are susceptible to the vagaries of climate especially extreme rainfall variability like droughts and floods . East Africa is a region of extremely varied and heterogeneous terrain which renders the region to have complex climatologic zones. The impacts of rainfall anomalies on agricultural activities vary from one zone to another, and inter-annual rainfall variability is quite large. In addition to the negative impacts on agriculture, seasonal rainfall anomalies have negative impacts on a wide range of socio-economic activities which include forestry, wildlife, energy, Tourism, Transport, etc.

Rainfall anomalies therefore often have severe impacts on foreign exchange earnings and food security for the region. Reliable forecasts of seasonal rainfall expectations in East Africa would therefore be of great importance for the planning and management of all regional socio- economic activities. Many attempts have been made in the region to provide long range forecasts (Ogallo et al. 1988; Ogallo 1989; Ininda 1995; Farmer 1985) among many others. Details of these will be discussed in section 1.2. Operational forecasting models are however currently not available within the region. Many of the long range weather outlooks within the region are determined from the persistent patterns of the regional synoptic weather systems. The purpose of this study is therefore to explore predictive potential of East African rainfall using statistical models based on sea surface temperature modes as predictors. Details of the objectives of the study are

addressed to in the next section.

Generally, it is not easy to obtain real-time sea surface temperatures for predictive purposes. It is therefore necessary to develop some proxies which could be used in predictive models to represent the regional SST modes. In this study attempts were made to examine relationship between sea-surface temperatures (SST) modes and surface air temperature (SAT) of some coastal towns. Derivation of SST and SAT relationships depended on the availability of SAT data along the coastal towns. Lastly also an attempt was made in this study to examine the relationship between upper level circulation and regional rainfall anomalies . Hectapascal (Hpa) is a unit of measuring atmospheric pressure. Due to scarcity of upper air data , only Nairobi 200 Hpa temperatures have been used in this study to quantify the characteristics of the upper air circulations. Details of the specific objectives of the study are presented in the next section.

1.1 OBJECTIVE OF THE STUDY

(i) Determine specific modes of the Indian and Atlantic Oceans that are highly correlated with seasonal rainfall in each of the East African rainfall homogeneous regions.

(ii) Determine potential SST proxies which could be used as alternative predictors of seasonal rainfall over East Africa. The two alternative predictors include upper level temperatures and surface air temperature of some coastal towns.

(iii) For all regions and predictors with significant correlations, attempts will be made to develop predictive models for seasonal rainfall for each region.

(vi) Improve the skill of early warning system in the region. Accurate and timely warning

of the expected seasonal rainfall anomalies is of great socio-economic importance through strategic planning for agriculture, water, food and other rain dependent socio-economic activities of the region. This will also ensure optimum use of natural resources to ensure sustainable socio-economic development.

Some of the work which are relevant to this study are discussed in the next section.

1.2. LITERATURE REVIEW

Models are the major basic tools for producing skillful forecast. This section reviews some of the basic modelling techniques which may be relevant to the study.

1.2.1 PREDICTIVE MODELS

Predictive models generally provide some information on future expectation of any variable. Predictive models used in weather and climate predictions can broadly be classified as statistical and statistical-dynamic models and dynamic models.

1.2.1.1 STATISTICAL MODELS

Several attempts have been made to use statistical techniques in the long range weather forecasting. Such statistical methods are based on the meteorological statistics derived from observed climatological samples. Some of the statistical forecasts are based on the probability of occurrence of certain events Ogallo (1980). Correlation techniques have been however the most common statistical method for searching for the predictors. The predicted value of the weather element is often expressed as a mathematical function of the observed numerical values of the chosen predictors. This approach has been discussed in detail by Ogallo (1980). With the availability of high speed computers, several sophisticated statistical techniques have been developed based on complex regression methods . Some of

the techniques include the exponential smoothing models (Brown 1959, 1962), the Box-Jenkin approach (Box and Jenkins 1967, 1976, Anderson 1976,1977a,1977b,1977c), the combination forecasts (Bates and Granger 1969, Newbold and Granger 1974, Barbara 1976). Detailed review of the statistical models which have been used in the East African region is given in section 1.2.2.

1.2.1.2 DYNAMIC MODELS

Dynamic models are based on the dynamic,physical, thermodynamic and chemical processes of the Earth-system. These processes are represented by equations expressing the conservation of momentum,energy,mass,moisture and other atmospheric constituents. These equations are solved simultaneously for the domain in question using various numerical techniques. The dynamic model used to study the earth's climate include Atmospheric General Circulation model (AGCM),Ocean General Circulation Model (OGCM) and coupled ocean atmosphere GCMs which allow for the interactive thermodynamic sea-ice formulation, meridional heat transfer by oceans, global ice cover, changing solar output, increased stratospheric aerosols loading, effect of changing sea-surface temperatures and land use patterns . Recent GCM also include the biosphere by using the atmosphere,ocean and Biosphere-Atmosphere transfer schemes (BATS) which attempted to accommodate among others:

(i) Treatment of canopy énergy and moisture balance,

(ii) Interception of precipitation by vegetation & subsequent evaporation,

(iii) Moisture uptake by plant roots, distribution of moisture between the lower and upper soil layers,

(iv) stomatal resistance to transpiration.

Recent studies have shown that if the slowly varying surface processes such as soil moisture, snow cover, sea-ice extent and sea surface temperatures are included in the GCMs, the forecast is improved beyond two weeks, Palmer(1988), Keshavamurty (1982) and Parker (1988).

Some of the current climate models include:-

- The 10-layer Canadian Climate Center (CCC),
- The 2 layer atmosphere and 60 m deep mixed layer ocean model of the Oregon State University (OSU),
- The 9-level atmosphere coupled with 50 m deep mixed ocean layer of National Center Atmospheric Research (NCAR),
- The 9-level atmosphere coupled with a static mixed-layer slab ocean of Geophysical Fluid Dynamic Laboratory (GFDL),
- The 15-Level coupled with a 50 m deep ocean mixed layer of UK Met. office (UKMO),
- Goddard Institute for Space Studies model (GISS),
- The 4-level Australian Model (CSIRO).

Climate general circulation models when nested to the Biosphere atmospheric transfer process models have given improved regional rainfall simulation outputs. Although the dynamic models are promising, the capital and other facilities required are still a prohibitive factor for many scientists and nations. In addition there is generally a shortage of manpower in the developing countries besides the general lack of adequate data. Details of these can be obtained from Tyson et al. (1993) among many others.

1.2.1.3 STATISTICAL-DYNAMICAL MODELS

Statistical-dynamical models are a combination of statistical and dynamical methods. The outputs of the dynamic models can for example be used as inputs of the statistical model in a technique known as perfect prog. In this case the outputs derived from the forecast of the dynamic models are used as predictors. On the other hand the outputs of the dynamic model can be refined to represent the observed variate by using statistical methods. This method is known as model output statistics. Details of the statistical-dynamic methods are found in Thapliyal (1982a,b; 1984; 1987); Klein (1982). Alternatively, the predictor can be forecasted using the statistical method and then used in the dynamic simulation, Ward et al. (1991). The statistical-dynamic methods have gained popularity over the pure dynamic or statistical techniques. Some of the work done in East Africa is presented in the next section. Detailed review of the work done in East Africa by using dynamic methods is reviewed in section 1.2.3.

1.2.2 STATUS OF MODELLING AND FORECASTING WITHIN THE REGION USING STATISTICAL MODEL

Attempts have been made in the region to use periodicity and trends of regional rainfall derived from time series studies. Variations in East African rainfall have been associated with fluctuations in the global parameters. Teleconnection which is the simultaneous correlation between temporal fluctuations in meteorological parameters at widely separated points on the earth has been observed to play a significant role in climatic variations in the region. Teleconnection is therefore a measure of the global scale variability (Ininda 1995). Due to the persistent nature of some of the global teleconnection patterns, the basic principles of teleconnection have been recognized as useful tools in Long range weather predictions. El-NIño/Southern oscillation, SST anomalies, Quasi-biennial oscillations have

been some of the persistent climatic systems which have been teleconnected with global and East African weather anomalies (Farmer 1988, Ogallo 1988 among many others). Teleconnection between the tropical and extra-tropical circulation have been explained in terms of Rossby Waves which emanate from tropical heat sources Ininda (1995). Johnson and Mörth (1960) indicated that there were linkages between East African weather and mid-latitude circulation. The linkages were reflected in the low and medium level pressure oscillation spanning across the equatorial Pacific and Indian ocean usually referred to as the Southern Oscillation (Cadet 1985, Ogallo 1988 Farmer 1988 among many others).

Empirical orthogonal function techniques have also been used besides other methods. Temporal and spatial characteristics of annual, monthly and daily rainfall in East Africa have been investigated by (Lumb 1970; Johnson 1962, Johnson et al. 1960; Tomsett 1969; Thompson 1966; Davies 1985; Trewartha 1961) among many others. Findlater (1977) examined relationship between Afro-Asia monsoon and summer rainfall over India.

Cycles of 2-2.5,3-3.7,4.8-6,10-12 years were for example found when the various regional time series were subjected to spectral analysis (Ogallo 1980; Rodhe and Virji 1976; Ininda 1987 among many others). Trends of the regional rainfall have also been examined by many authors (Nyenzi 1993; Lamb 1966, among many others). Lamb (1966), for example attributed high precipitation which caused a rise in lake Victoria and other inland lakes in 1960's to general circulation over the globe. No systematic trends have been observed in the regional rainfall apart from occasional occurrences of above and below normal rainfall.

Attempts have also been made to use regionally averaged records in statistical modelling. Regionalization of East Africa into rainfall homogeneous regions has been done by several researchers using harmonic analysis and various empirical orthogonal techniques

like Principal Component Analysis (PCA) and Rotated Principal Component Analysis (RPCA) (Atwoki 1975; Bärring 1987; Ogallo 1980/1989; Basalirwa 1991, among many others). Ogallo (1980,1989) used annual series to delineate East Africa into homogeneous regions figure 1(a). Basalirwa (1991) used seasonal data to delineate Uganda into 13 homogeneous climatological regions. Bärring (1987) used logarithmic transformed daily rainfall to generate eleven homogeneous regions in central Kenya. The complexity of the regional climatology is evident from the use of factor analysis and harmonic analysis (Atwoki 1975; Bärring 1987). Ogallo (1980) noted that although some stochastic models like ARIMA could give reasonable patterns of standardized mean annual regional rainfall, the models under estimated rainfall amounts especially in the extreme cases.

Southern Oscillation (SO) which is a quasi regular, inter-annual and global scale fluctuation reflecting a shift of air masses between the Indonesia equatorial low pressure cell and the south-east subtropical anticyclone over the Pacific ocean has been used to study inter-annual variability of climate in East Africa (Ininda 1995).

In terms of circulation , SO is viewed as the variation in the equatorial zone east-west Walker's circulation. The intensity of SO is measured by using an index which is the difference between normalized Sea-level pressure at Tahiti and Darwin (Tahiti minus Darwin). The measure of the SO intensity is referred to as Southern Oscillation Index (SOI). Quasi-regular warming of equatorial central and eastern parts of Pacific ocean which is referred to as EL-NIño and the cooling phase as La-nina is closely linked with SO. The SOI has large positive values during Lanina events and negative values during EL-Niño events. Due to linkage between the EL-Niño/Southern Oscillation (ENSO) is used to refer to both systems.

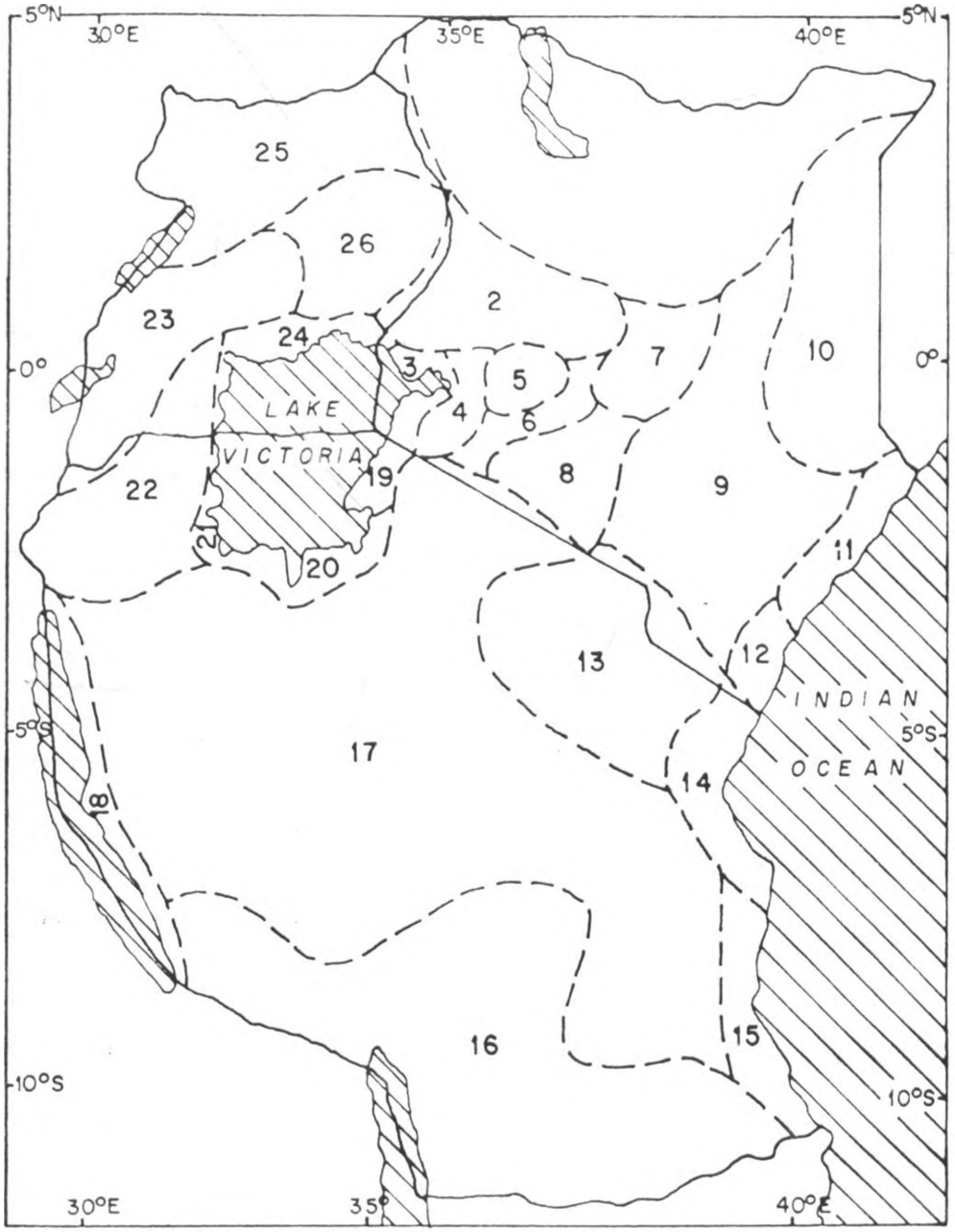

Fig.1(a): Climate zones of East Africa, *After Ogallo (1989).*

ENSO has many manifestations which include the variations in the Asian monsoon wind flow (Cadet 1985 among many other). ENSO events have been used to study inter-annual and seasonal variations in East African climate as indicated below.

The statistics of the temporal and spatial characteristics of East African annual and seasonal rainfall and the characteristics of Indian, Atlantic and Pacific oceans have been also investigated by using a variety of methods including temporal and spatial correlation techniques, Nyenzi et al. (1990) and Nyenzi (1993). Spectral peaks of 5-6 years were dominant in the Atlantic and Indian oceans. Southern oscillation index (SOI) and equatorial rainfall over East Africa exhibited similar peaks. But Nyenzi et al. (1990) and Nyenzi (1993) observed that Sea-surface temperature fluctuations in both oceans influenced rainfall in East Africa. Nicholson et al. (1990) investigated characteristics of the rainfall regime over East Africa and also obtained quasi-periodic fluctuations of 5-6 years.

Using lagged correlations between SST modes and seasonal rainfall, Ogallo (1989) found significant correlations between SST anomalies and some seasonal rainfall modes. He observed maximum correlations at zero time lag between SST anomalies in Pacific ocean and the Autumn rainfall. He obtained significant negative correlations between the summer rainfall over the western regions and the SST anomalies over the parts of equatorial Atlantic ocean, North of Indian ocean and the Arabian sea region. He also noted that negative SST anomalies over the above oceanic regions resulted into intensification of sea-level pressure which favoured the advection of moisture onto East Africa . He further noted that positive SST anomalies over coastal North-west Africa reduced the influence of Azores anticyclone due to reduction in the flow of modified sahalian air mass into the western areas of East Africa as a result of relaxation of the sea-level pressures.

Cadet (1985) established high correlation between pressure, SST, air temperature

fields and the Southern Oscillation Index (SOI) north of 10°S over Indian ocean. He also observed that the evolution of the zonal winds indicated a weakening of the westerly winds north of the equator which appeared at the beginning of EL-Niño. He also noted that very weak EL-Niño events over the Pacific seemed to have normal intensity over the Indian ocean. He further indicated that air-sea interactions seemed to play a certain role in controlling the 3.5-5 year cycle of SST associated with the SO over the Indian ocean. He suggested the existence of the eastward propagation zonal wind anomalies over the Indian ocean. He also showed that warming over the East Indian ocean occurred simultaneously with the warming over the central pacific ocean.

Southern Oscillation Index (SOI) has been associated with the occurrence of droughts and floods in Eastern Africa. Correlations between rainfall and SOI during the months of July-December have been observed although the spatial patterns of the observed correlations varied significantly from one location to another (Ogallo 1987; Farmer 1987; Ininda 1987). It was further noted that most of the years of strong SST & SOI (ENSO) events coincided with the occurrence of the droughts in Northern and Southern Africa although some droughts occurred in absence of ENSO events. It was suggested that there could be some other factors that control rainfall fluctuations in the region of Eastern and Southern Africa. Extreme occurrences that is floods and droughts in East Africa have also been associated with anomalous circulations in the low levels (Anyamba 1983; Anyamba and Kiangi 1985; Minja 1984 among many others).

Farmer (1988) used SOI of June to August to predict seasonal rainfall of September to December for the Indian ocean coast of Kenya. He identified SOI as one of the potential predictors of seasonal rainfall at one seasonal time lag.

Tyson (1993) indicated that of all the parameters that cause seasonal variability, sea-

surface temperature changes in the oceans around South Africa appeared to exert a greater influence on the rainfall than did ENSO on year to year basis. He also noted that in the early part of Southern Summer rainfall season (October to December) more variability over a wider area of South Africa could be explained by a combination of variables when the Quasi-biennial Oscillation (QBO) was easterly. He also noted that during the season of January to March a greater amount of variability over a greater area could be accounted for when QBO was westerly. Quasi-biennial oscillation (QBO) is another feature which has been used to study characteristics of seasonal rainfall in East Africa (Ogallo 1993). QBO refers to the regular alternation of zonally symmetric westerly and easterly winds in the mean winds of the tropical stratosphere. The reversal period of the easterly/ westerly is about 23-30 months. The successive westerly/easterly wind regimes first appear around 30 hpa and then propagate downwards. QBO has been identified in several of the stratospheric and tropospheric variables like temperature (Rassmusson et al. 1981), ozone (Funk and Garnham 1962), Indian monsoon rainfall (Mukherjee et al. 1985), African rainfall (Rodhe and Virji 1976, Ogallo 1979, 1982), ENSO phenomenon (Berlge 1966). QBO is attributed to the upward propagating equatorial waves like mixed Rossby-gravity waves and Kelvin waves (Holton and Lindzen 1972, Plumb 1984, among many others).

The average rate of downward propagation of westerly and easterly wind phase over East Africa was observed as - 1.3 Km/month. Although QBO accounted for relatively low percentage of seasonal rainfall variance, probability of 0.8 was associated with stratospheric westerly wind and above normal rainfall while the corresponding probability for below normal rainfall cases and stratospheric easterly wind phase was about 0.7 (Ogallo et al. 1993). Ogallo et al. (1993) also observed that QBO could provide useful Long range signals for expected seasonal rainfall anomaly especially during short rainfall season.

Rowell et al. (1994) found strong correlations between East African rainfall and the global SSTs on the month time scale during the short rainfall season and lack of correlations during the long rainfall season. He observed that rainfall variability during the month of April could be attributed to internal chaotic atmospheric circulations. Using General Circulation Models (GCM) , Rowell et al. (1994) further observed a higher forecasting skill during the season of October-November and the month of May indicated a higher skill compared to the month of April.

Hastenrath et al. (1993) established the existence of low pressures over the entire Indian ocean during the season of April to May and also observed existence of high pressures over west Indian ocean which were associated with low pressure over the Eastern Indian ocean during the season of October to November. He observed that such a configuration in the latter season induced an oceanic jet of westerly winds over the equatorial Indian ocean. The jet was linked to the strong SO phase. He noted that such a configuration caused rainfall over the East African Indian ocean coast during the short rains. The dipole circulation depicted ascending portions over Indonesia and subsidence near the African coast. He also noted that abrupt pressure rises at Darwin during the season of April to May led to a drastic drop of the SOI at this time of the year. He observed strong negative correlations between SOI and East African rainfall during the season of October-November and weak positive correlations during the season of January-February and March-May. He further noted that the correlation patterns between the East African rainfall and indicative atmospheric and oceanic fields in the Indian ocean were less distinct in the April-May and strong correlations were observed in the October-November season. He attributed the weak patterns in April-May to the change in phases of SO during boreal spring. Hastenrath (1993) also established that SST exerts a forcing on the surface pressure and thus indirectly on the equatorial Indian

ocean westerly winds. He also noted higher variability in most parameters in the October-November season compared to low variability in the April-May season. Weak correlations between East African rainfall and most parameters were observed in the latter season compared to the former season.

Research on linkage between climate anomalies and the 40-50 day oscillation has been investigated by many authors including (Madden and Julian 1971; Yasunari 1980; Weickmann 1985; Anyamba 1993 ; Lau et al. 1986; Murakami et al. 1984 among many others). The oscillation is believed to originate from the interactions between moisture and dynamics which could involve Conditional Instability of the Second Kind (CISK), wave CISK, evaporation-wind feedback mechanisms or processes involving the hydrological cycle (Anyamba 1993).

The 40 day oscillation has been noted to influence intra seasonal variability (Yasunari 1980; Anyamba 1993). Using outgoing long wave radiation (OLR) for the Tropical region (30°S - 30°N) , Anyamba (1993) found that the 50-day oscillation contributed about 25% of the total variance in the Indian Ocean. The oscillation was associated with eastward propagation between 50°E and 170°W. Anyamba (1993) also established a 25-day oscillation which has highest contribution of 10-15% of the total variance in the south Indian ocean and Pacific ocean. The oscillation was found to have mean polarward propagation phase: anomalies emanating from the Equatorial west Indian ocean and propagating northwards across the Arabian sea with a speed of 2-3 m/s and southward towards south Indian ocean. The oscillation's dominant spatial mode was found to be weakest in June-July period and most intense in the October-December (Anyamba 1990). Decrease in the amplitude of the 30-60 day oscillation during the ENSO period has been observed (Lau and Chan 1986).

1.2.3. STATUS OF DYNAMIC MODELLING WITHIN EAST AFRICA

In East Africa,dynamic models have been developed by several authors who include (Okeyo 1987; Semazzi 1978 among many others). The meso-scale circulations were found to play a significant role in weather activities. Mukabana (1992) examined the influence of the large-scale monsoonal wind systems on the diurnal weather patterns over Kenya. He found that convergence zones were in areas where the meso-scale circulations were in direct opposition to the prevailing large scale flow while the divergence zones existed in regions where the meso-scale circulations and the large scale monsoonal flows at low levels were in the same direction. Mukabana (1992) noted that Strong horizontal temperature and pressure gradients induced meso-scale circulations which extended up to 4 km.Above Mean Sea-Level (ABMSL) with sea-breezes being stronger than land breezes due to the solar insolation which enhanced vertical mixing of the atmosphere in the planetary boundary layer. He identified maximum rising motion of 1.0 cm per second against sinking motion of -0.5 cm per second at 0500Z compared to 3.3 cm. per second and -2.9 cm. per second respectively at 1600Z. He indicated rising motion over water bodies in the morning and subsidence in the afternoon and a reverse flow over land masses. He also showed that the precipitation generated in the convergence zones were controlled and advected by the large scale flow fields.

Semazzi et al. (1992) observed that in response to SST anomaly regimes, the rainfall deficits over West & Southern Africa in 1973 compared to 1950 were associated with continental-scale diffluent low-level circulation anomalies. He indicated that the anomalous circulation weakened the continental bound moist monsoon trade winds and thus reduced the amount of moisture reaching the interior of the continent. He further observed that the opposite rainfall anomaly over Equatorial Africa was caused by enhanced confluence over

East Africa due to the two continental anticyclonic regimes approximately 10° to the north and to the south of the Equator. The subsequent increase in convergence and vertical lifting over compensated for the reduction in supply of oceanic moisture. Semazzi et al. (1992) further recognized that deforestation reduces local moisture convergence. Using information from the Ground Survey of Tropical forests which was augmented by airborne sampling methods, Semazzi (1992) indicated that in several West African countries (Ivory Coast, Cameroon and Nigeria) the present rates of deforestation would probably deplete the forest resource within the next 20-30 years if business continues as usual in terms of these forests. He further indicated that according to the World Resource, (1990-1991), the central African state of Cameroon alone had estimation of deforestation rate of 80,000 hectares per year or 0.4% of the total national forest resource. He also observed that the relative impact of the current road construction in the presently inaccessible regions of Congo river basin and the general deforestation in the region would reach its peak in a few decades to come and the present knowledge would not be adequate to distinguish between the relative anthropogenic forcing and the effects of SST. The impact of deforestation in central Africa on the seasonal rainfall in East Africa especially the moist congo air mass is a subject that needs to be studied.

The relationship between Sea-surface Temperature anomaly patterns and the Inter-annual variability of Long and Short rainfall seasons over East Africa was examined by Ininda (1995). He found a higher degree of persistence in factors that influence rainfall during the short rainfall season and low persistence in the factors during the long rainfall season. He observed positive correlations between short rains and SST over Arabian Sea, central and eastern tropical Pacific ocean. He observed strong (weak) rainfall-SST correlations in May (April) during the Long rainfall season. He noted negative correlations

between East African rainfall and SST over east Pacific, central Pacific and south Atlantic ocean during the month of March. Negative correlations between SST and east Pacific and south west Indian ocean with rainfall over northern parts of East Africa were also observed in April. He also observed negative correlations between SST over south eastern Atlantic ocean and western regions of East Africa and he further noted positive correlations between SST over north western Indian ocean and coastal regions during the month of May.

Ininda (1995) further observed that the first global SST Empirical Orthogonal Function (EOF) mode represented general global warming/cooling pattern while the second and third global EOF modes were linked with the EL-Niño and southern oscillation (ENSO). Using General Circulation Models,Ininda (1995) also observed a better simulation skill of East African rainfall during the Short rainfall season which he attributed to the high degree of correlation between SST and seasonal rainfall. He noted high (lower) skill of simulation in May (April) during Long rainfall season.

Ininda (1995) also associated above (below) normal rainfall over East Africa with anomalous low level wind convergence (divergence) over western Indian ocean. He noted that the wind field was associated with fluctuations in Walker circulations which were linked with ENSO mode variations in the SST. He observed that east-west Walker circulations were strong during Short rains as compared to the Long rains. He also noted higher degree of variability in the southern local Hadley cell circulations as compared to northern cell both of which influence seasonal rainfall. He observed higher impact of the variations in the southern Hadley cell on East African seasonal rainfall during the Long rains when much of rainfall was associated with south easterlies.

Although the land processes could play an important role in modifying climate conditions, a large body of results based on numerical and statistical modelling indicated that

SST most likely was the primary cause of observed decadal variability in rainfall (Semazzi et al. 1989; Folland et al. 1986). **This literature formed the fundamental basis of this study.** A brief review of the climate of the region of study is presented in the next section.

1.3 THE LOCATION OF THE STUDY REGION:

This study has been conducted in East Africa. The term" East Africa" will be used to refer to the three countries of Uganda (240,000 km^2), Kenya (580,000 km^2) and Tanzania (940,000 km^2), Griffith (1972). The region is located within latitudes 5°N and 12°S and latitudes 29°E and 43°E. The next section describes the geography, climate and other physical characteristics of the region of study.

1.3.1 PHYSICAL FEATURES OF THE STUDY AREA.

East Africa is characterized by a complex of terrain which consists of low lands (below 1300 m) which run parallel to the Indian ocean in the east as shown in figure 1(b). There are isolated hills in south-eastern kenya and north-eastern Tanzania that rise above 1300 m. Central Kenya consists of highlands which are above 1800 m. These highlands extend to western Kenya including some parts of eastern Uganda. Southern Tanzania is characterized by highlands which rise above 1800 m while southern Uganda is occupied by high terrain which is above 1300 m. Specific mountains in the region include Ruwenzori (5109 meters), Elgon (4321 meters), Moroto (3084 meters), Kenya (5199 meters), Meru (4565 meters), Aberdare range (3999 meters), Kipengere range with the highest peak at 2961 meters, Kilimanjaro (5895 meters) and the Iringa mountain range. The mountains which rise to above 6,000 Meters have on their slopes a vast variety of vegetation and climates, going through dry to wet, cloud forests, open moorland and perpetual snow belt (Griffith, 1972).

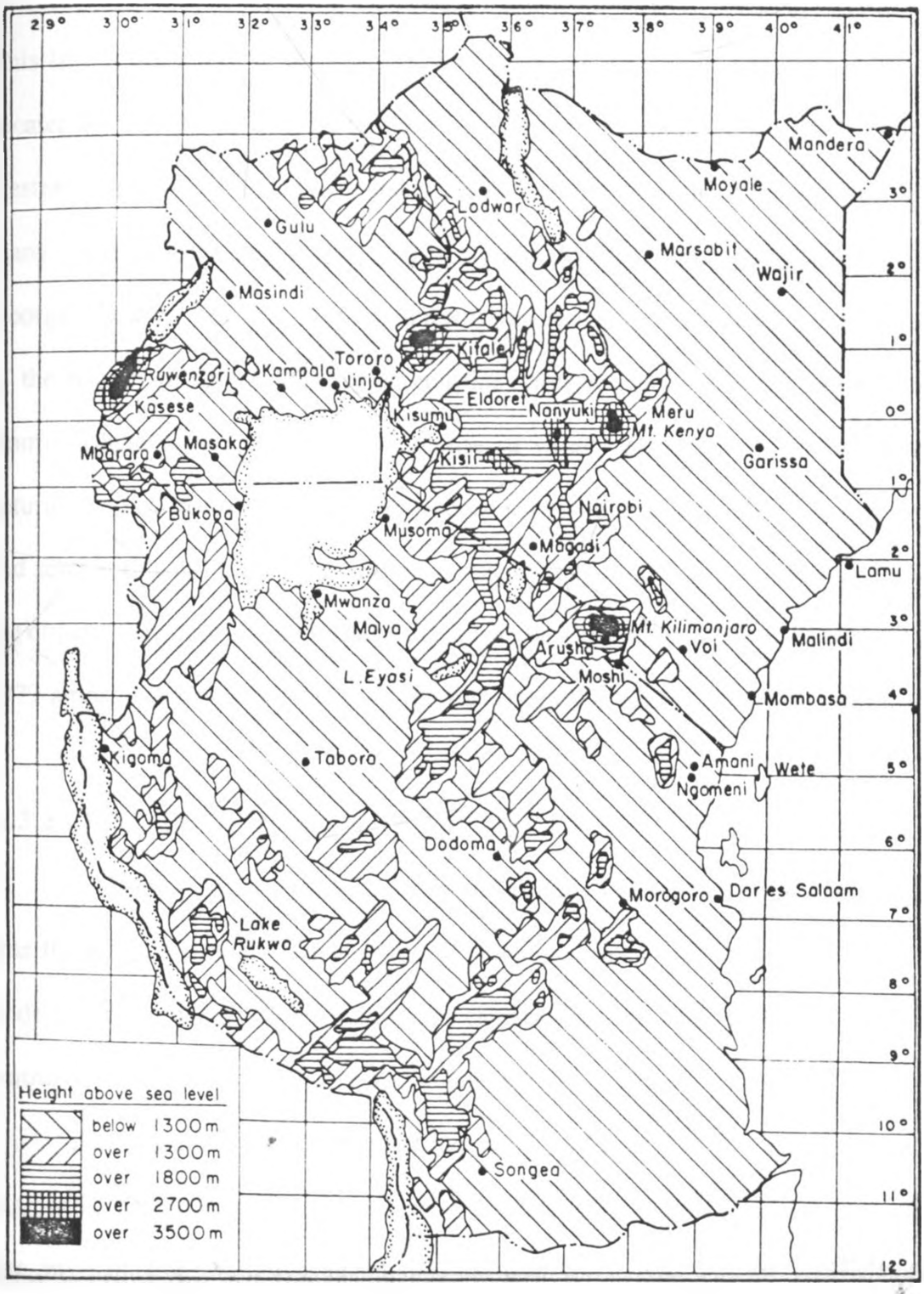

Fig. 1 (b) : Relief map of East Africa (after Johnson 1962)

Lake victoria with a surface area of 68,400 Km^2 lies in the plateau (100 - 200 m). This lake is the source of moisture and energy for the meso-scale circulations which have a greater impact on the climate of the neighbouring locations. For example hailstorms in western kenya are attributed to meso-scale circulations (Mukabana 1992, Okeyo 1987 among many others). Some of the inland lakes include ,Kyoga, Tanganyika, Naivasha, Edward, George, Turkana, Nakuru, Natron, and Rukwa . Indian Ocean lies to the eastern boundary of the region. In addition,the region contains eastern and western rift valleys which run from north to south. The region also has a variety of vegetation which ranges from natural Tropical forests and wetlands to open savannah grassland and thorny shrubs in arid and semi arid land. These physical features significantly modify the space-time variations of the climate over East Africa (Ogallo and Anyamba 1986; Okeyo 1986; Asnani and Kinuthia 1979 among others). The climate of the study region is given in the next section.

1.3.2 CLIMATE OF THE STUDY AREA

Climate of East Africa is shown in figure 1(c). The regions of high terrain and those near the water bodies are characterized of humid and moist sub-humid conditions. The low lands in northern and eastern kenya are characterized of arid conditions. Most areas in central Tanzania experience semi-arid conditions.

The spatial pattern of mean annual rainfall of East Africa is shown in figure 1(d). Highlands and regions which are near water bodies generally receive high rainfall. Generally, area in north-eastern Kenya including north eastern Uganda, eastern Kenya and Central Tanzania receive low rainfall. The variation of the mean monthly air Temperature through the year over the region is very small, usually being about 1-2°C over south-western

Uganda and the south-western half of Lake Victoria, to a maximum of 5-6°C over southern Tanzania. Nearly most locations experience relatively cold temperatures during the month of July which often spreads to August (Griffith 1972). Cool and cloudy weather experienced over eastern highlands in Kenya is attributed to the surge of cool and shallow south-easterly monsoons emanating from south-western Indian ocean. The existence of subsiding easterly winds aloft causes an inversion whose base is near 700 hpa and top is near 650 hpa. The inversion prohibits cloud development during June-August season (Asnani 1992).

Over most parts of the region, seasonal rainfall patterns are characterized by bimodal regimes. Unimodal regimes are however common over southern Tanzania. The first (long) rainfall season is experienced during March to May, with the second (short) rainfall season centered from around late September and persists to November/early December.

The Long and Short rainfall seasons are attributed to the convergence of wind field in the positions of the zonal component of inter tropical convergence zone (ITCZ). A number of locations in the west of the region however receive a third rainfall peak centered around July and August. This peak is attributed to the convergence of airmasses from south-eastern Atlantic ocean via moist Congo forest and south-easterly winds emanating from south-western Indian ocean. The convergence takes place in the positions of the meridional component of ITCZ. The coastal strip receives rain during June-August season due to the shears in the East African Low Level Jet (EALLJ) (Anyamba et al. 1985, Farmer 1987, Okoola 1989). Over othef parts, July/August is generally dry and cool. December-February season is however generally dry and hot (Ogallo et al. 1988). However, Southern Tanzania experiences a unimodal rainfall peak which spreads from November to March when zonal component of ITCZ is located in the southern hemisphere. Few locations near the large water bodies receive substantial rainfall throughout the year.

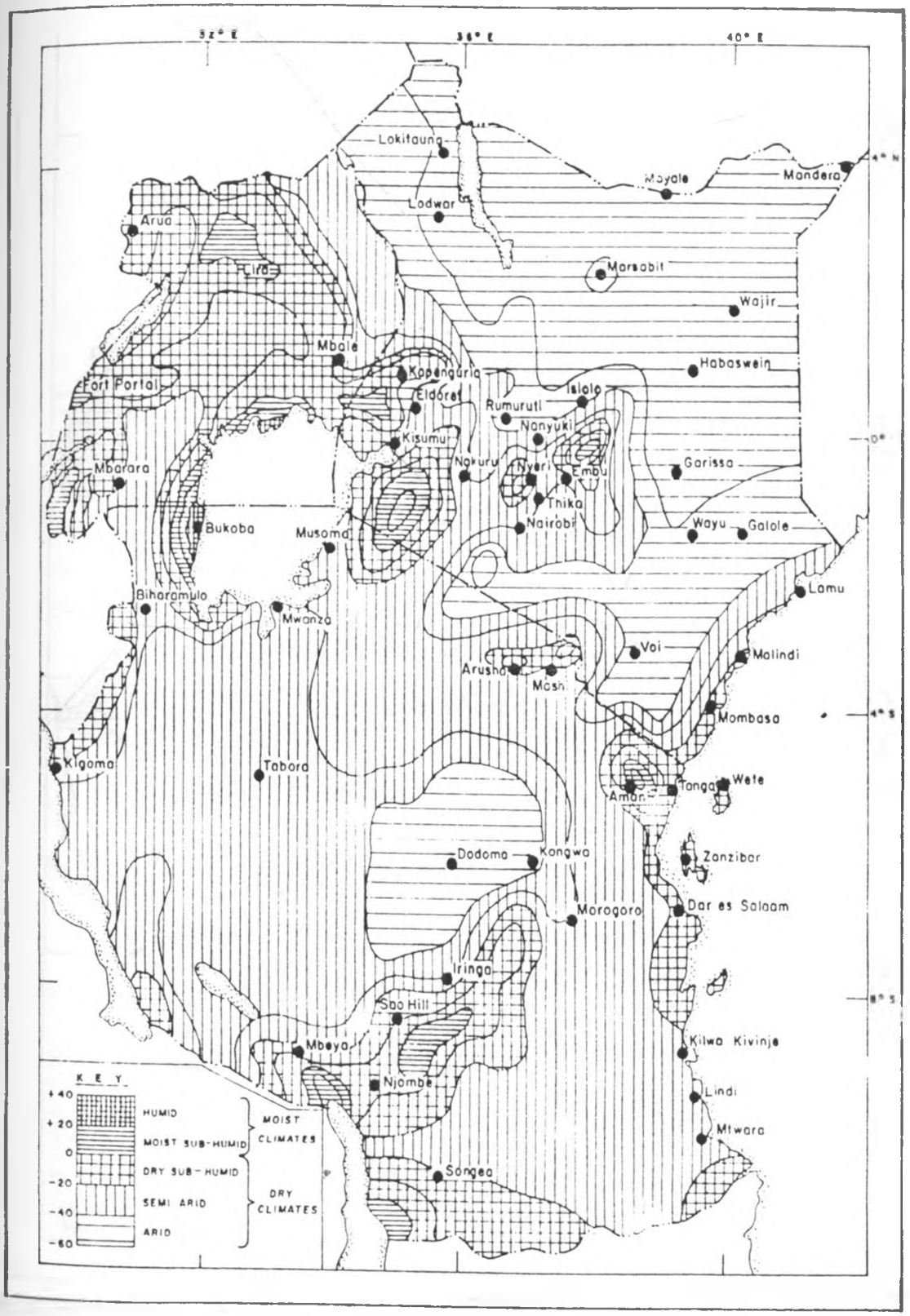

Fig. 1(c) : Climates of East Africa (After Pontel, 1971)

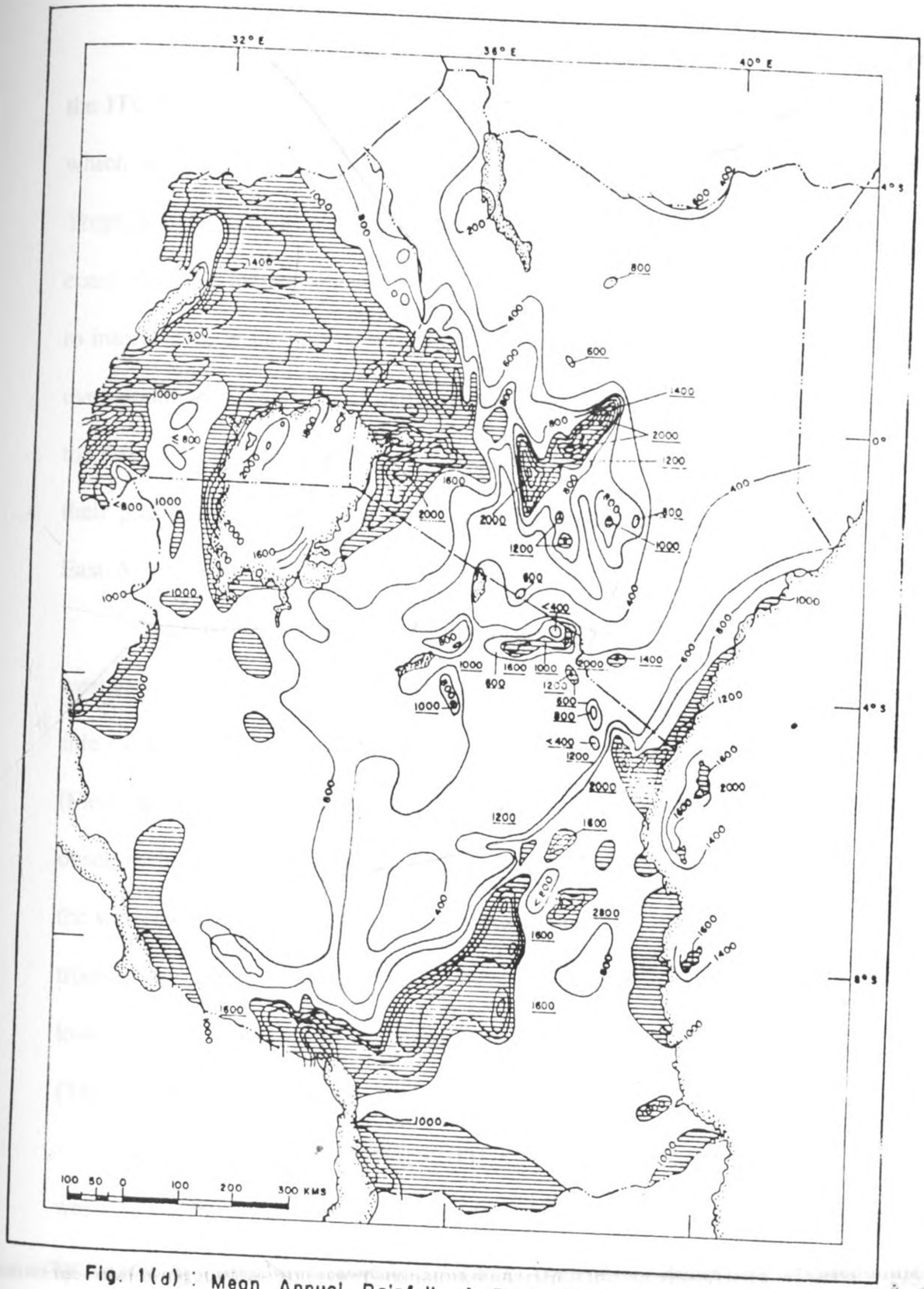

Fig. 1(d) : Mean Annual Rainfall of East Africa (After Pantel, 1971)

The onset and withdrawal of seasonal rainfall often follow the migration of the ITCZ (Asnani et al. 1980; Griffith 1972). In addition, there are other synoptic features which control the seasonal rainfall over the region. These include:,

Tropical cyclones which cause floods when the storm directly passes close to or hits the coast. Cyclone indirectly cause droughts in the locations which are far from the coast due to interference in the normal wind flow pattern. Although the tropical cyclones which form over South-west Indian ocean during the northern hemisphere spring and summer rarely hit the East African coast, they deflect the south-easterly wind and north-easterly winds towards their positions. Thus reducing moisture influx towards the land and reducing rainfall over East Africa (Griffths 1972),

Easterly/westerly waves influence seasonal rainfall in East Africa. Easterly waves are westward moving disturbances which form in the basic easterly current on the equatorward side of the subtropical pressure belts and these waves have been observed in East Africa (Fleming 1970, Krishnamurti 1971, 1979, Gichuiya 1970). However these waves have been observed to penetrate inland only slightly (Minja 1984, Njau 1982). During July and August the westerly waves mostly affect Uganda and Western Kenya (Davis et al. 1985). Upper level troughs in the extra-tropical westerly disturbances of the winter hemisphere penetrate into low latitudes and result in introduction of cool air aloft which leads to instability (Thomposon 1965, Trawartha 1961),

The meridional component of ITCZ which is a zone of convergence between the westerlies from the Atlantic ocean and the easterlies from the Indian ocean represents an ascending arm of the east-west circulation over equatorial Africa (Ininda 1995). The Component oscillates in the east-west direction over the western parts of East Africa and Central Africa,

Inter-annual variations in the mean positions of the four semi-permanent sub-tropical anticyclones (Azores high, St. Helena high, Mascarene high & Arabian ridge) influence inter-annual rainfall variations in East Africa. For example weaker Mascarene High is associated with below normal rainfall in East Africa (Minja 1982, 1984,; Ininda 1987),

During northern hemisphere winter, North-easterly monsoons prevail over East Africa. Since these winds are hot, dry and have land trajectory, they contain little moisture. During northern hemisphere summer, South-easterly monsoons prevail over East Africa Since south-easterly monsoons emanate from Mascarene High in south-western Indian ocean, they are moist and stronger than the north-easterly monsoons. The third type of air mass that prevails over East Africa is the moist westerly (Congo/Zaire) air mass which emanates from St.Helena High in south-eastern Atlantic ocean. The convergence of these monsoons in the positions of ITCZ results into convective activities that generate rain for the region (Tomsett 1969, Griffiths 1972, Anyamba 1984) among many others.

Seasonal characteristics of the monsoon wind systems causes seasonal rainfall variations in the East Africa,

Other factors include the African Jet streams especially East African Low Level Jet Stream, Global Teleconnetions which includes (EL-Niño and Southern Oscillation) which were discussed in section 1.2.2, Extra-tropical weather systems including frontal systems & Depressions, Blocking systems and polar circulation) together with thermally induced meso-scale circulations (Ogallo 1988b). These have been associated with complex geographical and temporal patterns of the East Africa climate (Griffith 1972; Ogallo 1988; Basalirwa et al. 1993). Rainfall is however the climate parameter with the largest space-time variability. Inter-annual rainfall variability especially the extreme case have therefore been associated with many socio-economic impacts.

1.4 JUSTIFICATION AND SIGNIFICANCE OF THIS STUDY.

This study attempts to explore predicative potential of the seasonal rainfall over the region of East Africa by using linear correlation and regression techniques derived from sea-surface temperature predictors. Past studies have indicated some significant teleconnections between Sea-Surface Temperatures (SST) and seasonal rainfall over East Africa at three months seasonal lag (Ogallo 1989; Nyenzi 1992; Ininda 1995; Hasternath 1993). This study will make an attempt to develop operational predictive model for each of the rainfall homogeneous regions of East Africa. The homogeneous rainfall regions will be based on principal component derived climatological zones (Ogallo 1988; Basalirwa 1993). A timely and accurate skillful seasonal rainfall forecast is a vital component of any early warning system for all rain dependent activities which include water, food, energy, and many other socio-economic activities.

The data used and the various methods which were adopted in the study are presented in the next section.

CHAPTER 2

DATA USED IN THE STUDY AND METHODS APPLIED

2.0 DATA AND METHODS

The data used in this study consisted of point (station) monthly rainfall, grid point sea-surface temperatures (SST) , surface air temperature for some coastal towns, island states in Indian ocean and 200 Hpa temperatures over Nairobi. Only SST for the ocean regions surrounding Africa have been included in the study namely Atlantic and Indian ocean respectively due to the close association between these oceans and Pacific ocean (Cadet 1985; Ogallo 1988/1989). In East Africa, monthly station rainfall data are some of the most readily available data for spatial and temporal climatological analyses. A total of 180 rainfall stations were used in this study. The density of the networks of stations used were however not uniform due to non availability of data at many remotely located areas. Figure 2 shows the spatial distribution of the stations. Table 1 gives the list of the rainfall stations used in this study. The study covered the period 1940-1990. Effort was however made to search for the stations which would ensure maximum representation of each of the homogeneous rainfall zones (Ogallo 1989).

The Meteorological Historical Sea-surface Data set (HOMSSDS) used contained Monthly mean SST anomalies calculated from a base climatology for 1951-1980 with a spatial resolution of 5° by 5° Latitude-Longitude. The raw SST records however extended back to 1856. The SST records were obtained from United Kingdom Meteorological Office (UK.Met. office) where quality control and other corrections had already been applied to compensate for the problems associated with historical SST data including the predominant use of uninsulated canvas buckets to collect sea water for making temperature measurements prior to 1942.

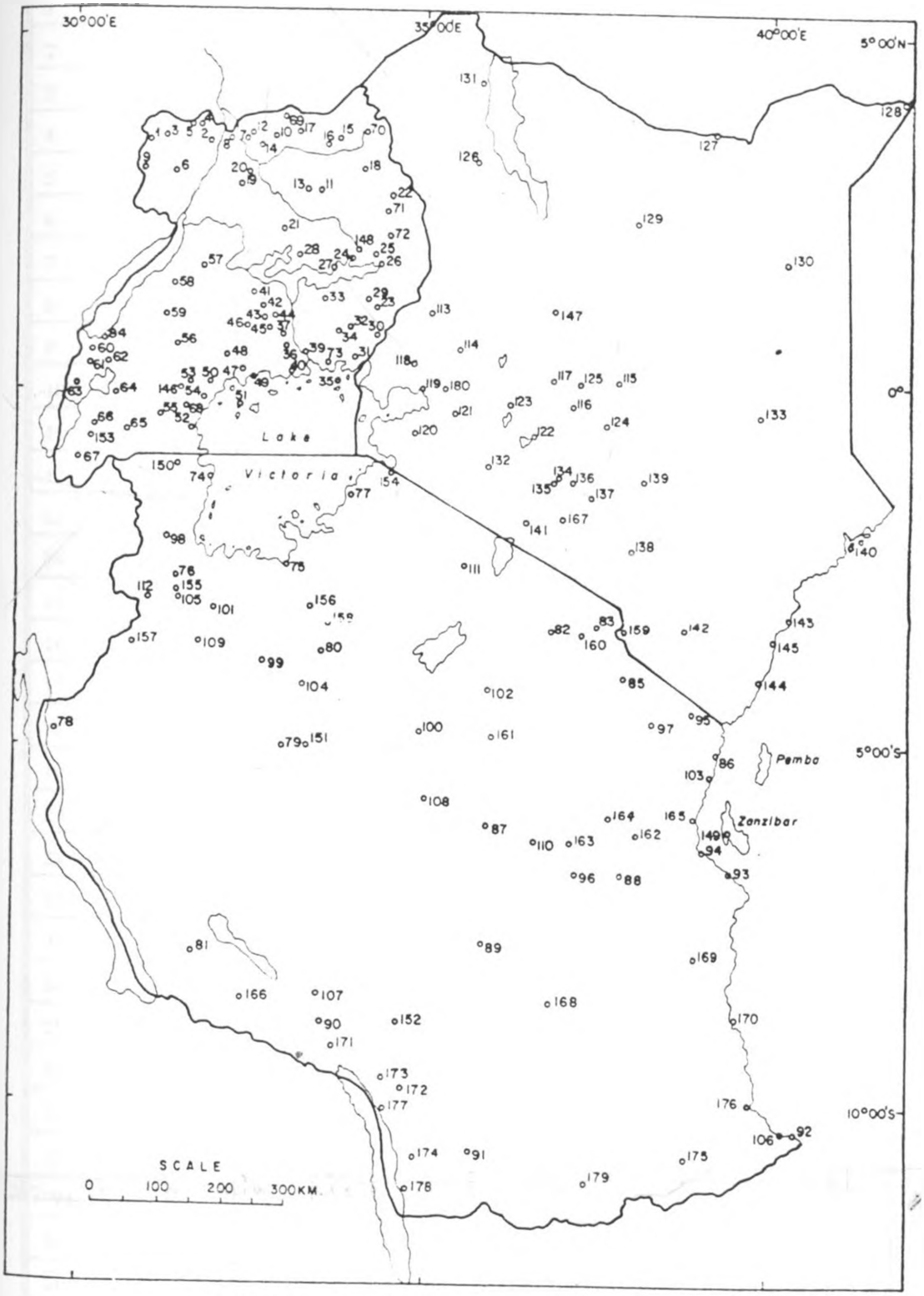

Fig. 2 — Stations used in the study.

Table 1:list of rainfall stations used in the study

Code number	Station name	Latitude deg.min.	Longitude deg. min.	Altitude (m)
1	Koboko Disp.	3 24N	30 59	1250
2	Adjumani Disp	3 22N	31 47	732
3	Yumbe Disp.	3 25N	31 14	1067
4	Laropi Disp.	3 34N	31 50	610
5	Moyo Boma	3 41N	31 41	1036
6	Obangi Disp.	3 14N	31 33	610
7	Zaipi Disp	3 22N	31 58	732
8	Pakelle N.T.C.	3 22N	31 52	762
9	Arua	3 03N	30 56	1204
10	Kitgum V.T.C	3 17N	32 53	937
11	Adilang	2 44N	33 28	1067
12	Padibe	3 29N	32 49	914
13	Patonga	2 47N	33 19	1067
14	Plabek	3 27N	32 34	914
15	Rom Gomb.	3 23N	33 33	1219
16	Naam okora	3 19N	33 19	1219
17	Mucwini Gomb.	3 26N	33 01	914
18	Kotido	3 01N	34 06	1219
19	Gulu	2 45N	32 20	1106
20	Abera For.stn	2 53N	32 25	1109
21	Lira	2 15N	32 54	1085
22	Moroto	2 15N	34 36	1524
23	Mbale	1 06N	34 11	1494
24	Ongino Leprosy	1 31N	33 58	1052
25	Serere C.M.C.	1 31N	33 27	1139
26	Ngora Agr.stn	1 27N	33 46	1128
27	Soroti	1 43N	33 37	1127
28	Kaberamaido Agr.stn	1 47N	33 10	1067
29	Bukedea	1 19N	34 03	1113
30	Tororo	0 42N	34 10	1226
31	Debani	0 28N	34 05	1219
32	Budumba	0 49N	33 51	1070

Table 1 continues on the next page

code number	station name	Latitude deg.min.	Longitude deg.min.	Altitude (m)
33	Vukula	0 57N	33 36	1097
34	Nuwanzu	0 33N	33 30	1189
35	Buvuma Island	0 11N	33 18	1158
36	Moninko Estate	0 23N	32 55	1250
37	Kivule	0 23N	32 47	1228
39	Jinja	0 26N	33 11	1134
40	Mukono Agr stn	0 21N	32 45	1184
41	Nakasongola	1 19N	32 28	1274
42	Kakoge H/MET	1 04N	32 28	1189
43	Bukalasa Agr.stn	0 43N	32 31	1128
44	Kawanda Agr stn	0 25N	32 32	1196
45	Nsimbe	0 16N	33 26	1219
46	Bakijulula	0 28N	32 03	1219
47	Mpigi Ag.stn	0 13N	32 20	1250
48	Kabasanda	0 17N	32 13	1153
49	Entebbe	0 03N	32 28	1173
50	Nkozi	0 01S	32 01	1189
51	Bumagi W.F.M.	0 19S	32 14	1143
52	Katera Sango Bay	0 55S	31 38	1189
53	Katigondo W.F.M.	0 13S	31 44	1311
54	Kyanamukaka	0 30S	31 41	1219
55	Lyantonde Disp.	0 20S	31 09	1219
56	Mubende H/MET	0 35N	31 22	1553
57	Masindi	1 41N	31 43	1146
58	Bulindi For.stn	1 28N	31 28	1036
59	Matiri	0 32N	30 46	1341
60	Kijura tea Estate	0 48N	30 25	1524
61	Kyembogo Ag.stn	0 41N	30 20	1524
62	Kisomoro	0 31N	30 09	1585
63	Bugoye	0 17N	30 06	1829
64	Kicheche	0 05S	30 24	1372
65	Mbarara	0 37S	30 39	1443
66	Bushenyi D.F.I	0 33S	30 12	1631

Table 1 continues on the next page

station code	Name of station	latitude deg min	Longitude deg.min	Altitude (m)
67	Kabale	1 15S	29 59	1871
68	Kiteredde Mission	0 37S	31 34	1219
69	Madi Opei Admin.	3 46N	33 01	1372
70	Kaabong	3 17N	34 05	1500
71	Nabilatuk	2 10N	34 36	1250
72	Kangole	2 28N	34 25	1311
73	Bwavu	0 21N	33 01	1280
74	Bukoba	1 20S	31 47	1144
75	Mwanza	2 32S	32 53	1140
76	Biharamulo Agr.stn	2 36S	31 18	1478
77	Musoma	1 30S	33 49	1147
78	Kigoma	4 50S	29 37	885
79	Tabora	5 03S	32 53	1190
80	Shinyanga	3 30S	33 24	1219
81	Sumbuwanga Agr.stn	7 57S	31 36	1722
82	Arusha	3 23S	36 43	1372
83	Moshi	3 21S	37 20	813
84	Fortportal	0 40N	30 17	1539
85	Same	4 05S	37 44	860
86	Tanga	5 07S	39 07	9
87	Dodoma	6 10S	35 46	1120
88	Morogoro	6 48S	37 46	579
89	Iringa	7 43S	35 37	1428
90	Mbeya	10 42S	33 29	1826
91	Songea	10 42S	35 40	1067
92	Mtwara	10 18S	40 12	113
93	Dar-Es-Salaam.	6 50S	39 17	53
94	Bagamoyo Agr.stn	6 24S	38 54	9
95	Amani malaria unit	5 06S	38 36	911
96	Kilosa Agr.stn	6 48S	37 00	491
97	Handani	5 24S	38 00	677
98	Igabiro	1 48S	31 36	1524

Table 1 continues on the next page

station code	station name	latitude deg min.	Longitude deg min.	Altitude (m)
99	Kahama	3 48S	32 36	1219
100	Singida D.O	4 48S	34 48	1498
101	Shanwa	3 12S	33 48	1341
102	Lushoto	4 48S	38 18	1396
103	Pangani Agr.stn	5 24S	39 00	9
104	Nzega	4 12S	33 12	1219
105	Ngara Agr.stn	2 30S	30 36	1798
106	Mikindani	10 12S	40 06	51
107	Madibira	8 12S	34 48	1158
108	Manyoni	5 42S	34 48	1248
109	Mbulu D O	3 54S	35 36	1737
110	Mpwapwa vet.office	6 18S	36 30	1128
111	Dangodesh Mission	4 06S	35 24	2042
112	Kagondo Mission	2 30S	32 54	1140
113	Kitale Ag.stn	1 01N	35 10	1896
114	Eldoret Ag.stn	0 31N	35 17	1985
115	Meru Ag.stn	0 37N	37 39	1571
116	Nyeri Ag.stn	0 33S	36 56	1830
117	Rumuruti	0 16N	36 32	1856
118	Kakamega Ag stn	0 28N	34 50	1585
119	Kisumu Ag.stn	0 06S	34 45	1146
120	Kisii Ag.stn	0 41S	34 47	1768
121	Kericho Ag.stn	0 23S	35 17	1981
122	Naivasha	0 43S	36 26	1900
123	Nakuru	0 17S	36 04	1836
124	Embu	0 32S	37 27	1372
125	Nanyuki	0 01N	37 04	1947
126	Lodwar	3 07N	35 37	354
127	Moyale	3 32N	39 03	1113
128	Mandera	3 57N	41 52	331
129	Marsabit	2 19N	37 59	1345
130	Wajir	1 45N	40 04	244

Table 1 continues on the next page

station code	station name	Latitude deg min	Longitude deg.min.	Altitude (m)
131	Lokitaung	4 15N	35 45	2377
132	Narok	1 08S	35 50	1890
133	Garissa	0 29S	39 38	183
134	Wilson Airport	1 19S	36 49	1676
135	Dagoretti Corner	1 18S	36 45	1798
136	Jomo kenyatta I.A.	1 19S	36 55	1615
137	Machakos Ag.stn	1 35S	37 14	1463
138	Makindu	2 17S	38 50	1000
139	Kitui	1 22S	38 01	1177
140	Lamu	2 16S	40 54	9
141	Magadi	1 53S	36 17	615
142	Voi	3 24S	38 34	560
143	Malindi	3 14S	40 06	20
144	Mombasa	4 04S	39 42	16
145	Kilifi	3 40S	39 51	3
146	Masaka H/MET	0 21S	31 47	1280
147	Maralal	0 56N	37 23	1830
148	Katakwi	1 45N	33 59	1159
149	Zanzibar	6 06S	39 12	18
150	Kaisho Agr.stn	1 36S	31 42	1296
151	Kipalapala seminary	5 00S	32 48	1265
152	Njombe D.O.	9 18S	34 42	1829
153	Rwashamaire D.O.	0 50S	30 08	1646
154	Nyabassi (Nyarero)	1 21S	34 34	1829
155	Runazi	2 47S	31 29	1402
156	Ngudu	2 57S	33 21	1219
157	Kibondo D.O.	3 34S	30 40	1515
158	Maswa H/MET	3 10S	33 46	1341
159	Rombo Mission	3 12S	37 36	1433
160	Kivungi	3 24S	37 19	762
161	Kondoa Maji	4 55S	35 48	1372
162	Tungi sisal Estate	6 46S	37 42	503
163	Scutari sisal Estate	6 47S	37 10	457

Table 1 continues on the next pa

station code	station name	latitude deg.min.	Longitude deg.min	Altitude (m)
165	Kizimbani Agro.stn	6 05S	39 16	67
166	Mkulwe Mission	8 32S	32 18	1067
167	Kajiado	1 52S	36 48	1754
168	Mahenge Hospital	8 41S	36 42	1106
169	Utete Agr stn	8 01S	38 45	52
170	Kilwa Masoko	8 55S	39 31	14
171	Tukuyu Hospital	9 15S	33 38	1646
172	Lugalawa Pri.sch.	9 49S	34 41	1372
173	Dansland	9 36S	34 38	2164
174	Limbo Mission	10 57S	34 50	1433
175	Masasi Mission	10 42S	38 49	457
176	Lindi Agr.stn	10 00S	39 42	41
177	Mwita	10 17S	40 05	51
178	Mbamba Bay customs	11 18S	34 46	488
179	Tunduru Agr.stn	11 06S	37 22	701
180	Chemilil	0 06S	35 07	1241

Agr.stn = Agriculture station. W.F.M. = White Fathers Mission. Disp = Dispensary. Gomb = sub-county headquarters. N.T.C = National Teachers College. V.T.C. = Variety Trial Center. D.O. = District Office. Pri.sch = Primary School. D.F.I. = District Farm Institute. C.M.S = Church Mission Society. For. stn = Forest station. H/Met. = Hydrometeorological station. I.A = International Airport.

It has been noted by United Kingdom Meteorological office that uninsulated bucket tends to lose heat to the atmosphere mainly through evaporation of sea water from outer surface of the bucket before the temperature of the water in the bucket can be read. The subjected corrections vary with location and sea but a typical value would be about +.3°C and ranges between about +.1°c and +.9°c. Maps of the corrections are in Bottomley et al. (1990) with detailed discussion in Folland and Parker (1990).

The 10° by 10° sea-surface temperature anomalies (SSTA) data were also used. These have been obtained by averaging the available 5° by 5° monthly anomalies Bottomley (1990). Folland et al. (1991) noted that the 10° by 10° SST records gave more realistic results especially with respect to the investigations of issues related to large scale systems.

In most cases, SST values are not readily available for the real-time analysis. It is therefore necessary for prediction purposes to develop some proxies which could be used in the absence of real-time SST data. Possible proxies include coastal surface air temperatures which are relatively available on real-time basis. Surface air temperature data from coastal stations of Mombasa, Lamu, and island states of Seychelleys and Aldabra were therefore included in this study for these purposes. Other records which were used in this study include 200 Hpa level temperature over Nairobi.

Data were subjected to several analyses as highlighted in the next section. These included correlation and regression methods. The quality of the records were however first examined. The next sections are devoted to all methods which were used to investigate the various objectives of the study. The first part was however devoted to data quality control and estimation of missing records followed by correlation and regression analyses.

2.1 DATA QUALITY CONTROL

It has been realized that errors are often introduced in many climatological data due to shifts of the station locations, changes in the instrument used at the station which may include changes in the instrument model and replacement of spare parts, besides human error etc. In this case the data ceases to be homogeneous (a sample from the same statistical distribution). The quality control methods attempt to identify any heterogeneity in the climatological records. Standard statistical methods are available for adjusting the heterogeneous component of the data sets. The methods which were adopted in this study include mass curve analysis. Under this method cumulative values of a variate are plotted against time. A linear relationship (straight line) indicates that the records are homogeneous (sample from same statistical distribution) otherwise the records are assessed to be heterogeneous. Gradients of the respective heterogeneous portions of the curve can be used to adjust the heterogeneous components of the records in order to restore the homogeneity of the data. Double mass curve technique can also be applied if two variates are associated eg rainfall from neighbouring locations.

It should be noted that the quality controlled data included the missing records which had been estimated using various techniques together with the areally averaged records. Methods which were used to derive areally averaged records are also presented. The methods which were used to quantify point rainfall anomalies (rainfall indices) are however presented first.

2.2 RAINFALL ANOMALY INDICES

In order to quantify the magnitude of the rainfall anomalies which were observed during the individual months, seasons or year (t), a simple rainfall anomaly index (Z) was used as expressed in the equation (1):

$$Z_t = \frac{x_t}{\bar{X}} * 100 \qquad (1)$$

Where $\bar{X}$ represent long term average of observation at time (t)

(X_t) and $x_t = X_t - \bar{X}$.

Alternatively Z_t anomalies (Z'_t) can as well be expressed as departures of X_t from $\bar{X}$ (equation 2)

$$Z'_t = \left(\frac{X_t - \bar{X}}{\bar{X}}\right) * 100 \qquad (2)$$

Such indices have been used in many studies (Ogallo 1988; Ininda 1987; Basalirwa 1991).

Equation (2) was adopted in this study. It has been noted by many authors that areally averaged records give better representation of the large scale features which are generally associated with rainfall anomalies. Areally averaged rainfall records were therefore included in this study. The next section gives a brief discussion of these areally averaged records.

2.3.0 AREAL INDICES

It has been observed that areally averaged indices are capable of removing errors which may be associated with the individual locations. They also give better expressions of

the synoptic features. Areally averaged indices which were also used in this study include simple averaging methods and time coefficients derived from Principal Component Analysis dominant modes.

2.3.1 SIMPLE AREAL AVERAGES Simple areal rainfall average (Z_t) for the individual homogeneous rainfall zones were expressed as:

$$\overline{Z}_{tj} = \sum_{j=1}^{n} \frac{Z_{tj}}{n} \qquad (3)$$

$$\overline{Z}_{tj} = \sum_{j=1}^{n} \frac{Z'_{tj}}{n} \qquad (4)$$

Where n is the number of stations in the respective homogeneous zones.

2.3.2 TIME COEFFICIENT OF THE PRINCIPAL COMPONENT ANALYSIS (PCA) MODES

Time coefficient series are generated from the weighted average of observed normalized variates as derived from Principal Component Analysis (PCA). Only a very brief account will be given here. Details of PCA are given in section 2.6.7.1. Under this method, factor loadings of PCA derived eigenvectors are used as weights and areal indices are obtained from the averages of the series as indicated in the equation (5)

$$Z_{ij} = \frac{1}{N}\sum_{j=1}^{n} a_i X_{ij} \qquad (5)$$

where z_{ij} is the areal index ,a_i is the weight at eigenvector i and location j and X_{ij} is normalized variate at location j and eigenvector i. Details of these may be obtained from (Ogallo 1988; Basalirwa 1991; Folland 1991). Principal component analysis will be discussed in section 2.7. This method was used by (Ogallo 1988; Folland et al. 1991 among many others). This method was adopted in this study . The various rainfall anomalies indices were subjected to several spatial and temporal analyses including Trend, spectral, correlations and principal component analysis. Trend analysis is presented in the next section.

2.4 TREND ANALYSIS

Temporal variations in the time series are analyzed in these methods. Graphical and statistical approaches are applied to analyze the trends. Under graphical analysis,graphical representation of time averaged values or running averages are considered. Running averages can either be overlapping or non overlapping. The resulting plots are examined for any significant departures.

Under the statistical methods parametric and non parametric methods are used. Accumulated sums of the deviations from the mean can be used to indicate fluctuations in the series (Basalirwa 1991). In this study statistical methods were used by applying spearman rank correlation test on areal seasonal series. The spearman rank correlation (Γ_s) is calculated from equation (6) bellow:

$$\Gamma_s = 1 - \frac{6\sum_{i=1}^{N} d_i^2}{N(N^2-1)} \qquad (6)$$

where $d_i = K_i - i$, K_i is the rank of the series X_i and N is the total number of observations. The value of the Spearnam rank correlation is tested for significance by computing the statistic (t) defined by:

$$t = \Gamma_s \left[\frac{N-2}{1-\Gamma_s^2}\right]^{\frac{1}{2}} \qquad (7)$$

The t-value is compared with the probability points of student's t-distribution with N-2 degrees of freedom.

Spectral analysis which was used to examine cycles in the seasonal series is presented in the next section.

2.5.0 SPECTRAL ANALYSIS

Spectral Analysis is the modern method for searching for cycles in a time series . The time series must be made stationary (time series with constant mean & variance) before the data are subjected to spectral analysis. Filters which are quantified in terms of mathematical expressions are normally used to make time series stationary. The most common filter used in time series is the difference filter which may be expressed as:

$$Y_t = X_t - X_{t-j} \qquad (8)$$

Where j = order of the filtering.

The development of Spectral Analysis has a long history and some of the methods which have been established include the Fourier Transform of Autocovariance, Fast Fourier Transform (FFT) and Maximum Entropy Method (MEM) (Jenkins & Watts 1968; Cooley et al. 1967; Burg 1972). FFT method is based on harmonic analysis and it is most applicable for analyzing long data sets. The data is grouped into subsets and dominant modes in the subsets are compared.

The Maximum Entropy Method is derived from the concept of entropy in a time series. This method is suitable when short period of data is considered. The method has a high resolving power and it is applicable when weak signals are analyzed. MEM also gives unbiased spectral estimates since no fixed smoothing window is required. Despite these advantages over other methods, MEM has the following disadvantages:

(i) The significance of the spectral peak cannot be tested.

(ii) There are difficulties in choosing the maximum time lag or coefficients to be applies, Agwata (1992). The autocovariance method which was used in this study is presented in the next section.

2.5.1 AUTOCOVARIANCE TRANSFORM METHOD

In this method,the spectral density function $D_t(f)$ is expressed as a Fourier transform of the autocovariance function, $R_t(K)$ or autocorrelation function, $r_t(K)$. Therefore spectral density function can be expressed as:

$$D_x(f) = \sum_{K=-N}^{N} r_x(K) \exp^{-i2\pi fk} \qquad (9)$$

or

$$D_x(f) = \sum_{K=-N}^{N} R_x(k) \exp^{-i2\pi fk}, K = 1,2,3,... \qquad (10)$$

$$i = \sqrt{-1}$$

for normalized time series when the variance, $\sigma^2 = 1$.

$r_x(k)$ = Autocorrelation function at lag (k) and it is given as:

$$r_x(K) = \frac{\frac{1}{N}\sum_{t=1}^{N-K} (X_t - \bar{X})(X_{t+k} - \bar{X})}{\frac{1}{N}\sum_{t=1}^{N} (X_t - \bar{X})^2} \qquad (11)$$

Where X_t = observation at time t, N = Total number of observations, K = time lag (=0,1,2,.....M) = time lag where M is the maximum time lag. Autocorrelation is based on the concept of correlation which will be discussed in details in section 2.6.0.

Correlogram which is a graphical plot of the autocorrelation function against time lag k is used to give some information about the periodicities in a time series. However, correlogram is in a form of damped harmonic functions and it becomes difficult to estimate

the periods. The standard method of detecting cycles from spectral analysis is to plot the spectral density function D.(f) against f. Random variations in this function are removed by applying spectral windows to smoothen the spectral density function. When spectral windows are applied, then the smoothed spectral density function can be presented as:

$$D'_X(f) = \sum r(K)\, W(f) \exp^{-i2\pi fk} \qquad (12)$$

Where W(f) = spectral window.

Equation (12) can be rewritten as:

$$D'_x(f) = 2\left[1+2\sum_{k=1}^{M-1} r(k)\, W(f)\cos(2\pi fk)\right] for; 0 \le f \le \frac{1}{2} \qquad (13)$$

After applying the spectral windows, then cycles appear as peaks in the plot of D'.(f) against f.

The statistical significance of the peaks is tested by applying either the 'White' or 'Red' noise hypothesis. The 'White' noise hypothesis assumes that the generation process of the time series is random while the Red noise hypothesis assumes inter-correlation between neighbouring points of a time series.

When White noise hypothesis is assumed in the time series, then equation (13) becomes:

$$D'_x(f) = \frac{\sigma^2}{2\pi}, for\ \ all\ \ frequencies, f \qquad (14a)$$

$$D'_x(f) = \frac{1}{2\pi}, for\ \ normalised\ \ series, \sigma^2 = 1 \qquad (14b)$$

$$D_x'(f) = 0.16 \qquad (14c)$$

When Red noise hypothesis is assumed, the expression for the smoothed spectral function becomes:

$$D_x'(f) = D_x(f)\left(\frac{1-r_1^2}{1+r_1^2-2r_1\cos(\frac{\pi k}{M})}\right) \; ; \quad 0 \le K \le M \qquad (15$$

Where $D_x(f)$ = Mean of the raw Spectral peaks, M = Maximum time lag, r_1 = lag correlation for the first time lag.

Red noise hypothesis is rarely assumed in testing significance of the spectral peaks because equation (15) is complex . On the other hand, a Chi-square test statistic χ^2 for V degrees of freedom and at 95% confidence level is applied when White noise hypothesis is assumed. If the maximum time lag is M and the total number of observations is N, then the degrees of freedom ,V, for the Parzen window is given as:

$$V = 3.71\frac{N}{M} \qquad (16)$$

Then the white noise spectrum becomes:

$$D_X'(f)\chi_v^2(95) = 0.16\chi_{3.71}^2\frac{N}{M}(95) \qquad (17)$$

For a random series, the autocorrelation function $(r_1)t$ is approximately normally

distributed with mean

(-1/N-1) and variance N-2/(N-2)^2 . The exact one tailed significance points given by Anderson (1942) may be sufficient to base the significance test on a desired probability point of the Gaussian (normal) distribution especially when N is greater than 40 ,WMO (1966). The significance of r_1 is tested by comparing with the test value of $(r_1)t$ which is defined as:

$$(r_1)\,t = \frac{-1 \pm t_g\sqrt{N-2}}{(N-1)} \qquad (18)$$

Where N = Number of observations in years, t_g = standard normalized variate corresponding to the desired level of significance g.

At 95% confidence the value of t_g extracted from Gaussian tables for a one-tail series was 1.645 and 1.960 for a two-tail series. r_1 is significantly different from zero if it falls outside the confidence limits of the test value $(r_1)t$. In this study this technique was used to determine statistical significance of peaks in the seasonal rainfall and SST series. In this study the autocovariance method was used because it consumes less time,round off errors are few and there is flexibility in the selection of frequency bands.

2.6.0 CORRELATION ANALYSIS

This section gives a review of most of the correlation methods and highlights the specific methods which were adopted in this study.

2.6.1 SIMPLE CORRELATION ANALYSIS

Simple correlation coefficient (r_1) between the predictand (y_i) and any predictor at any time lag, k, (x_{ik}) may be expressed as:

$$r_k = \frac{\sum_{t=1}^{M} x_{t+k} y_t}{\left[\sum_{t=1}^{M} y_t^2 \sum_{t=1}^{M} x^2{}_{t+K}\right]^{\frac{1}{2}}} \qquad (19a)$$

where

$$x_{t+K} = X_{t+K} - \bar{X}; y_t = Y_t - \bar{Y} \qquad (19b)$$

where $-1 \leq r_k \leq 1$, Positive and negative values of (r_k) are indicative of the positive or negative relationship respectively.

This method assumes that there is no any other variable which is strongly associated to either X or Y. In this study correlation between seasonal rainfall and seasonal SSTs as well as lagged seasonal SSTs was evaluated. Principal Component Analysis was used to derive correlation matrices. Yevjevich (1972) and many others have shown that students t statistic is given by equation (20). Therefore , this technique was used to decide the significance of the correlations at 95% confidence limit.

$$t = \left[\frac{(n-2)\, r^2}{(1-r^2)}\right]^{\frac{1}{2}} \qquad (20)$$

Where n is the number of years covered and (r) is the correlation coefficient.

2.6.2 PARTIAL CORRELATION

This technique may be applied for multiple variables. Under this method,correlation between pairs of the variables is partially computed while other variables are kept constant.

2.6.3 SEMI-PARTIAL CORRELATION

Semi-partial correlation technique is applied when the dominant variables have been identified by partial correlation technique. In the second phase a second variable is introduced to check whether it significantly improves the skill. This method is simple enough but it is not accurate. Considering the complexity of climatological variables, this method is not of much use in meteorological analysis.

2.6.4 MULTIPLE CORRELATION

Multiple correlation technique gives total correlation between multiple variables. Thus if the relationship is linear, then multiple correlation coefficient can be specified by mean values , variances and covariances of the variables only and a knowledge of the exact distribution of the variables may not be necessary. Multiple correlation coefficient can be expressed as:

$$\rho_{yx} = \left[1 - \frac{\sigma^2_{y.x}}{\sigma^2_{y}}\right]^{\frac{1}{2}} \qquad (21)$$

where $\sigma^2_{y.x}$ = *Covarience of x , y*

and

$$\sigma^2_y = Variance\ of\ y$$

Details are found in Rao (1965).

For climatological purposes,long term observations of the variate are needed in order to apply multiple correlation techniques. In most cases long term observations of most variates are not generally available. Therefore the method is not readily applicable for most of climatological variables.

2.7.0 CLUSTER ANALYSIS

Many of the correlation methods are not able to delineate complex relationships between several variables. Some methods which have been used to delineate complex spatial and temporal relationships include cluster and Empirical Orthogonal Functions (EOF). Under the cluster method, variables with similar characteristics are grouped together. This method of clustering represents linkage analysis which can be applied to few groups of variables like station locations. The linkage analysis uses the inter-station correlation matrix to determine the stations which are closely related. This method works quite well when small numbers of variables/stations are being considered. Sorting out the inter relationship between the stations becomes complex as the number of variables increases,Basalirwa (1991).

2.7.1 EMPIRICAL ORTHOGONAL FUNCTION (EOF)

This method can give more information on the spatial and temporal distribution of complex variables. The advantages of the method include the following:

• The method has the ability to reduce large volumes of data by replacing them with fewer orthogonal functions which represent the physical processes of the original data. Therefore depending on the data being analyzed, it is possible to interpret the orthogonal functions in terms of some recognizable physical processes.

• The method does not require that stations should be equidistant from each other.

• The time coefficient of the eigenvectors are used as composite indices of the temporal anomalies while the loadings of the EOFs are used to derive rainfall homogeneous zones. Common Factor Analysis considers the unique factors of the variance whereas the principal component analysis neglects the unique properties of the variables. Common Factor Analysis and principal component analyses are presented in the next section.

2.7.2 COMMON FACTOR ANALYSIS (CFA) AND PRINCIPAL COMPONENT ANALYSIS (PCA)

Factor Analysis is a process of identifying and classifying characteristics which differentiate one object from another. The basic equation for CFA may be of the form:

$$Z_j = \sum_{k=1}^{m} a_{jk}F_k + a_kU_k \; ; \quad (j=1,2,...n) \qquad (22)$$

where: Z_j = the standardized variable j, a_k U_k = Unique variance and it is more difficult to evaluate, F_k = hypothetical factor k (principal component), a_{jk} = standardized multiregression coefficient of variable j on factor K (factor loading), m = the number of common factors, n = the number of variables.

The observed variables are transformed into a set of new variables (principal components)

which are uncorrelated. Hence, the new variables are orthogonal. The method is an 'algebraic' technique for decomposing the total variance in a data set into orthogonal components, Bärring (1987).

When a grouping of variables has a great deal in common, a factor between variables is said to exist and the interconnection constitutes a factor. The first factor accounts for the major portions of the common variance while the next three factors are group factors and factors above the fourth factor express the specific characteristics of variance, Child (1970). In this study, Burt-Banks formula which was applied to examine the spatial patterns of the factor loadings at 5% significance levels is given in equation (23).

$$SEl = SEC \sqrt{\frac{n}{n+1-r}} \qquad (23)$$

where SEL = Standard Error of a Loading,SEC = Standard Error of a correction,n = The number of variables/years in the analysis period,r = The factor number that is the position of the factor during extraction. The standard error of correlation was obtained from the tables of Pearson product moment correlation coefficients. The unique component of the variance U_t is very difficult to estimate. This component is often omitted in many studies. In such a case equation 22 reduces to simple PCA as shown in the next section.

2.7.2.1 PRINCIPAL COMPONENT ANALYSIS (PCA) .

When the term a_tU_t is neglected in equation 22, CFA reduces to simple PCA. PCA mode may be expressed as :

$$Z_j = \sum_{k=1}^{m} a_{jk} F_k \qquad (24)$$

where: Z_j, F_k, a_{jk}, m and n have the same meaning as defined in equation 22

The loadings are either obtained from covariance matrix or correlation matrix. In this study correlation matrix was used because it has the advantage of assigning equal weighing to the stations and assigns perfect correlation between a variable and itself.

In meteorology, the principal components may not be completely independent of each other due to the physical, dynamic and thermodynamic processes that contribute to weather conditions. Therefore, this factor is achieved by rotating the components. The two common methods of rotations are the 'Orthogonal' and the 'Oblique' rotations. In the orthogonal (varimax) rotation the reference axes are maintained at 90° whereas in the case of oblique rotation the components are partially correlated. The Varimax orthogonal is more popular than the oblique rotations. The Oblique types of rotation include Oblimax, Oblimin, and many others. The details of factor and principal component analyses have been discussed by Ogallo (1980). In this study orthogonal varimax rotation (Nie et al. 1970) has been applied. Rotated principal components are superior to unrotated components Farmer (1981). Rotated principal components were used by (Ogallo 1980/1986/1988; Bärring 1987; Basalirwa 1991 among many others).

Significant components which adequately explain the total variance were retained in the analysis. The methods which have been developed for selecting significant components include:

(i) The Kaiser criteria (1959) whereby all eigenvalues greater than unity are considered to

be significant.

(ii) The Castell-Scree test of (Castell 1966) uses a plot of eigenvalues against the factor numbers and the non significant vectors (noise) is assumed to generate a linear relationship.

(iii) The Logarithm of Eigen Values (LEV) of Craddock (1965/1973; Craddock et al. 1969/1970) first transforms the eigenvalues into logarithms which are then plotted against the factor numbers of the variables. Again the highest eigenvalue corresponds to the first ordinate point where noise is detected by the linear relationship.

(iv) The sampling errors test by North et al. (1982) is based on the comparison of the sampling errors for the eigen values and the separation in the neighbouring eigen values. The sampling error ($\lambda_i(2/N)^{1/2}$) indicates whether a sample eigenvalue is a faithful representation of the eigenvectors. Here λ_i refers to the eigenvalue i and N refers to the total number of records. The spacing between the eigenvectors (λ_i-λ_i) is greater than the sampling error ($\lambda_i(2/N)^{1/2}$) up to a point when the sampling error becomes greater than the spacing between the eigenvectors. Such a point would mark the truncation in the extraction of the significant eigenvectors. In this study, Significant eigenvectors were identified by applying all the four methods. The next section presents the technique of communality analysis.

2.7.2.2 COMMUNALITY ANALYSIS

The method of communality indicates the proportion of the total variance at each station that is shared by all other stations. This technique may also reveal the effect of some common rainfall generating functions and the influence of the unique properties at the individual stations. The communality of each variable Z_i given by (h^2) has been given by Nie et al. (1970) and many others as:

$$h_j^2 = \sum_{k=1}^{m} a_{jk}^2 \quad (j = 1,2,\ldots,n) \qquad (25)$$

where: a_{jk} ,m and n are as defined in equation (22)

In this study,the station which is best correlated with the rest of other stations within a given climatological grouping was used to represent the individual homogeneous zones based on communality principles which ensured that such stations were realistic and could represent most of the regional information. Communality analysis was also applied to the SST modes in order to select the grid-points which exhibited highest communality in each of the modes. The stations and the grid-points which were selected by using the communality method were used in the lagged correlations. Since real-time SSTs may not be easily obtained for operational seasonal forecasting, effort was made to develop proxies which would be used to represent SSTs. The following section presents the method of lagged correlation.

2.8 LAGGED CORRELATIONS

The relationship between a variable (Y) at time (t) and another variable (X) at time lags (t-1),(t-2)...,(t-K) , where K is the maximum time lag, represents the time lagged correlation between the two variables at the respective time lags.

In this study ,lagged correlations were used to examine time relationship between seasonal rainfall and seasonal SSTs. The SST seasonal time series were lagged behind the seasonal rainfall time series . The significant correlations between the seasonal SSTs and seasonal rainfall were selected from the correlation matrices after applying equation (20) at

95% confidence limit.

Many of these correlation methods cannot be able to delineate complex relationships between several variables. Empirical Orthogonal Functions analyses which were used to delineate complex spatial and temporal relationships between SST and rainfall was presented in section 2.6.7.1

2.9 INDIAN OCEAN PROXIES

Under this section analytical method was used to derive proxies which may be used to represent SST over Indian ocean in absence of Indian ocean SSTs. The most used data here were surface air temperatures (SATs) from Aldabra, Lamu, Mombasa and Seychelles. The SATs were correlated with the grid-pints SSTs values for Indian ocean. Equation (20) was used to determine the significant correlations from the correlation matrices.

2.10 REGRESSION ANALYSIS

Regression models are used to express the mathematical relationship between the variables. The independent variables are known as the predictors and the dependent variables are known as the predictands. This section presents the basic regression methods.

2.10.1 MULTIPLE LINEAR REGRESSION ANALYSIS

The value of the predictand might depend on several predictors which might have interrelationship such that the value of one of them may be influenced by many others. Multiple regression helps to study the joint effect of the predictors on the predictand. The linear basic equation for the simple relationship between the predictors (m) at time (t) and the predictand (Y) at lead time (K) may be expressed as:

$$Y_{t+k} = a + b_1X_{1t} + b_2X_{2t} + b_3X_{3t} + \ldots + b_mX_{mt} \qquad (26)$$

Again this equation assumes simple relationship between the predictand (Y_{t+k}) and the SST predictors X_{1t}, X_{2t},.....X_{mt} . If $b_1 \ldots b_m = 0$,then equation (26) reduces to a simple regression equation.

The significance of the predictors in regression equations is tested by the magnitude of the variance ratio and the square of multiple correlation/explained variance as given below:

$$F = \frac{R^2}{1-R^2}\frac{n-p-1}{p} \qquad (27a)$$

Where F = variance ratio and R^2 = explained variance by the model which may be expressed as:

$$R^2 = \frac{b_1S_{01} + \ldots\ldots + b_3S_{03}}{S_{00}} = SMC/EPV \qquad (27b)$$

Where SMC is Square of Multiple Correlation and EPV is Explained Variance,n = sample size,p = number of independent variables, S_{oi} = corrected sum of the product. S_{oi} can be represented as:

$$S_{oi} = \sum (y_t - \bar{y})(x_t - \bar{x}) \qquad (27c)$$

In this study, the model parameters were identified from correlation matrices as

explained in section 2.7.2.1. under PCA.

2.10.1.1 STEP-WISE REGRESSION MODEL

Step-wise regression was used in this study to introduce the individual predictors $X_1,..,X_n$ in equation 26 into the regression equation. A single predictand is added to the equation based on the variance of the predictand which can be accounted by the new variable. Thus the first variable X_1 accounts for most of the variance followed by $X_2, X_3, ...X_n$ respectively. The regression equation during the first step is of the form :

$$Y_{t+K} = a + b_1 x_{1t} \qquad (28)$$

K and t have the same meaning as defined in section 2.10.1 and equation 26.

when the second variable is introduced at the second step,the equation takes the form:

$$Y_{t+K} = a + b_{1t} x_{1t} + b_2 x_{2t} \qquad (29)$$

K and t retain the same meaning as defined above.

The regression equation is in form of equation 26 at the m^{th} stepwise regression step where $b_1, b_2, ...b_n$ are regression constants. The time lag (t) of the predictors used in equation 26 and stepwise solutions were based on results from time lag correlation analysis.

The results which were obtained in this study are presented in chapter three.

CHAPTER 3

RESULTS AND DISCUSSION

This chapter presents the results which were obtained when the data were subjected to the various methods which were adopted in the study. The details of the various methods were presented in chapter two. These included the estimation of missing records,data quality controlling using mass curve analysis, together with trend,cyclical analysis,correlation and principal component analysis. The results from the fitted models are also presented in this section.

3.1 ESTIMATED RECORDS AND MASS CURVE ANALYSIS

Typical examples of the uncorrected mass curves which were obtained from the rainfall records of the various locations are given in the figures 3(a), 3(c) and 3(e). Although the results indicated that the mass curves were linear at most of the locations,twenty one (21) locations out of the one hundred and eighty (180) used in the study indicated some form of heterogeneighty. The names of these stations are given in table two (2): Three, eight and ten of these stations are located in Kenya,Tanzania and Uganda respectively. Figure 2 which was given in section 2.0 indicates that there was no spatial uniformity in the distribution of heterogeneity status as most of these heterogeneighty did not generally extend to the neighbouring stations. Causes of data heterogeneity have been addressed by many authors (Ogallo 1987/88; Basalirwa 1991) among many others. The causes of heterogeneity in the data include: shift of station, change of instruments,change of instrument spare parts, and human error due to miss reading of the instruments.

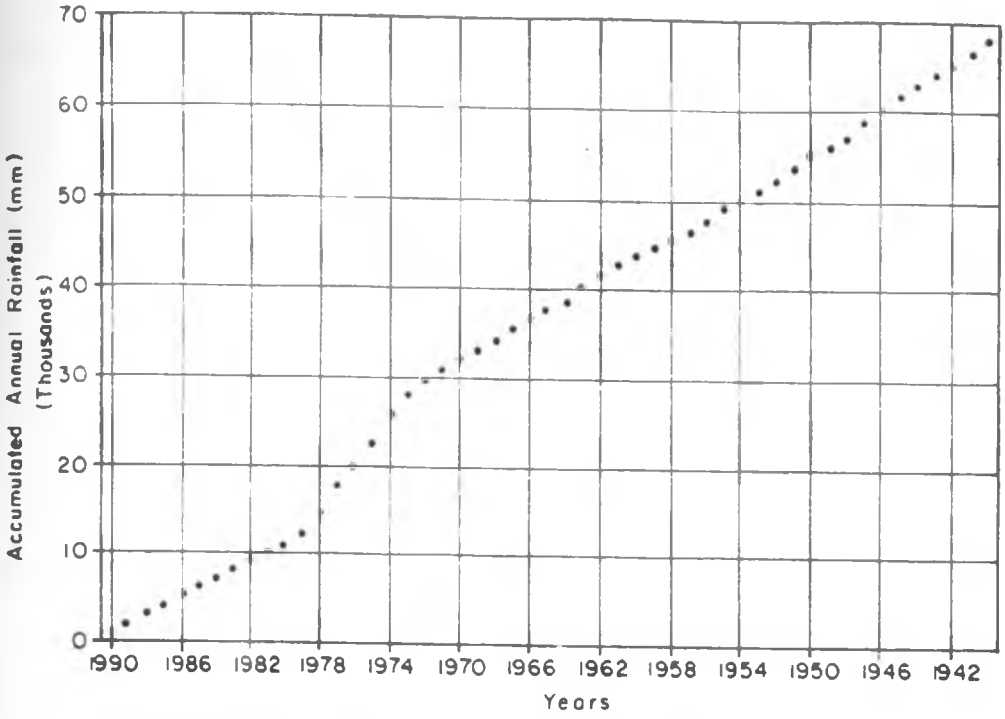

Fig. 3(a). Mass Curve for Lugalawa before corrections.

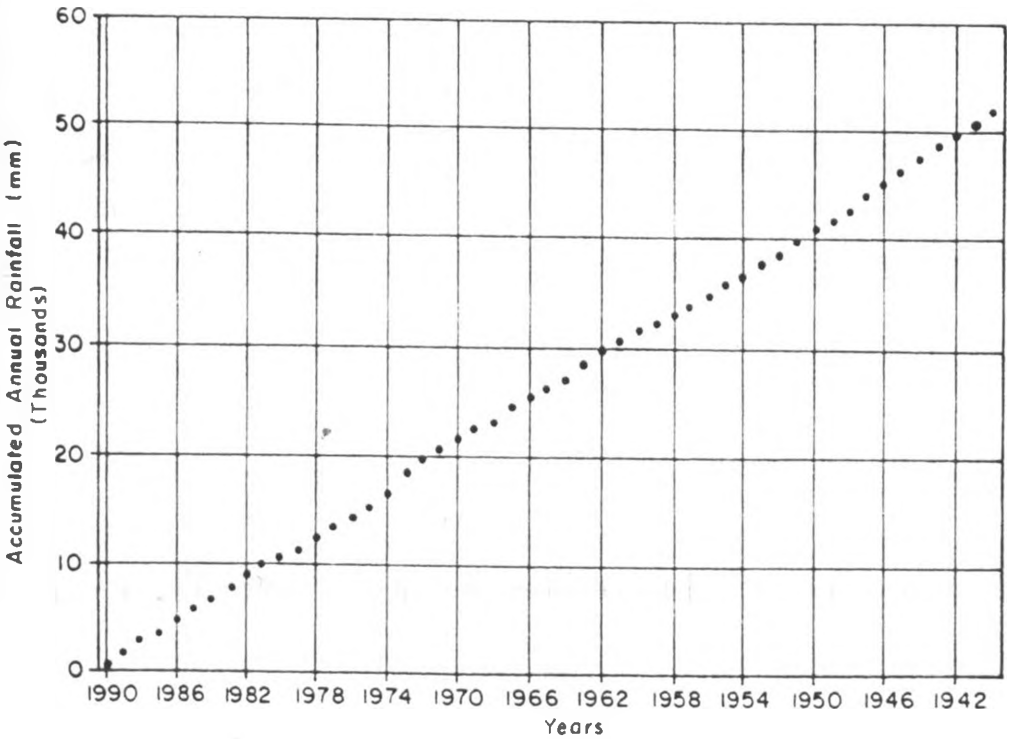

Fig. 3(b) : Mass Curve for Lugalawa after corrections.

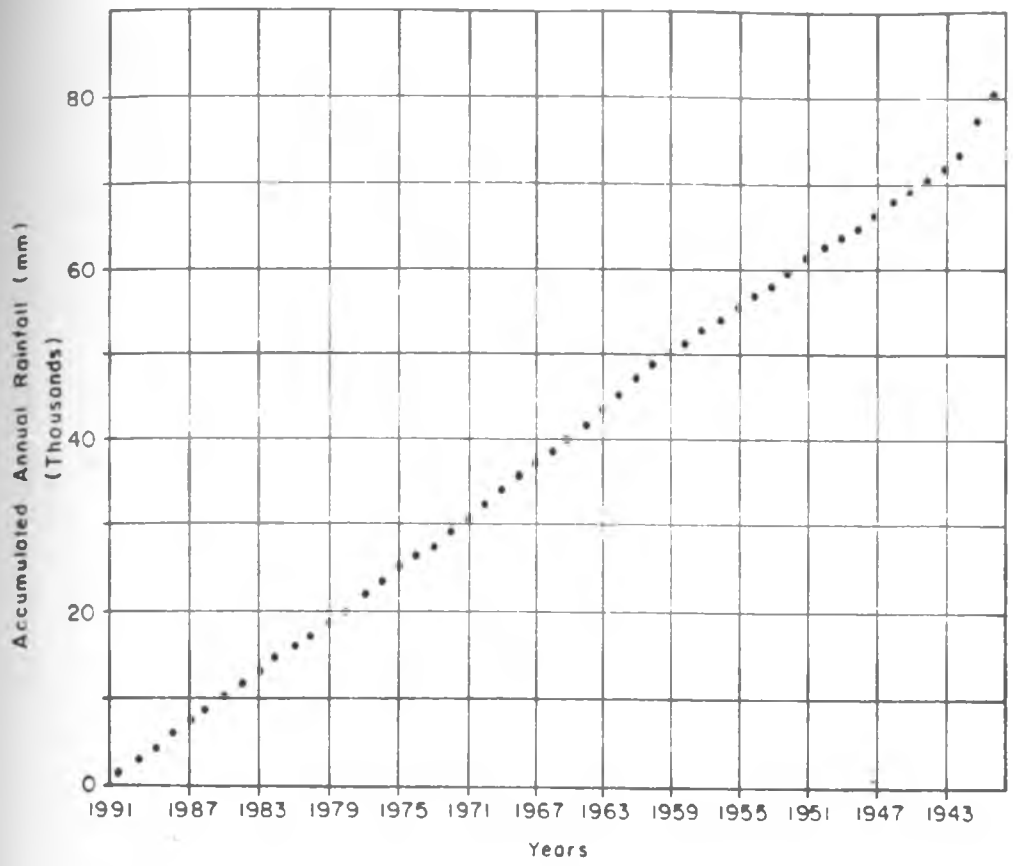

Fig. 3(c) : Mass Curve for Tororo before corrections.

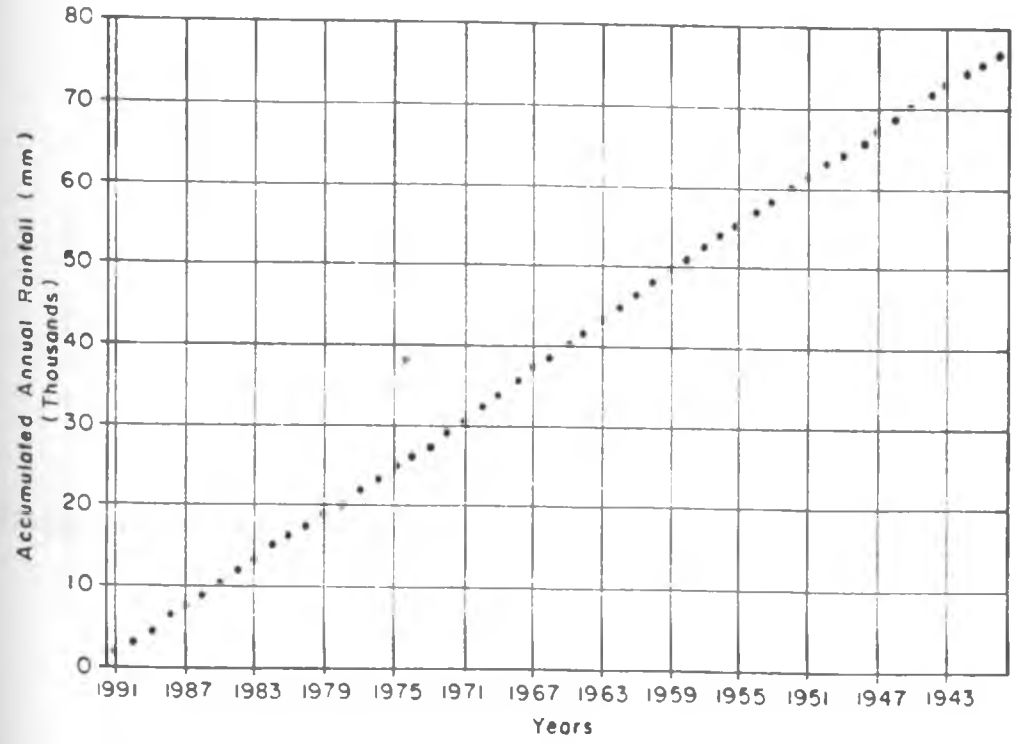

Fig. 3(d) : Mass Curve for Tororo after corrections

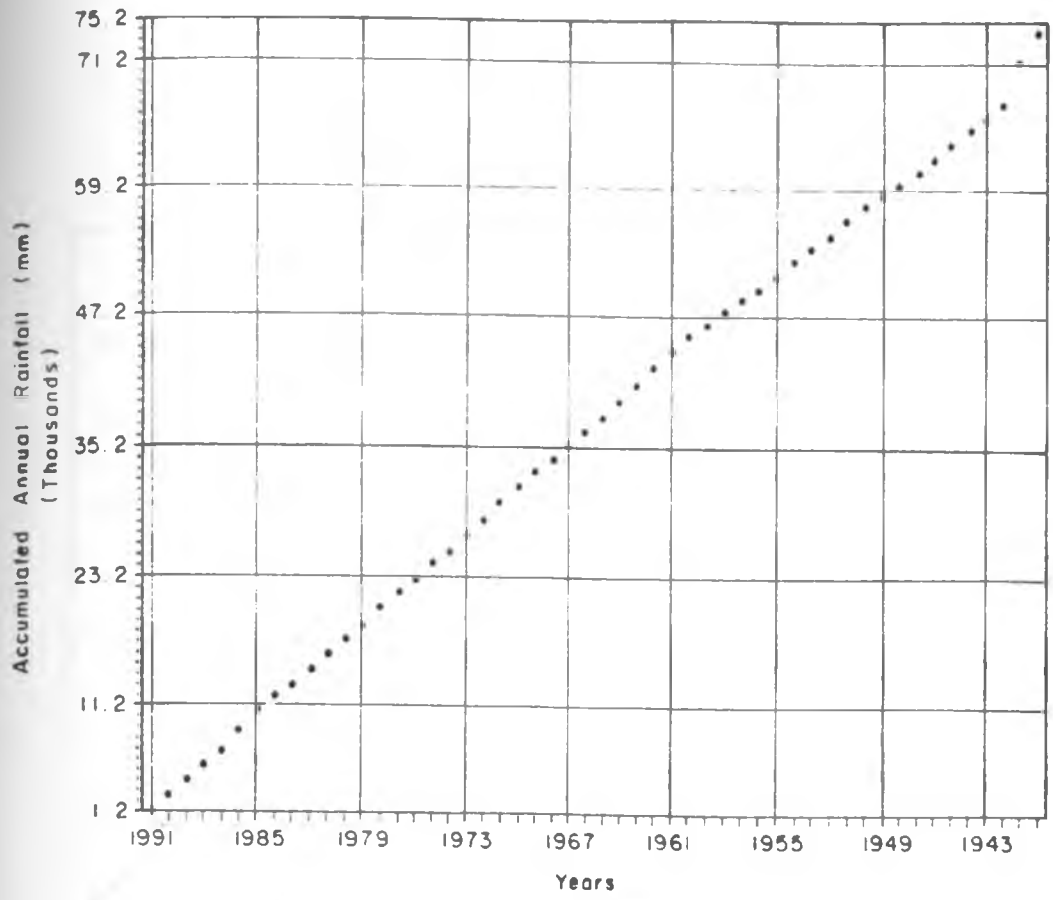

Fig 3(e). Mass Curve for Masindi before corrections

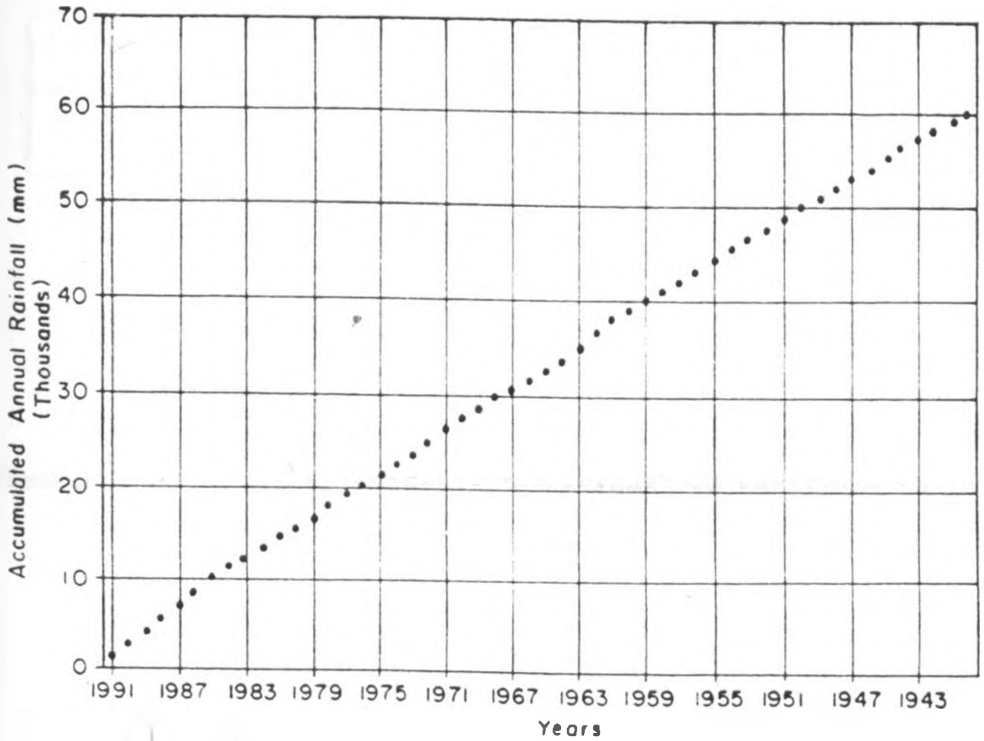

Fig. 3(f) : Mass Curve for Masindi after corrections

Table 2: Stations which were heterogeneous

STATION NAME	PERIOD CORRECTED
Dansland	1942-40, 1951-43, 1975-52
Kibondo	1942-40, 1943-60, 1961-67
Runazi	1942-40, 1943-61
Arusha	1954-40, 1978-55
Moninko	1942-40, 1947-43, 1961-48,
Katigondo	1942-40, 1975-43,
Adilang	1942-40, 1953-43, 1961-54
Rom	1942-40,1969-43
Masindi	1942-40, 1962-43, 1963-86
Kyembogo	1942-40, 1959-43, 1965-60
Nyeri	1942-40, 1943-59, 1968-60
Lugalawa	1940-73,1974-79
Wilson Airport	1940-54, 1955-73, 1974-77

Table 2 continues on the next page

STATION NAME	PERIOD CORRECTED
Nyabasi	1940-61, 1962-73, 1974-79
Lushoto	1940-42, 1943-56, 1957-62, 1963-77
Mukono	1940-42, 1943-55, 1956-63, 1964-79
Tororo	1940-42, 1943-59, 1960-63
Bakijulula	1940-42, 1943-65, 1966-84
lokitaung	1940-42, 1943-47, 1948-61, 1962-68, 1969-77, 1978-83, 1984-88
Rwashamaire	1940-42,1973-77

The causes of heterogeneity were not investigated here, but the unbiased records were adjusted using double mass analysis. Typical examples of the adjusted records were shown in figures 3(b), 3(d), and 3(f). The quality controlled data were the ones subjected to the various analyses which were presented in chapter 2. The following section will present the results obtained from each of the methods.

3.2 DRY/WET PATTERNS

The major rainfall months for East Africa are March-May and October-November. In this section dry/wetness anomaly indices were examined for areal rainfall anomalies for the individual seasons, years and climatological zones. The patterns of the indices during the EL-Niño and la-Nina years were also examined. According to analysis by Rasmusson (1984), Ropelewski (1993) and others, the major El-Niño years during the period 1891 to 1993 occurred in 1891, 1900, 1902, 1905, 1911/1912, 1914, 1917, 1919, 1923, 1925/1926, 1929/1930, 1932, 1939, 1940/ 1941, 1943/1944, 1946, 1948, 1951/1952, 1953/1954, 1957/1958, 1963, 1965/1966, 1969/1970, 1972/1973, 1975/1976, 1982/1983, 1986/1987, 1992/1993. The computed index values indicated that for the long rainfall season (March-May) driest years were recorded in 1940, 1941, 1943, 1945,1949, 1952,1953, 1954, 1956, 1958,1960, 1961,1962, 1966, 1967, 1970, 1971, 1972, 1973, 1979, 1983, 1984, 1986, 1987.

Out of these years, 11 years corresponded to El-Niño events giving a mean probability of 0.46 of occurrence of drought during EL-Niño. The probability however ranged from 0.15 to 0.73 in the coastal and lake Victoria shore regions of western Kenya respectively.

The largest wet anomaly indices were recorded in 1942, 1947, 1948, 1950, 1951, 1956, 1957, 1959, 1961, 1962, 1963, 1966, 1967, 1968, 1974, 1975, 1977, 1978, 1979,

1981, 1982,1985, 1990, 1991. Out of these, 15 years corresponded to la-Nina events giving a mean probability of 0.63 of occurrence of wet events during la-Nina. However, the probability of getting maximum wet anomaly during El-Niño years in the long rainfall season varied significantly from 0.1 to 0.68 in central southern region of Tanzania and southwestern Uganda respectively.

For the short rainfall season (September to November),the computed indices indicated that driest years were recorded in 1941, 1942, 1943, 1949, 1954, 1957, 1958, 1962, 1964 1969, 1970, 1971, 1974, 1976,1983, 1987. Out of these years 10 corresponded to the EL-Niño events giving a mean probability of 0.63 of occurrence of drought during EL-Niño. The probability, however was as low as 0.22 over Northwestern Tanzania.

The largest wet anomaly indices for the short rains were recorded in 1944, 1948, 1953, 1959, 1961, 1965, 1966, 1967,1971, 1972, 1977, 1982. Out of these 4 events corresponded to la-Nina giving a mean probability of occurrence of 0.31. It should be noted that although the mean probability of getting a positive anomaly during EL-Niño years during the short rainfall season was also about 0.31, the probability was however as high as 0.67 over the coastal and lake Victoria regions.

December-February is the peak rainfall season for southern Tanzania. The computed values indicated that the driest years for the December to February season were recorded in 1941, 1942, 1944, 16946, 1948, 1949, 1953, 1958, 1961, 1967, 1972, 1974, 1975, 1977, 1988, 1990, 1991 . Out these, 8 years are EL-Niño events which gives a mean probability of 0.47 of drought occurrence. When the individual regions in southern Tanzania were considered , the probability of getting drought ranged from 0.43 to 0.64 for the southern part near the border with Mozambique and the southern regions on the Indian ocean coastline respectively.

The largest wet anomalies in southern Tanzania were recorded in 1945, 1956, 1962, 1964, 1966, 1968, 1973, 1979, 1984, 1986, 1987. Seven of these are la-Nina events which gives a mean probability of 0.64 of wet anomaly occurrence. Considering the individual regions, the probability of getting a wet year, during la-Nina event ranged from 0.5 to 0.82 for central southern Tanzania and southern regions near the border with Mozambique respectively.

June-August is normally a wet season only over western parts of the region especially northern and eastern Uganda. Substantial rainfall is also recorded in the coastal region linked with East African Low Level jet. Driest years for June to August season were recorded in 1940, 1941, 1942, 1944, 1945, 1949, 1950, 1951, 1952, 1953, 1954, 1955, 1956, 1957, 1960, 1959, 1963, 1964, 1966, 1965, 1968, 1969, 1970, 1971, 1972, 1973, 1976, 1979, 1980, 1982, 1985, 1986,1990 . Out of these 14 are EL-Niño years which gives a mean probability of 0.42 of drought occurrence. When the individual regions within this sector were considered, the probability of drought occurrence ranged from 0.36 to 0.57 for regions to the north of lake Kyoga and central northern Uganda respectively. During this season, the largest wet anomalies in northern Uganda were recorded in 1946, 1947, 1948, 1958, 1961, 1962, 1967, 1974, 1975, 1977, 1978, 1981, 1984, 1985, 1988, 1989 and 1991. Out of these, 10 years were la-Nina events which gives a mean probability of 0.59 of wet anomaly occurrence. Considering individual regions, the probability of wet anomaly ranged from 0.55 to 0.76 for the regions around lake Kyoga and central northern Uganda respectively. The spatial patterns of seasonal rainfall during some of the EL-Niño and la-Nina years are shown in figures 4 to 13. Figures 4 and 7 give the spatial patterns of the index when cooling conditions were observed over Atlantic ocean and warming conditions were observed over Indian ocean (Ininda 1995). Reversal changes in the spatial patterns of rainfall during the EL-

Niño and la-Nina years are quite evident in some regions. The coastal and lake Victoria regions for example received substantial rainfall during the EL-Niño period while they are relatively dry during the la-Nina events. In addition some parts of central Kenya, northeastern Kenya, Northwestern Kenya including northeastern Uganda experienced drought conditions while southern Tanzania received above average rainfall during the long rainfall season in la-Nina events as indicated in figure 13.

The short rainfall season of 1961 has remained the highest on record with widespread coverage and highest rainfall amounts. Yet this season was neither EL-Niño nor la-Nina event figure 14. Anyamba (1984) attributed the anomalous high rainfall of Short rains to zonal orientation of the Arabian High which strengthened the northeasterly monsoon. Driest conditions of 1949 also occurred during non EL-NIño or La-nina years, but the positive SST anomalies were however recorded over Southeastern Pacific, South east Atlantic ocean (St. Helena region) and south east Indian ocean.

Negative SST anomalies were observed over western Indian ocean, western Pacific and over the Azores high region (Ininda 1995). It may be concluded from the patterns that although EL-Niño signals are discernable in the seasonal rainfall patterns of the regions, factors other than EL-Niño have been linked to several rainfall anomalies over the region. Such factors have included anomalies in cyclone activities, ITCZ, monsoon wind patterns among many others. Okoola (1978) for example attributed wet index/dry index over the coast to convergence of southeasterly monsoons and the meso-scale circulations/ convergence of meso-scale circulations with dry northeasterly monsoons respectively. Long rainfall deficit of 1984 , figure 13, was attributed to the low and medium level diffluence patterns over western Indian ocean regardless of the medium level anomalous westerlies Ininda (1995).

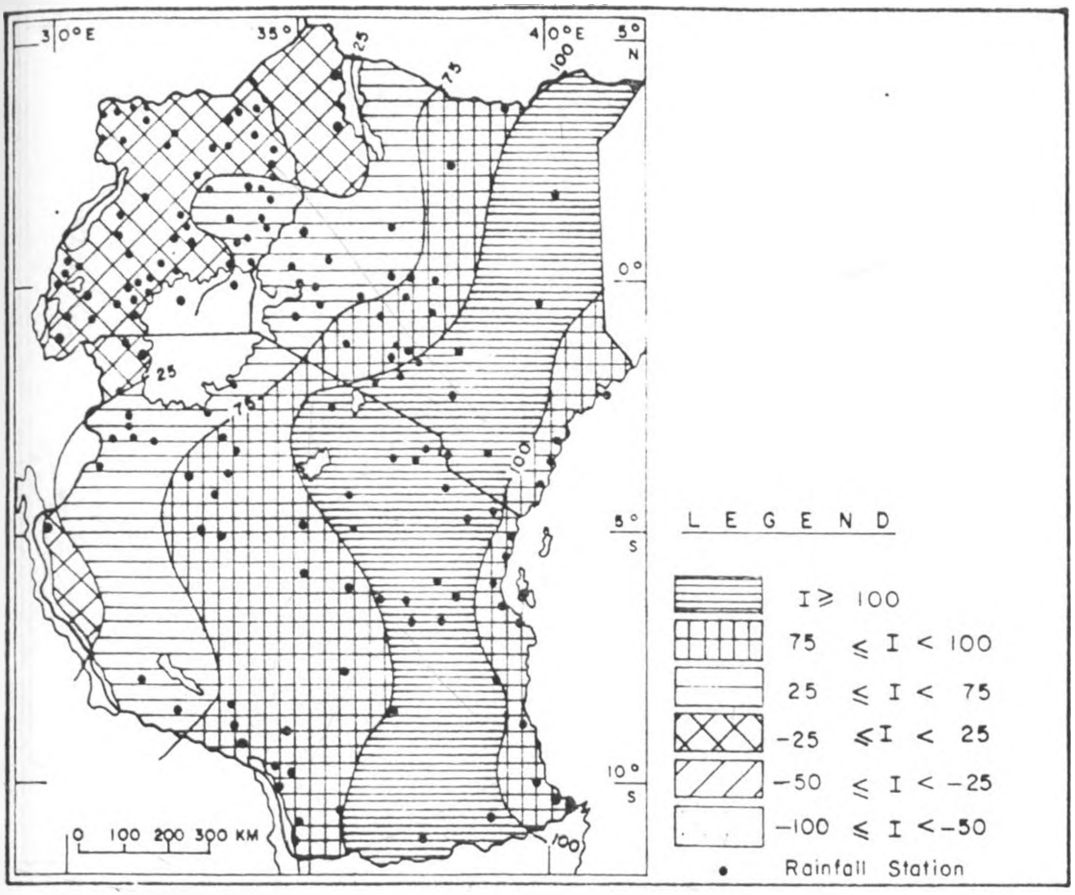

Fig. 4 : Spatial patterns of wet/dry index during the season of September — November, 1982 (EL Niño event)

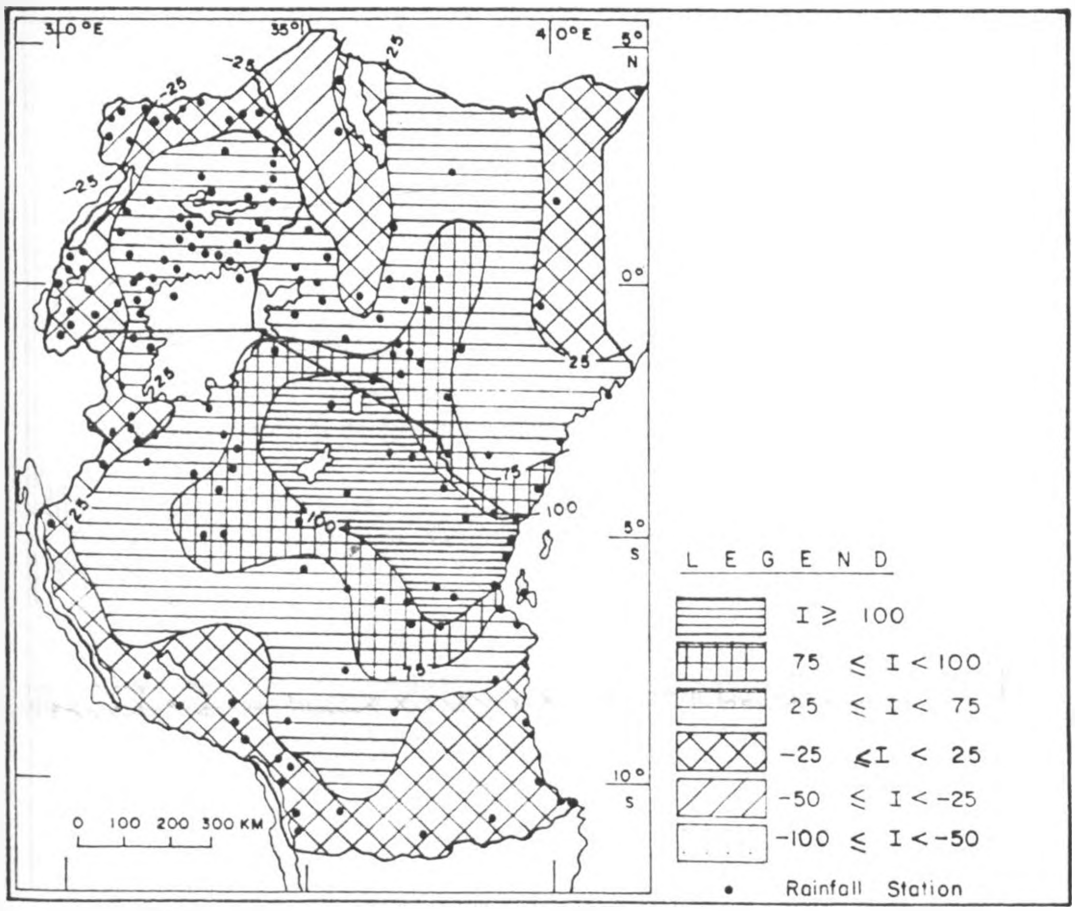

Fig. 5 : Spatial patterns of wet/dry index during the season of September — November, 1972 (El Niño event)

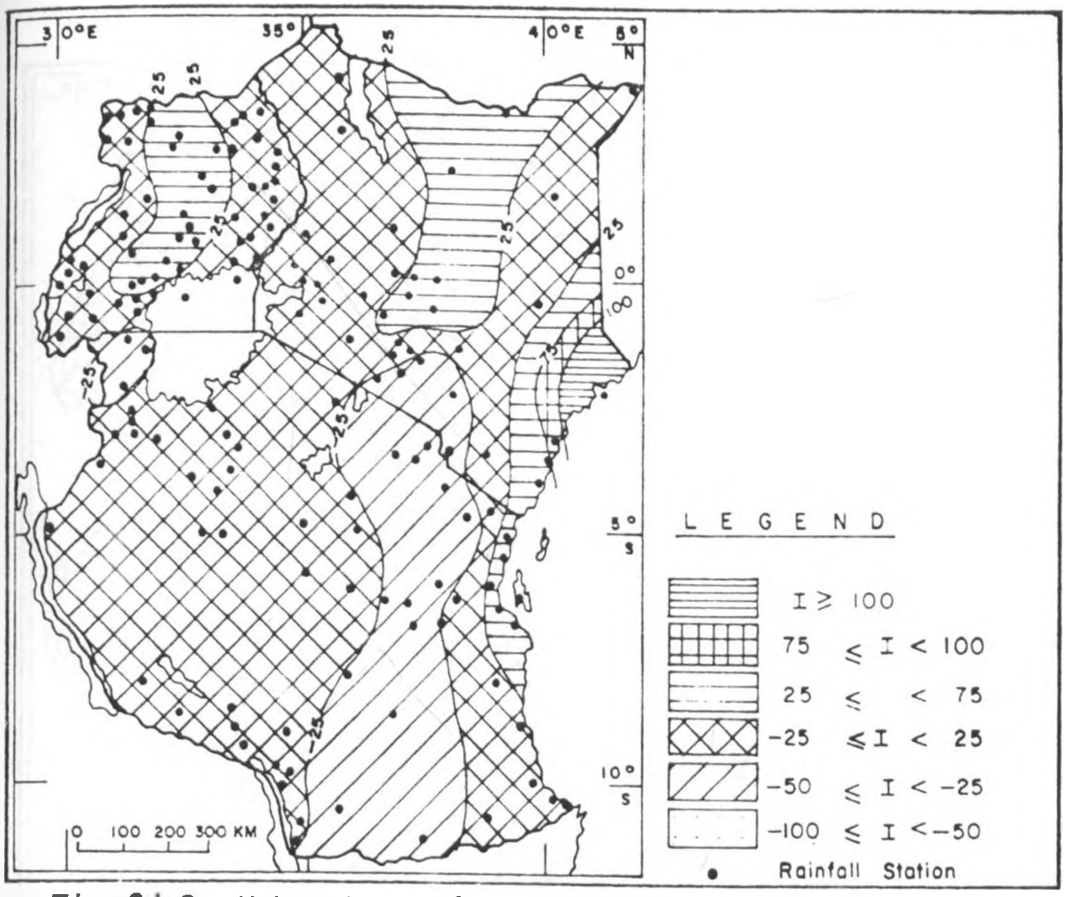

Fig. 6: Spatial patterns of wet/dry index during the season of March—May, 1972 (El Niño event)

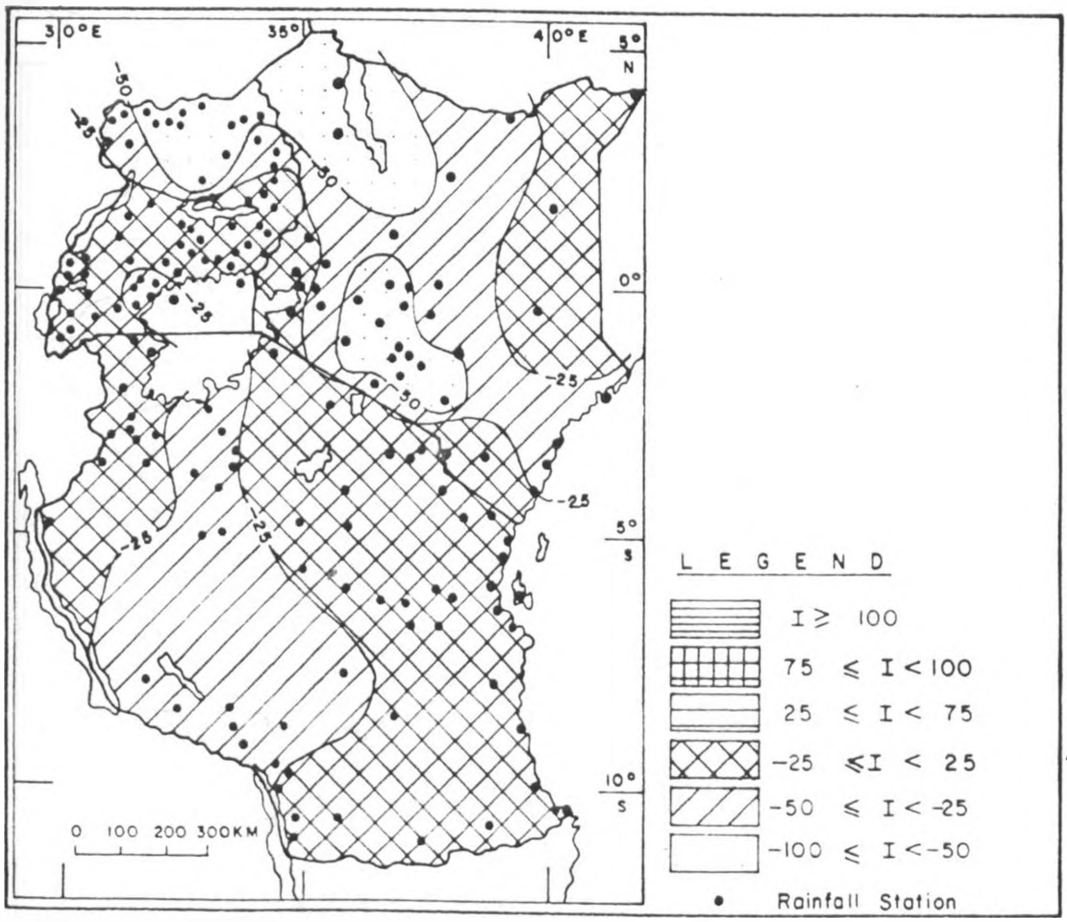

Fig. 7: Spatial patterns of wet/dry index during the season of March—May, 1982 (El Niño event)

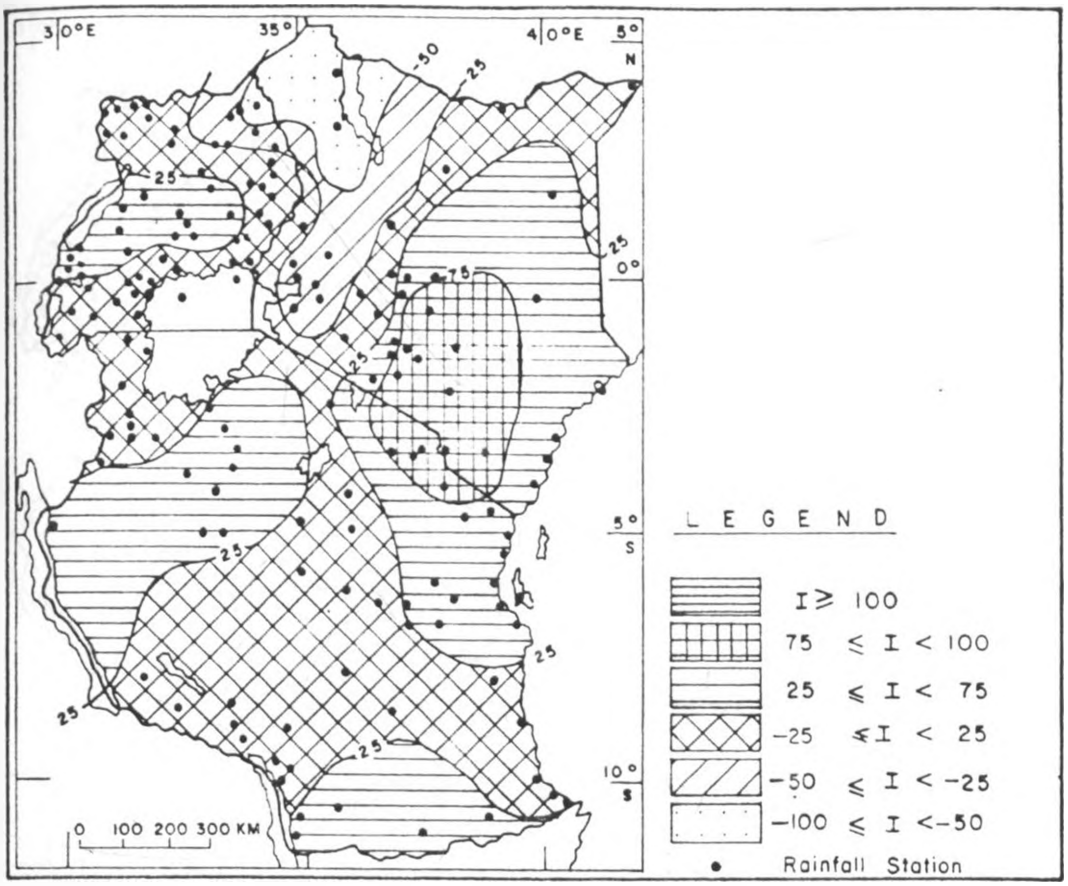

Fig. 8: Spatial patterns of wet/dry index during the season of September — November, 1984 (La Nina event)

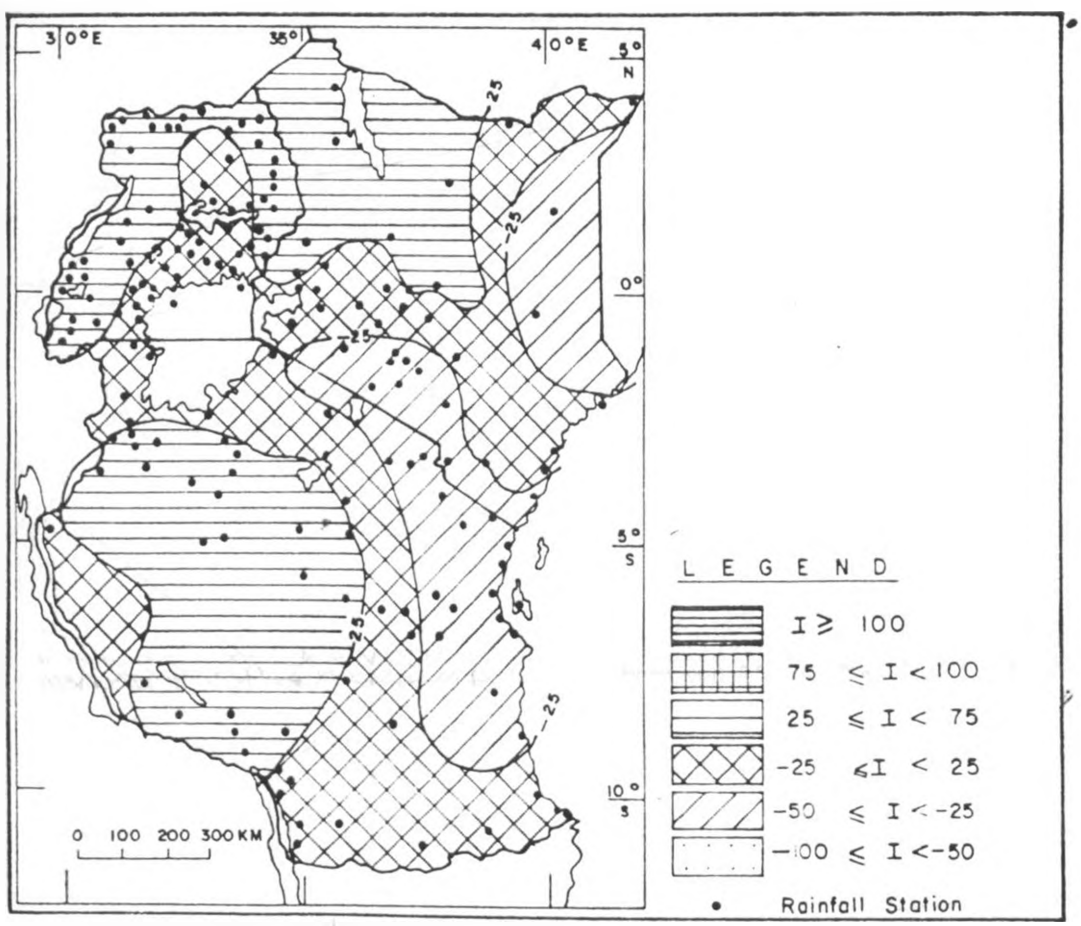

Fig. 9: Spatial patterns of wet/dry index during the season of September — November, 1988 (Normal Year) CAC 1993

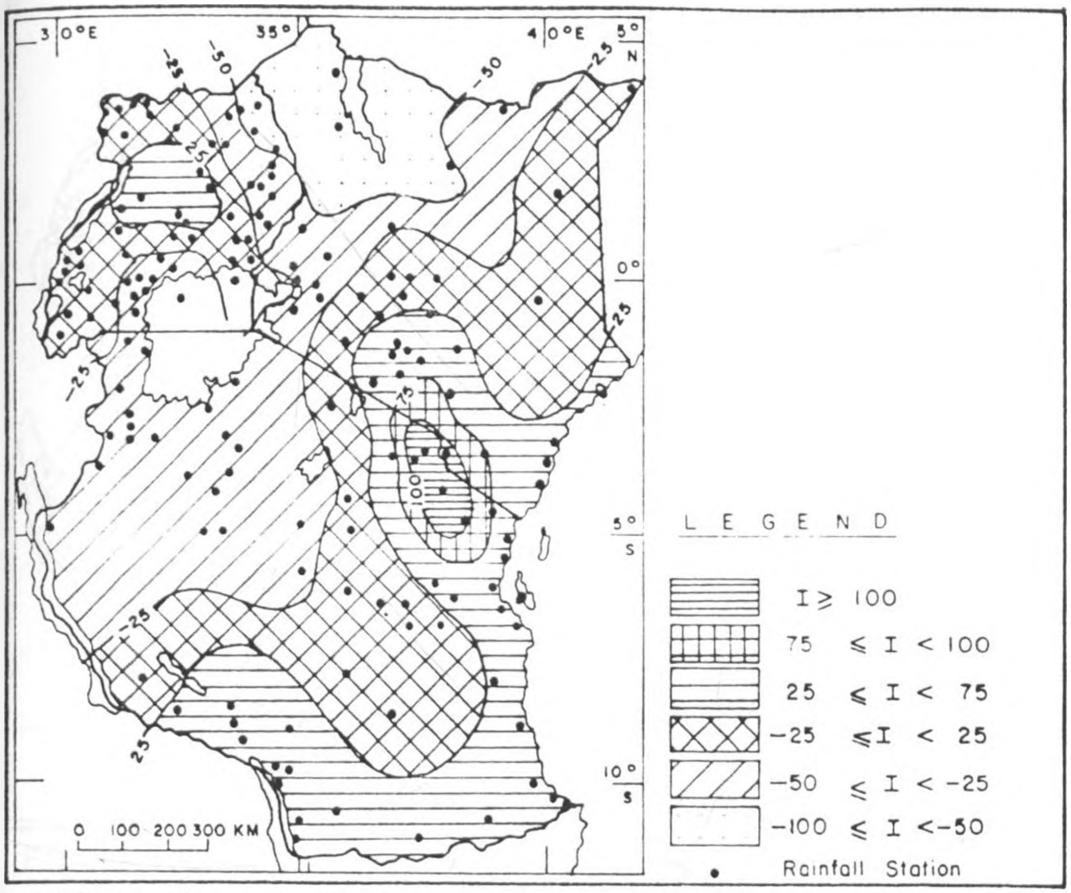

Fig. 10: Spatial patterns of wet/dry index during the season of September—November, 1990 (Normal Year) CAC 1993

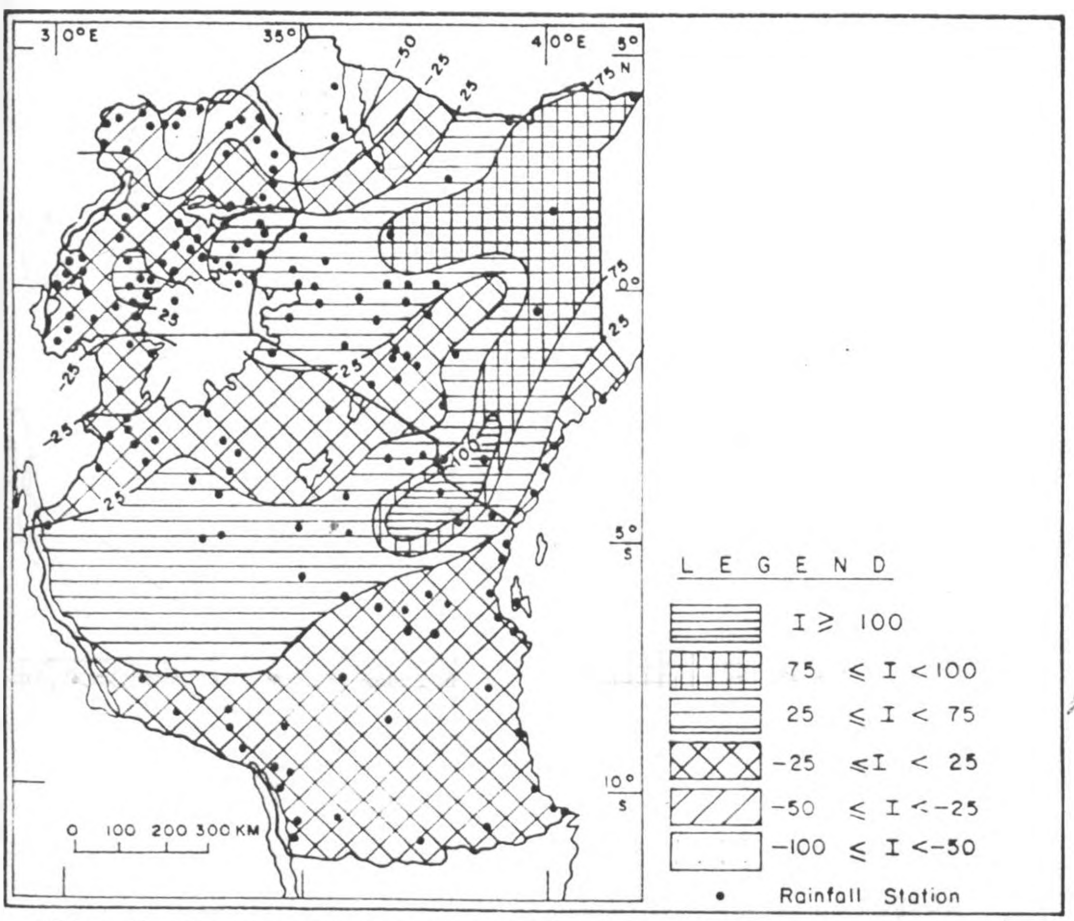

Fig. 11: Spatial patterns of wet/dry index during the season of March—May (Normal Year) CAC 1993

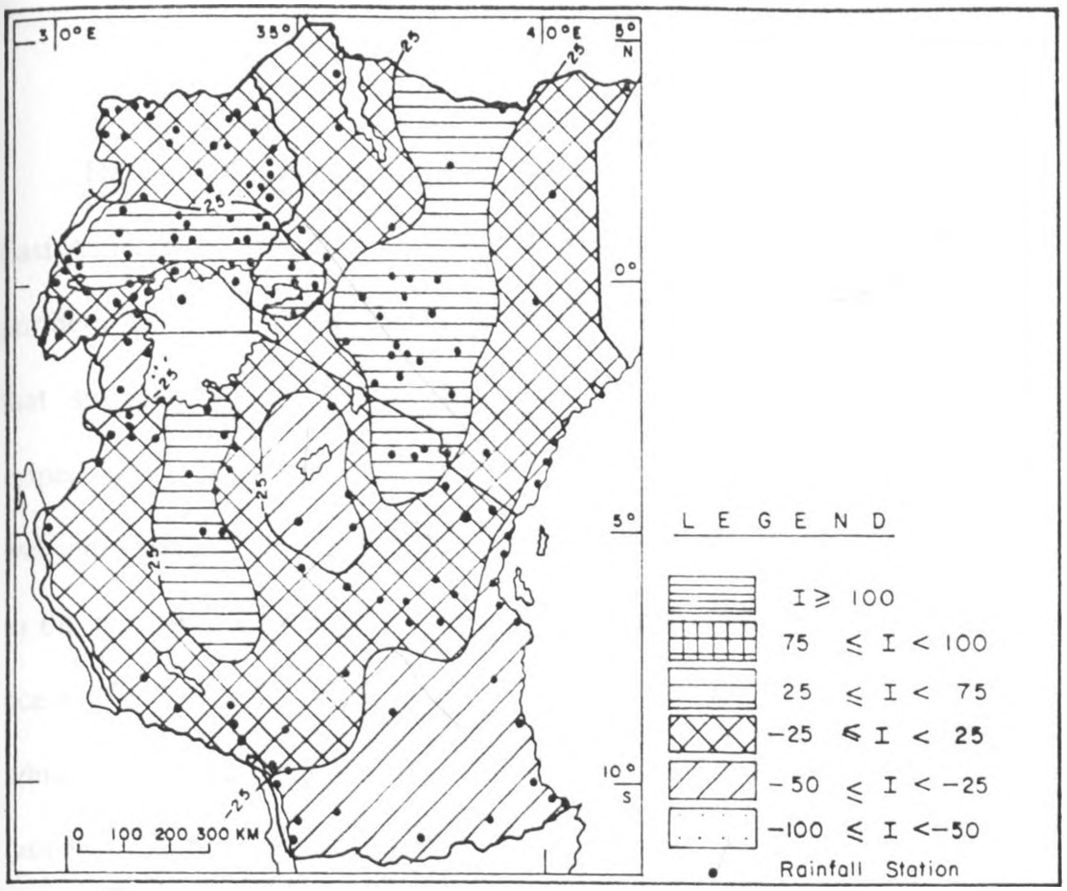

Fig. 12 : Spatial patterns of wet/dry index during the season of March — May, 1988 (Normal Year) CAC, 1993

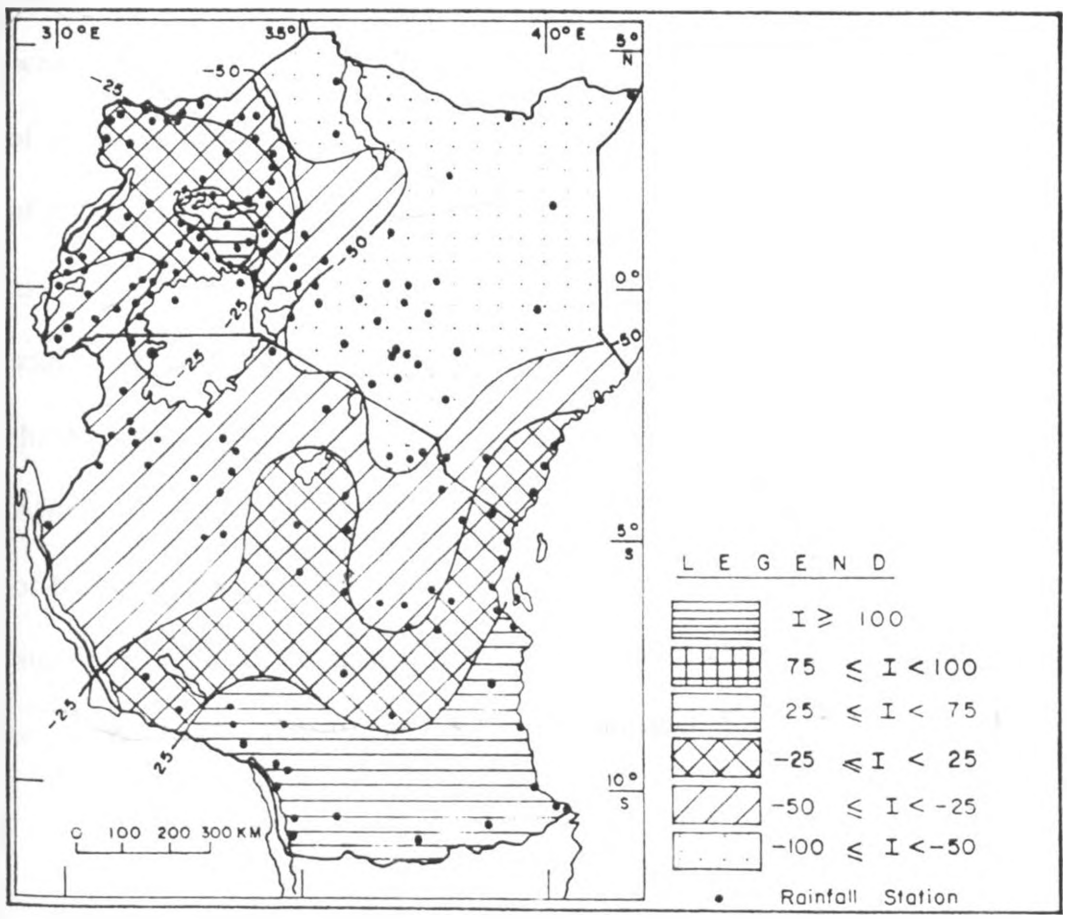

Fig. 13 : Spatial patterns of wet/dry index during the season of March — May, 1984 (La — Nina event)

He noted that anomalous low level easterlies/westerlies over the southern sector of East Africa were associated with wet index/dry index respectively. He observed that the northern sectors of East Africa also received moisture from Congo air mass. He further noted that stronger/weaker Walker circulations over equatorial Atlantic ocean/East Africa respectively enhanced eastward shift of ITCZ (meridional component) which would lead to wet index over western parts. The strength of the low level westerlies was therefore linked to the intensity of St.Helena which was also associated with cooling in southern Atlantic ocean. The intensities of the Mascarene and Arabian Highs were related to the Hadley cell which influenced the ITCZ (zonal). For example he observed northward shift of ITCZ (zonal) and associated wet index in 1986 due to northward shift of Arabian High during the long rains. However, wet index in 1981/1982, figure 7, during long rains was attributed to negative SSTs anomaly over tropical Pacific, tropical southern Atlantic, southern Indian oceans and positive SST anomalies over Arabian sea and central Indian ocean. The dry index of 1970 was attributed to warming over tropical Pacific , equatorial Atlantic and most parts of Indian oceans. Wet/dry indices over coastal regions/western parts respectively have been associated with warming over north-western Indian ocean which cause weakening of southwesteries during EL-Niño events. Generally, simultaneous warming in the positions of the Mascarene, Arabian and St.Helena Highs would lead to wide spread droughts in East Africa. The major patterns exhibited by the wet/dry indices were, however, the recurrence of high and low values. The next sections present the results from spectral analysis which attempted to detect the major periodic fluctuations which were exhibited by the indices.

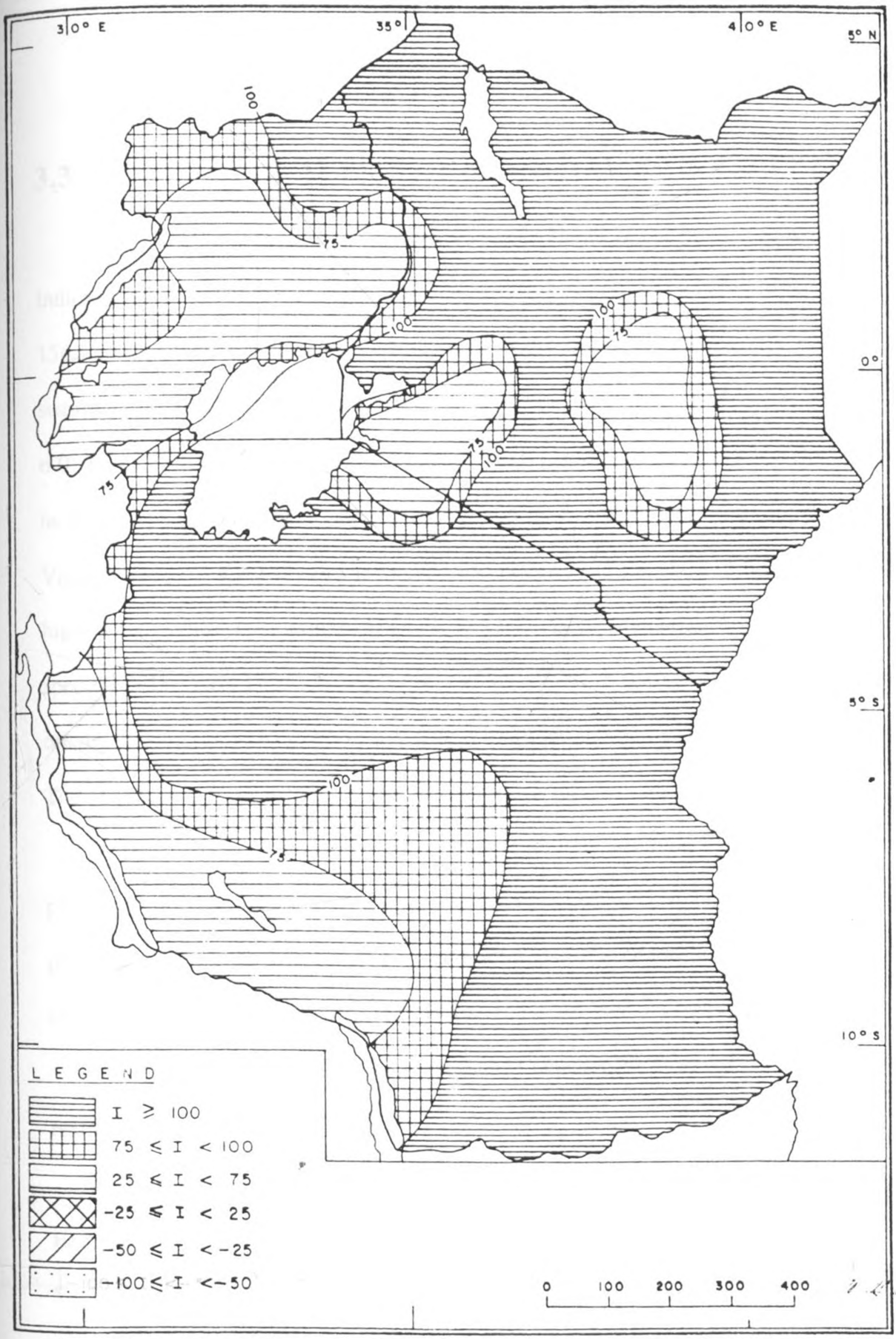

Fig. 14 : Spatial patterns of wet/dry index during the season of September — November, 1961 (Normal Year)

3.3 SPECTRAL ANALYSIS OF SEASONAL RAINFALL .

Spectral analysis for East African seasonal rainfall series for the period 1940-1990 indicated some unique spectral peaks in the seasonal rainfall time series. Figures 15(a) to 15(c) give some of the examples of the spectral peaks in seasonal rainfall. The results for the seasonal rainfall time series indicated dominant peaks in the period 2.2-2.8, 3.0-3.7, 4.9-6.0, 10-12.5 years. The periods of 2.2-2.8, 3.0-3.7 and 4.9-6.0 years were most dominant in all seasons and locations. The 10-12.5 year peak was more dominant in shores of lake Victoria and lake Kyoga . This peak was also dominant in the areas of high terrain (Kenya high lands, highlands in western Uganda, and regions near mountain Kilimanjaro). Similar spectral peaks have been observed by Ogallo (1988); Nyenzi et al. (1992), among many others. In this study white noise hypothesis was used to test the significance of the peaks. The statistical significance of the spectral peaks varied from one region to another.

The periodic fluctuations in the seasonal rainfall are related to fluctuations of the physical processes of the general circulation system Ogallo (1982). The general circulation parameters which have been noted to have some periodic fluctuations include the sunspot cycles, EL-Niño, southern oscillation index, and quasi-biennial oscillation (QBO).

In this study no test was made to examine whether the observed cycles are physically realistic.

The 2.2-2.8 year cycle has however been observed in the QBO. Relationship between East African rainfall and QBO has been observed by Ogallo et al.(1993). The 3.0-3.7 and 5-6 year cycles are common in the El-Niño-Southern oscillation index. Such cycles have also been observed in many other meteorological parameters over the region (Ogallo 1982,1984; Nyenzi 1992).

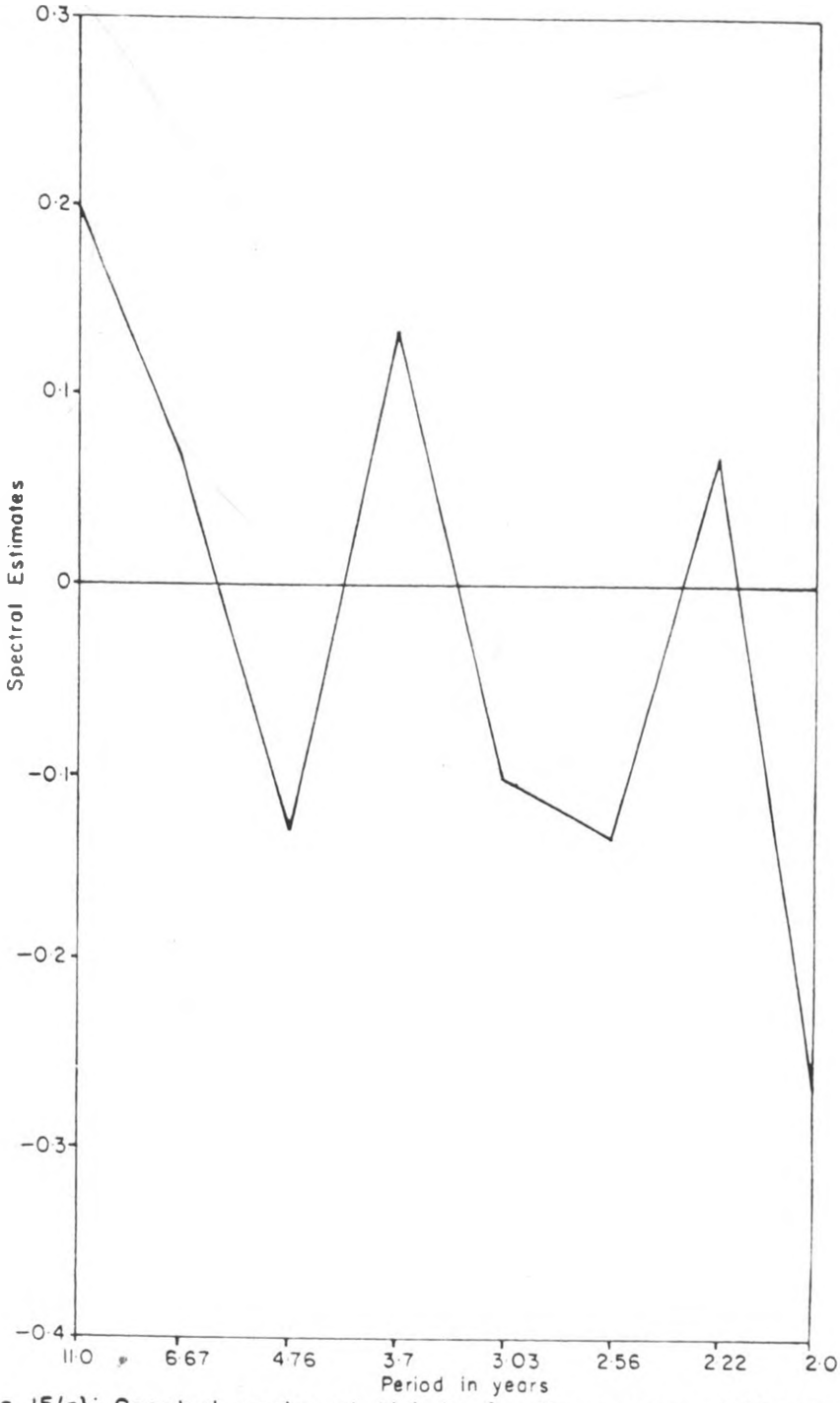

Fig. 15(a): Spectral peaks at Vukula for the season of March – May.

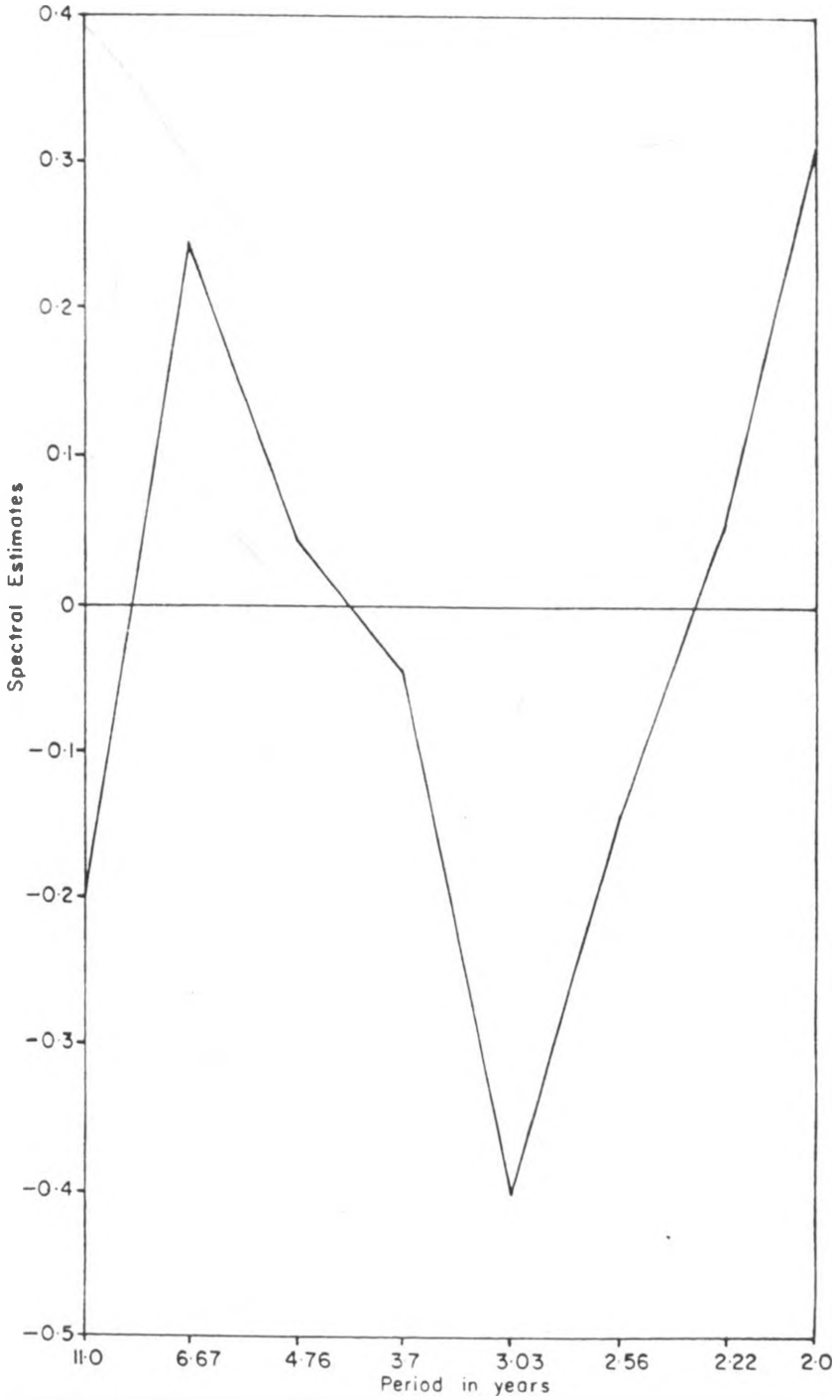

Fig. 15(b) : Spectral peaks at Embu for the season of September – November.

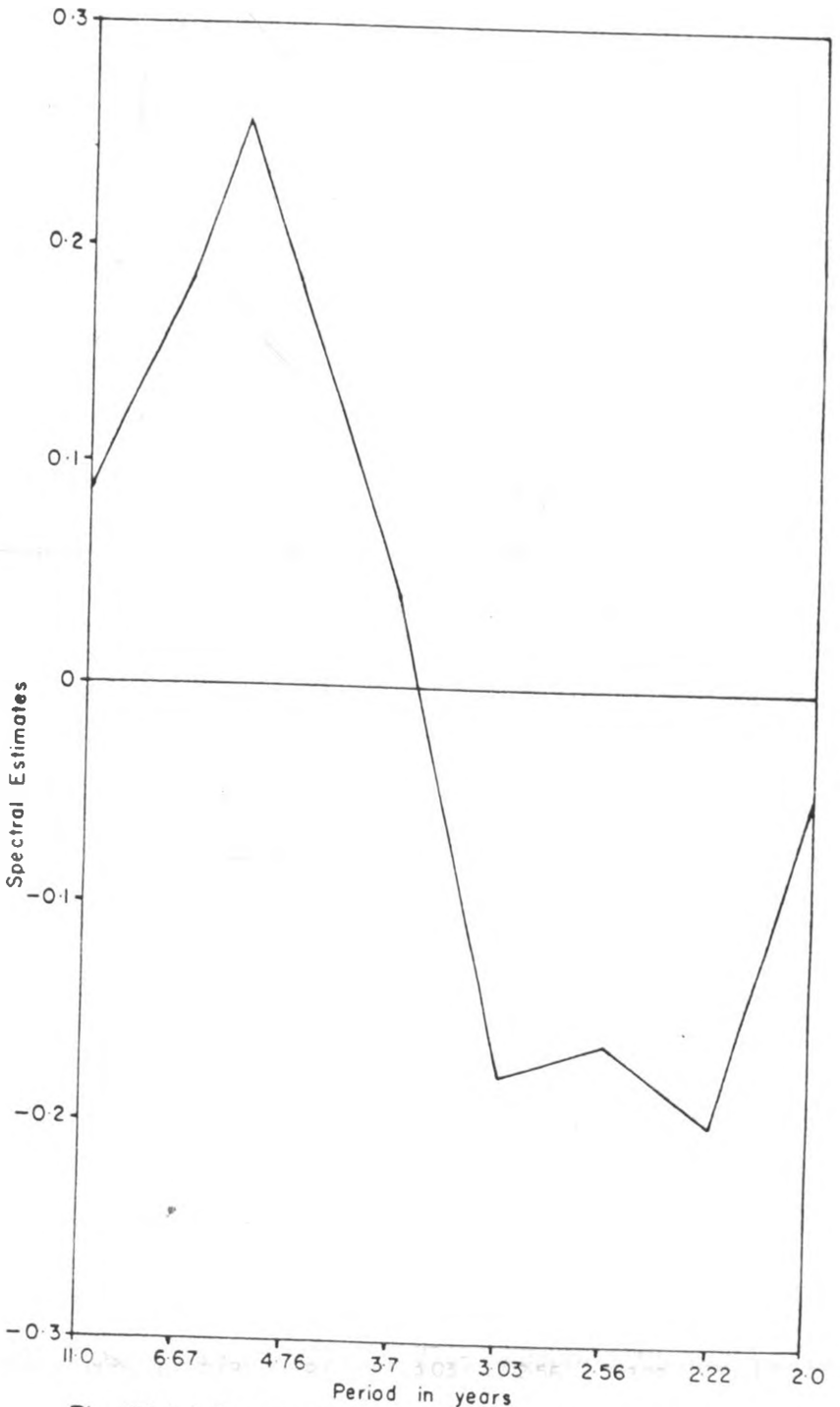

Fig.15(c) : Spectral peaks at Dar for the season of December – Februc

Cycles close to 11 years have been linked to solar cycles (Willet 1965; Deshpande 1967; Lawrence 1971).

3.4 TREND ANALYSIS .

The spearman rank correlation method which was discussed in section 2.4 was applied on the seasonal areal series in order to investigate existence of any systematic trends. The results from the study indicated that there were no significant trend in the seasonal time series at most of the locations. Examples of the time series without significant trends are given in figures 16(a)-16(b) while figures 16(c) and 16(d) give examples of positive trends. It should however be noted that the locations with significant trends were randomly distributed since most of the neighbouring regions did not show significant trends. Therefore, the observed trends may not be attributed to any systematic regional or large scale climate systems. Localized trends have been associated with urbanization, changes in surface parameters eg deforestation and overgrazing,heterogeneity in the data among many other factors. Similar results have been obtained by (Rodhe and Virji,1976; Ogallo,1980,1982). No attempts were made here to investigate the causes of the observed trends in few rainfall time series.

3.5.0 PRINCIPAL COMPONENT ANALYSIS.

The complex nature of the space-time characteristics of rainfall have been highlighted in the last few sections. In this section an attempt was made to use Empirical Orthogonal Functions (EOF) to cluster the observed patterns of rainfall variability. The EOF models used in this study were derived from rotated Principal Component Analysis Solutions.

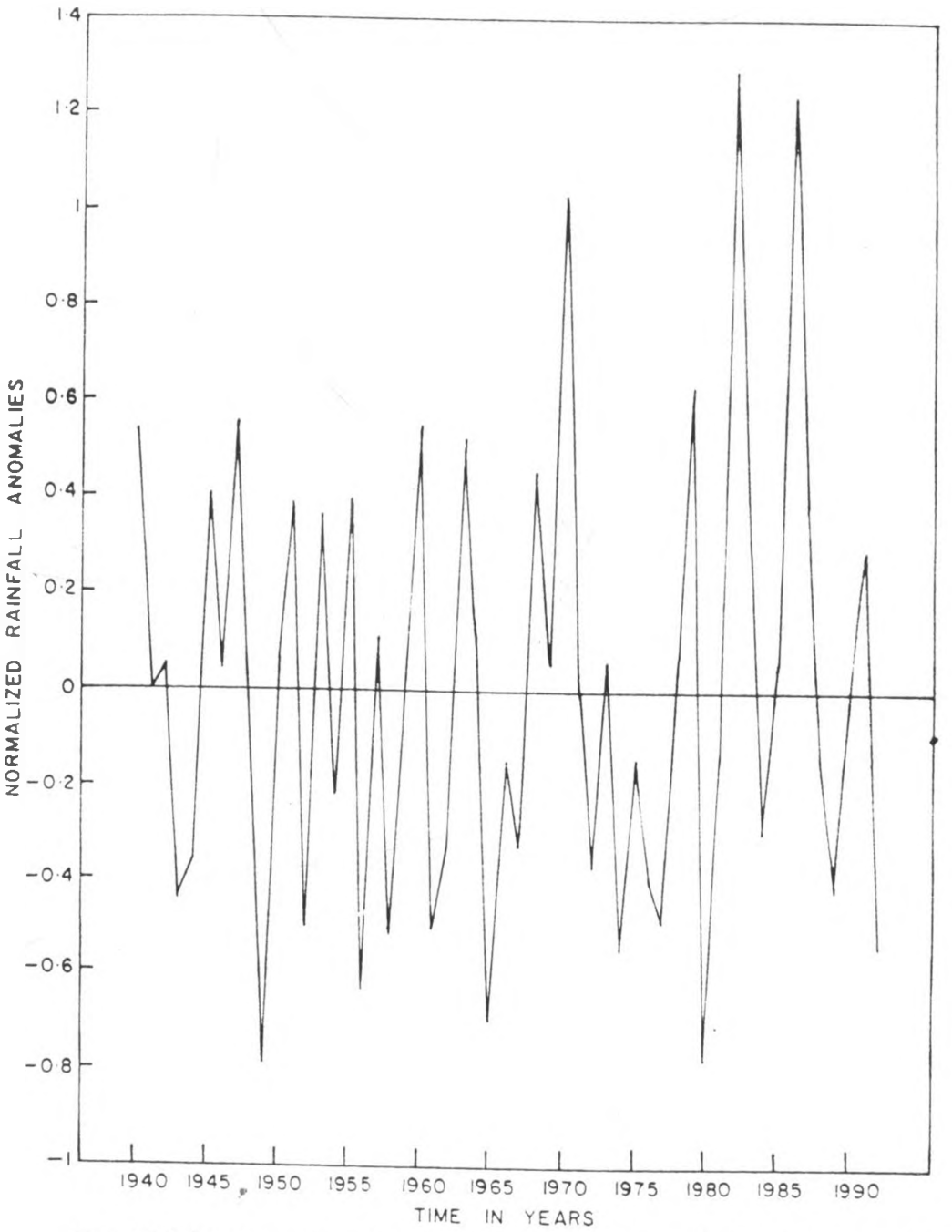

Fig. 16(a) : Example of no significant seasonal trends, zone 25 for March – May season.

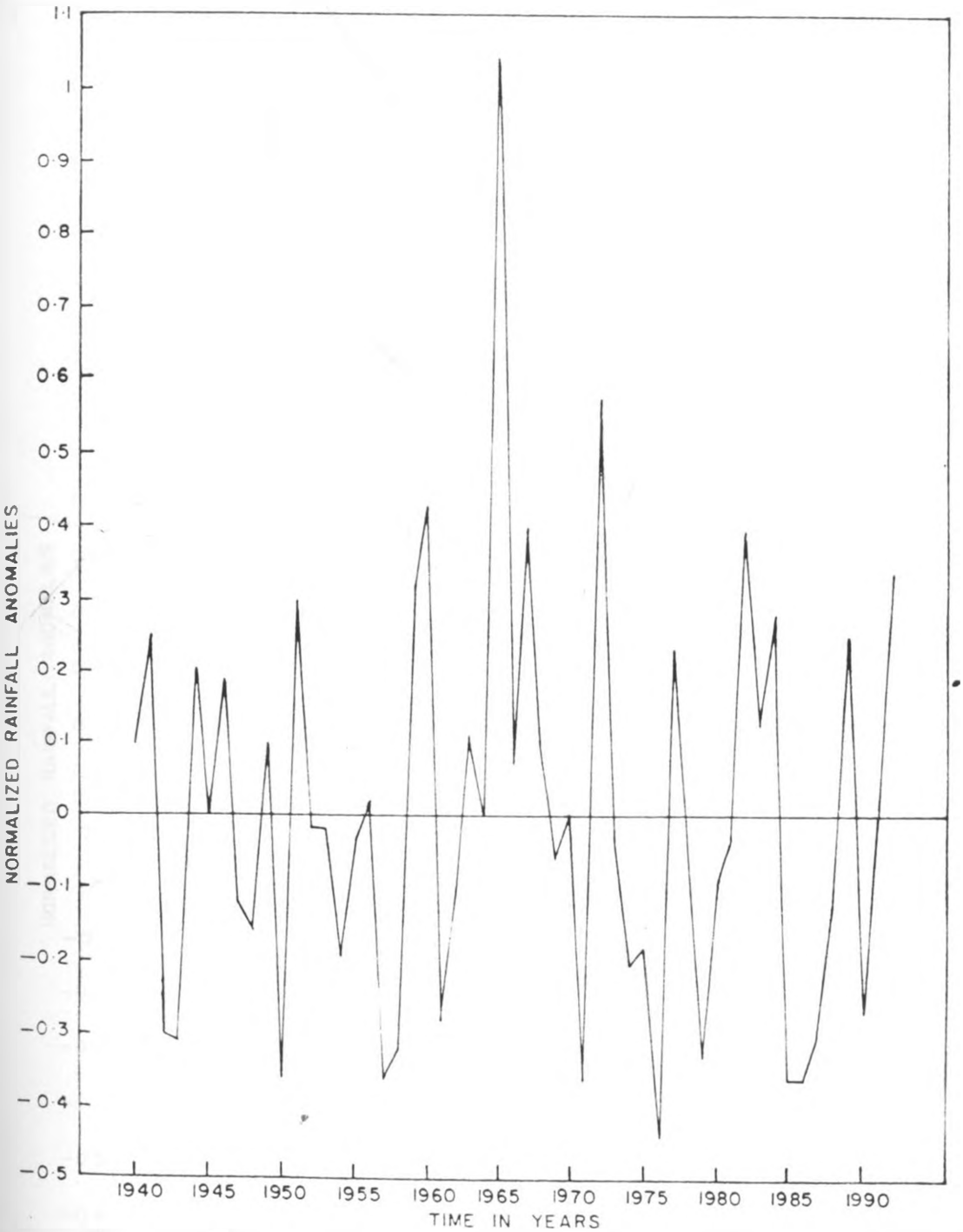

Fig. 16(b) : Example of no significant seasonal trends, zone 33 for September—November season.

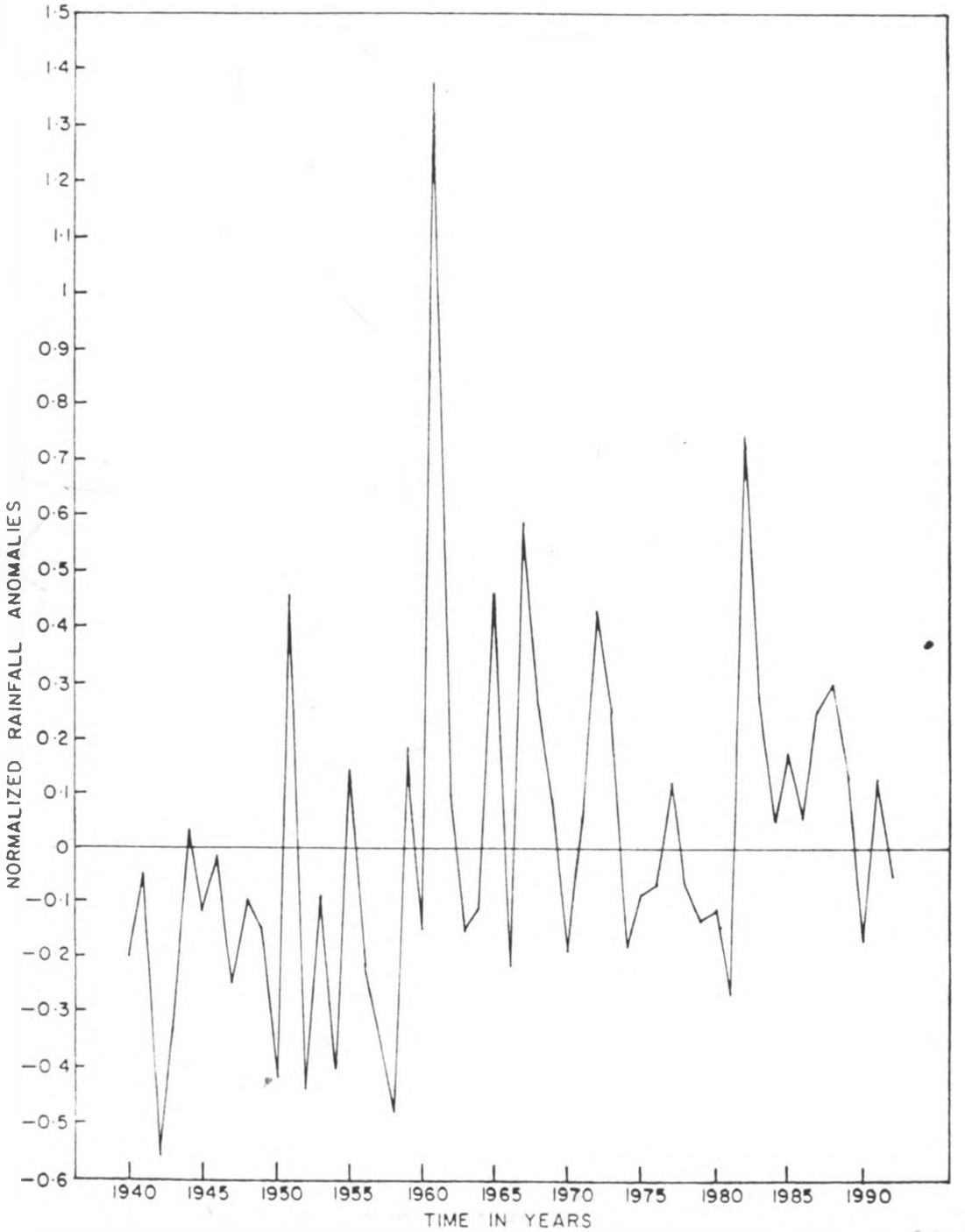

Fig. 16(c) : Example of positive seasonal trends, zone 34 for September – November season.

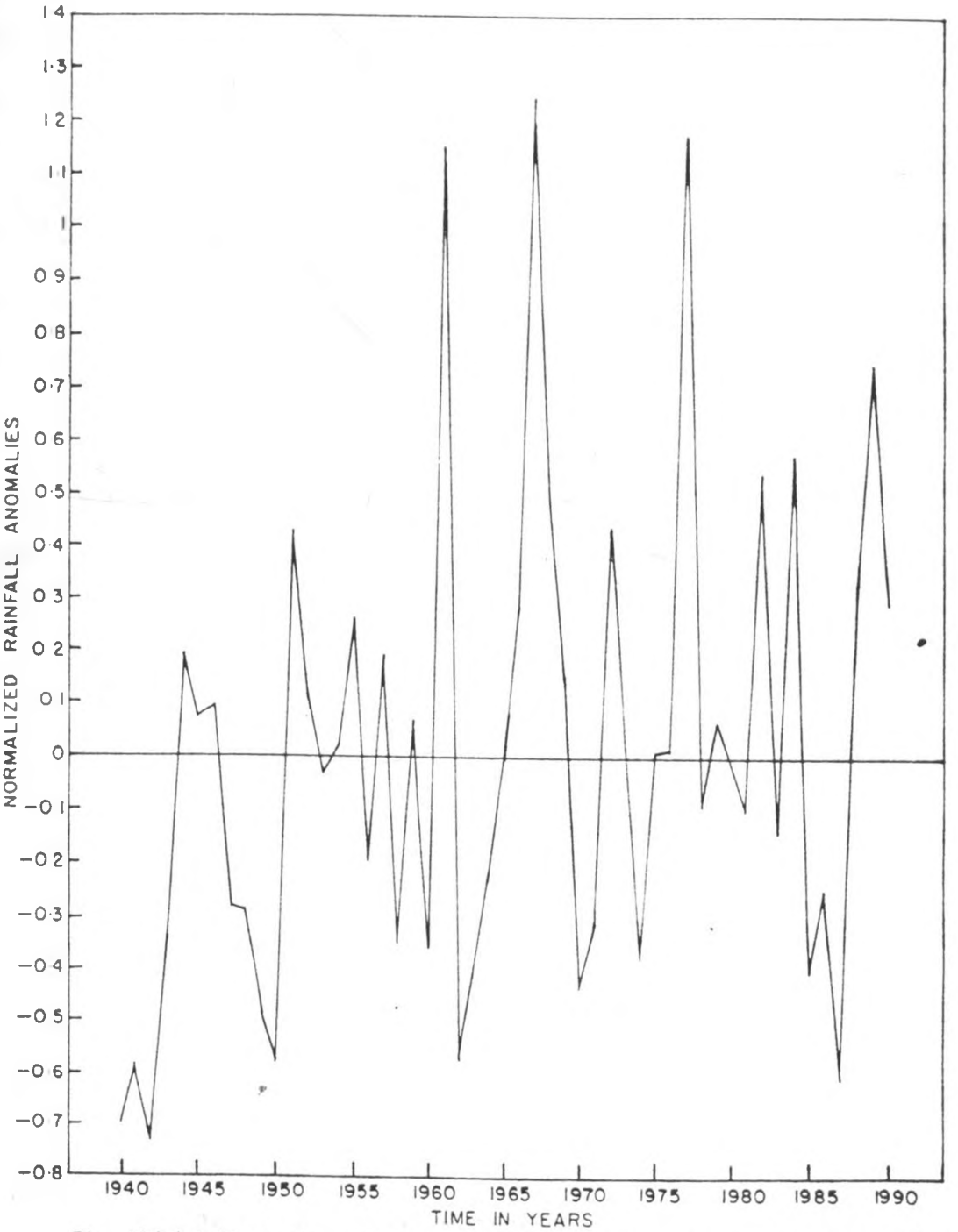

Fig. 16(d) : Example of seasonal positive trends, zone 31 for September—November season.

Under this method rotated principal components (RPCA) for each of the rainfall seasons within the period 1940 to 1975 were used to delineate the unique spatial patterns of the observed rainfall variability. Relationships with the dominant SST seasonal RPCA modes were also determined.

Results from sampling error technique which was used to test the statistical significance of the various components are included in tables 3 to 7. Other tests include the Scree test, Kaiser's criteria and logarithm of eigen vectors (LEV). Typical examples of the results from the LEV and Scree test are given in figures 17(a) and 17(b) respectively. From figure 17(a), its discernable that the Kaiser criteria extracted 19, 29, 32, 34 and 28 factors from the annual, December-February, March-May, June- August and September - November time series respectively. Although four tests were used in this study, the Scree test seemed to have produced the most consistent results. The number of significant components delineated by this method however was not significantly different from those which were delineated by the sampling and LEV methods.

Table 3: Summary of the RPCA results for the annual rainfall time series .

RPCA mode NO.	% variance accounted for	% cumulative variance	sampling error
1	67.5	67.5	23.9
2	7.3	74.8	2.6
3	3.4	78.2	1.2
4	2.6	80 8	1.0
5	2.3	83.1	0.8*
6	2.0	85.2	
7	1.8	87.0	
8	1.5	88.5	
9	1.4	89.9	
10	1.3	91.2	

* Truncation point of significant modes extracted by random error test. + significant modes extracted by Scree test = 5

Table 4: Summary of RPCA results for March-May season.

RPCA mode NO.	% variance accounted for	% cumulative variance	sampling error test
1	26.7	26.7	8.5
2	8.5	35.2	2.7
3	6.7	41.9	2.1
4	6 3	48.2	2 0*
5	6.0	54.2	
6	5.3	59 5	
7	4.4	63.9	
8	3.6	67.5	
9	3.5	71.0	
10	3.4	74.4	

* Truncation point of significant modes extracted by the random error test. + Significant modes extracted by Scree test = 4

Table 5: Summary of RPCA for June-August season.

RPCA mode No.	% variance accounted for	% cumulative variance	sampling error test
1	14.1	14.1	4.4
2	12 6	26.7	3.9
3	9.1	35.8	2.8*
4	6.8	42.6	
5	5.8	48.4	
6	5.3	53.7	
7	5.0	58.7	
8	4.3	63.0	
9	4.2	67.2	
10	4.0	71.2	

* Truncation point of significant modes extracted by sampling error test. + Significant modes extracted by Scree test = 4

Table 6: Summary of RPCA for November-September season.

RPCA mode No.	% variance accounted for	%cumulative variance	sampling error test
1	45.7	45.7	15.5
2	7.6	53.3	2.6
3	7.3	60.6	2.6
4	5.1	65.7	1.7*
5	3.7	69.4	
6	3.3	72.7	
7	2.9	75.6	
8	2.7	78.3	
9	2.6	80.9	
10	2.3	83.2	

* Truncation point of significant modes extracted by the random error test. + Significant modes extracted by Scree test = 4

Table 7: Summary of RPCA for December-February season.

PRCA mode No.	% variance accounted for	% cumulative variance	sampling error test
1	37.1	37.1	12.4
2	9.5	46.6	3.2
3	6.2	52.8	1.9
4	4.6	57.4	1.5*
5	4.4	61.8	
6	3.9	65.7	
7	3.8	69.5	
8	3.7	73.2	
9	3.2	76.4	
10	3.0	79.4	

4* Truncation point of significant modes extracted by random error test. + Significant modes extacted by the Scree test = 3

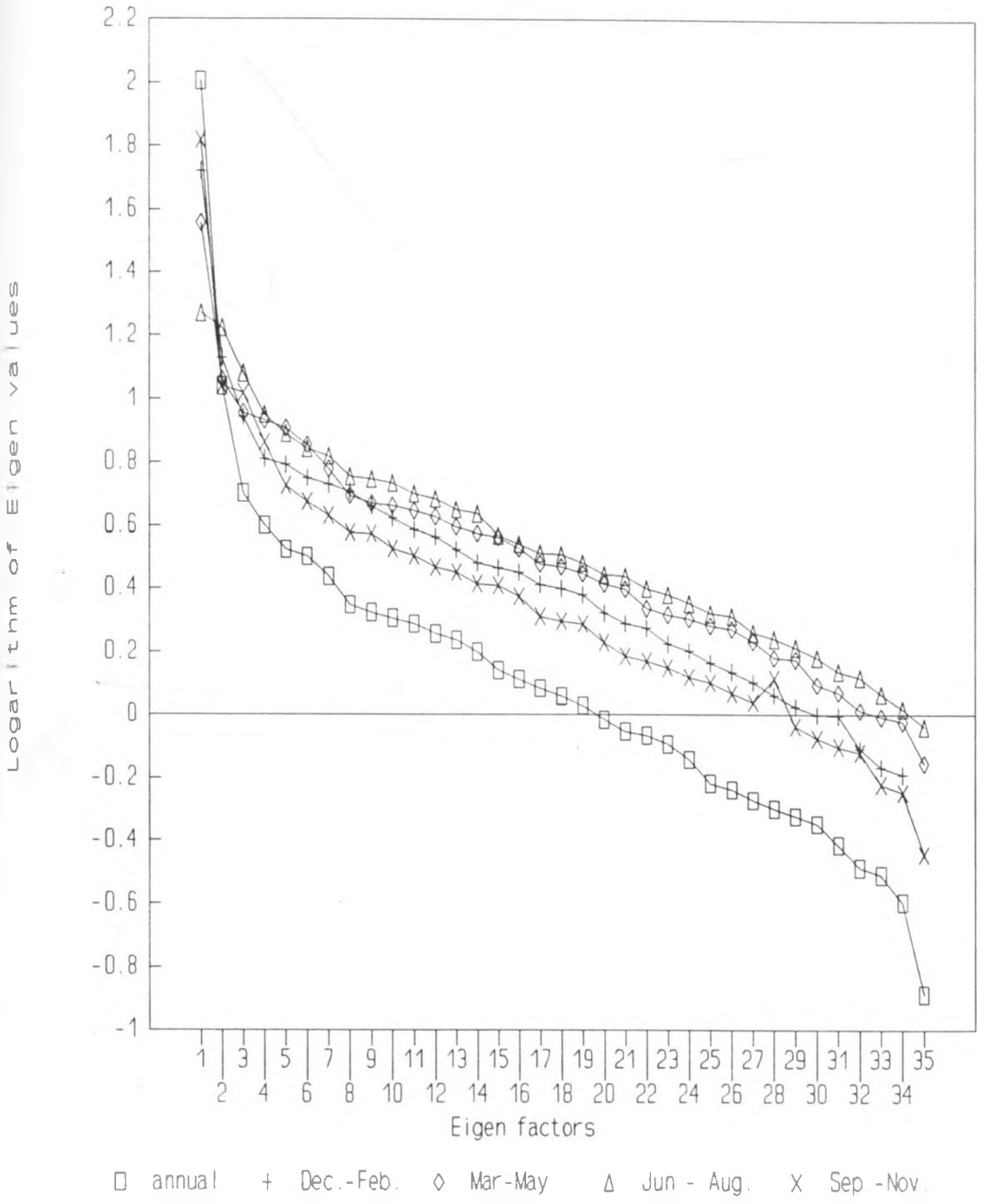

Figure 17a : dominant eigen factors (logarithm method)

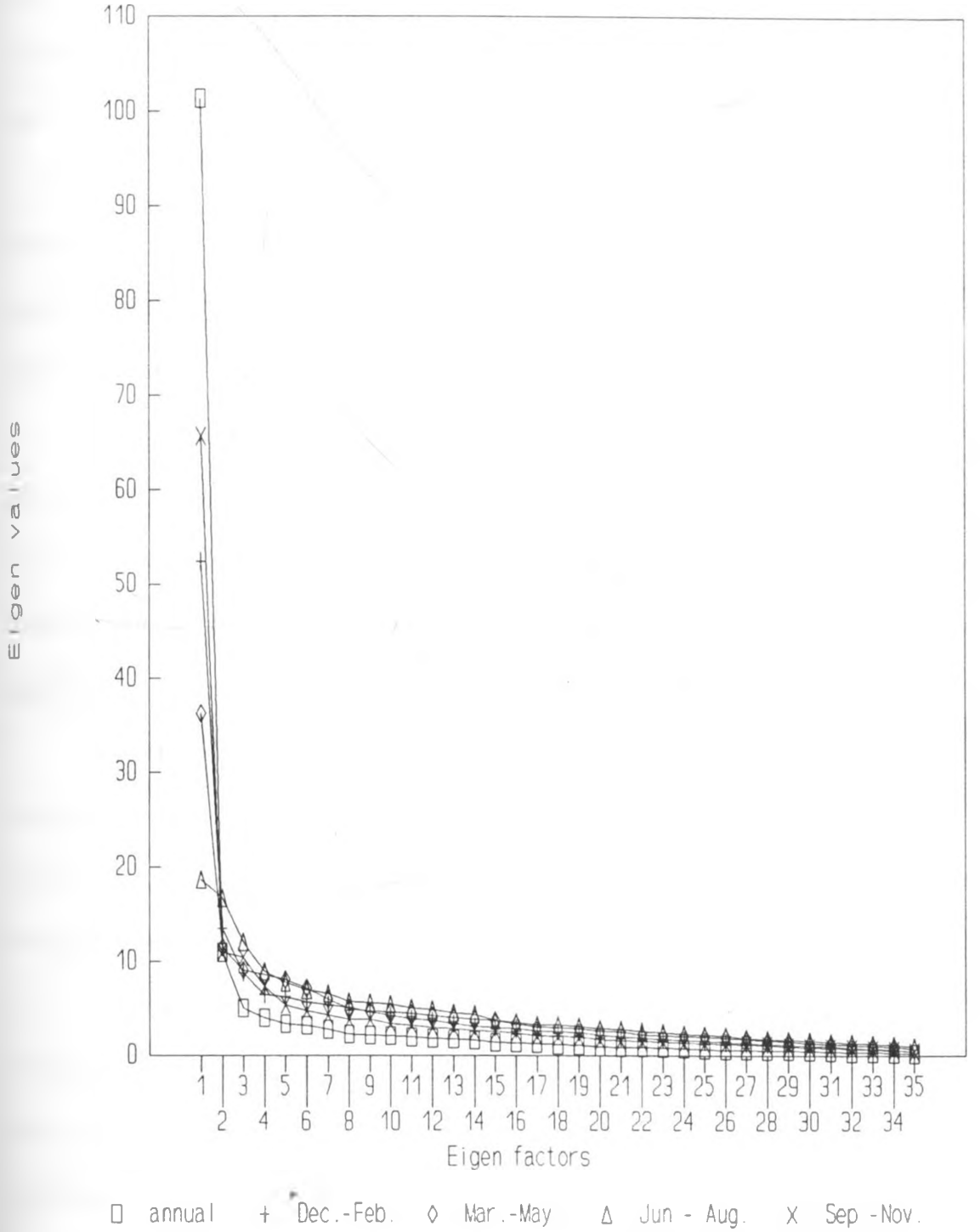

Figure 17b: dominant eigen factors (scree test)

Apart from Kaiser criteria, the other tests indicated that a maximum of about five principal component-modes were significant for the annual rainfall time series (table 3 and figure 17(a) and 17(b).

The March-May is the long rainfall season for the whole of East Africa. During this season, four principal component modes were significant. The first four components together accounted for a total variance of 48.2% of the seasonal variance with the first, second, third and fourth explaining 26.7%,8.5%, 6.7% and 6.3% respectively (table 4).

The spatial patterns of some of the significant RPCA modes are shown in figures 18(a)-18(d). Figure 18(a) shows the spatial patterns of first component during this season. It is dominant over the Kenya highlands, mountains (Ruwenzori, Moroto, Elgon) and southwestern highlands of Uganda. The northern part of the Indian ocean coastline also indicated significant positive loadings.

Figure 18 (b) shows the spatial patterns of second component which had maximum loadings over central Tanzania, northeastern Kenya, and northwestern Tanzania during this season. The third component indicated maximum loadings over northeastern Tanzania during this season and its spatial patterns are given by figure 18(c).

Maximum positive loadings and maximum negative loadings of the fourth component were indicated over on the coastal strip and near lake Tanganyika respectively as shown in figure 18(d). June-August is generally a dry season for most locations except for northern and eastern Uganda as well as western regions which receive substantial rainfall during this season due to moist westerly incursions. The lake basin gets occasional rainfall due to the influences of lake Victoria and lake Kyoga. The coastal strip also gets substantial rainfall due to the East African low level Jet. Table 5 showed that during June-August, the four (4) components were also significant .

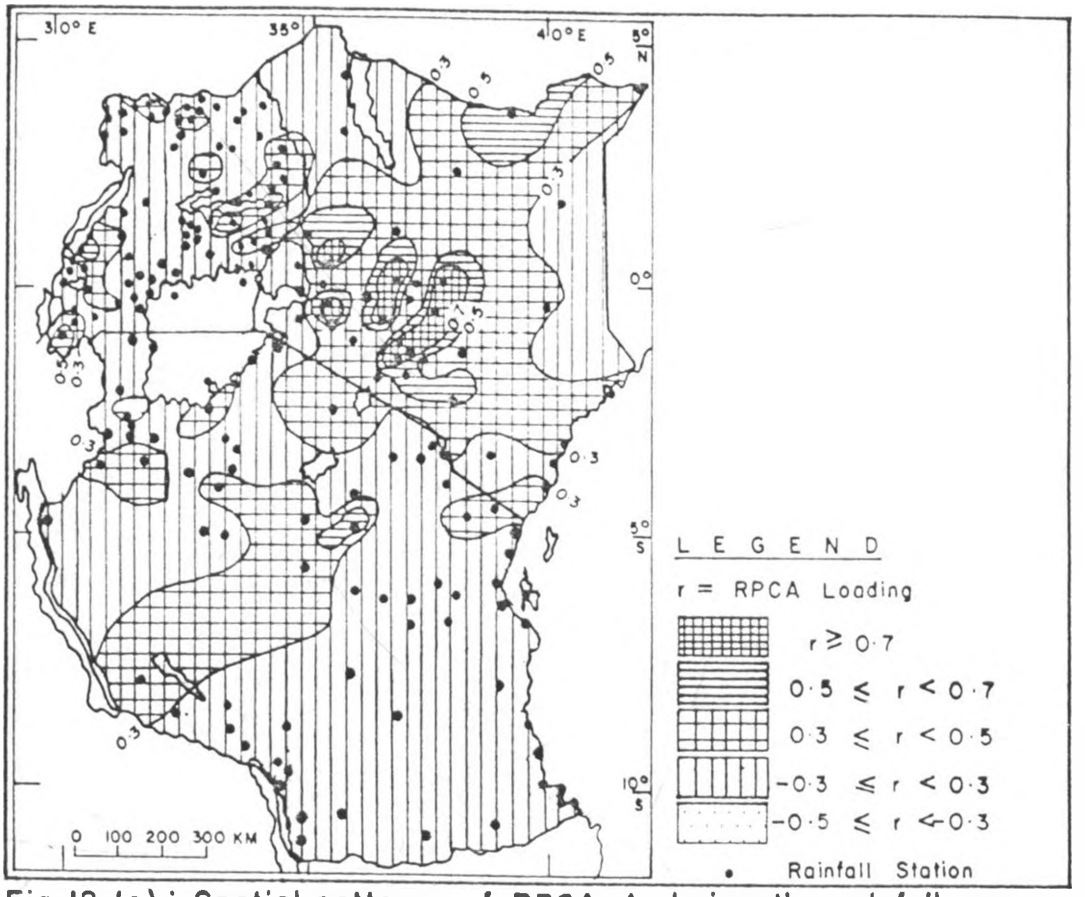

Fig.18 (a) : Spatial patterns of RPCA 1 during the rainfall season of March — May

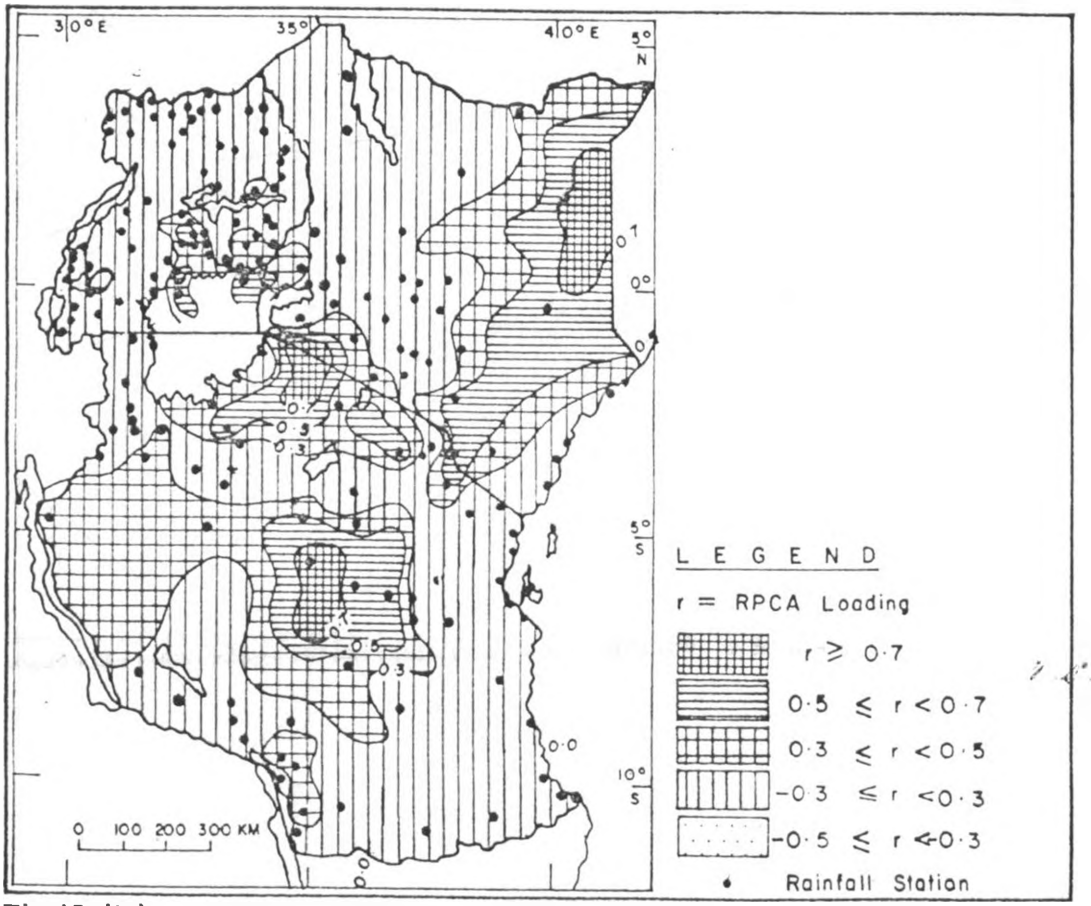

Fig.18 (b) : Spatial patterns of RPCA 2 during the rainfall season of March — May

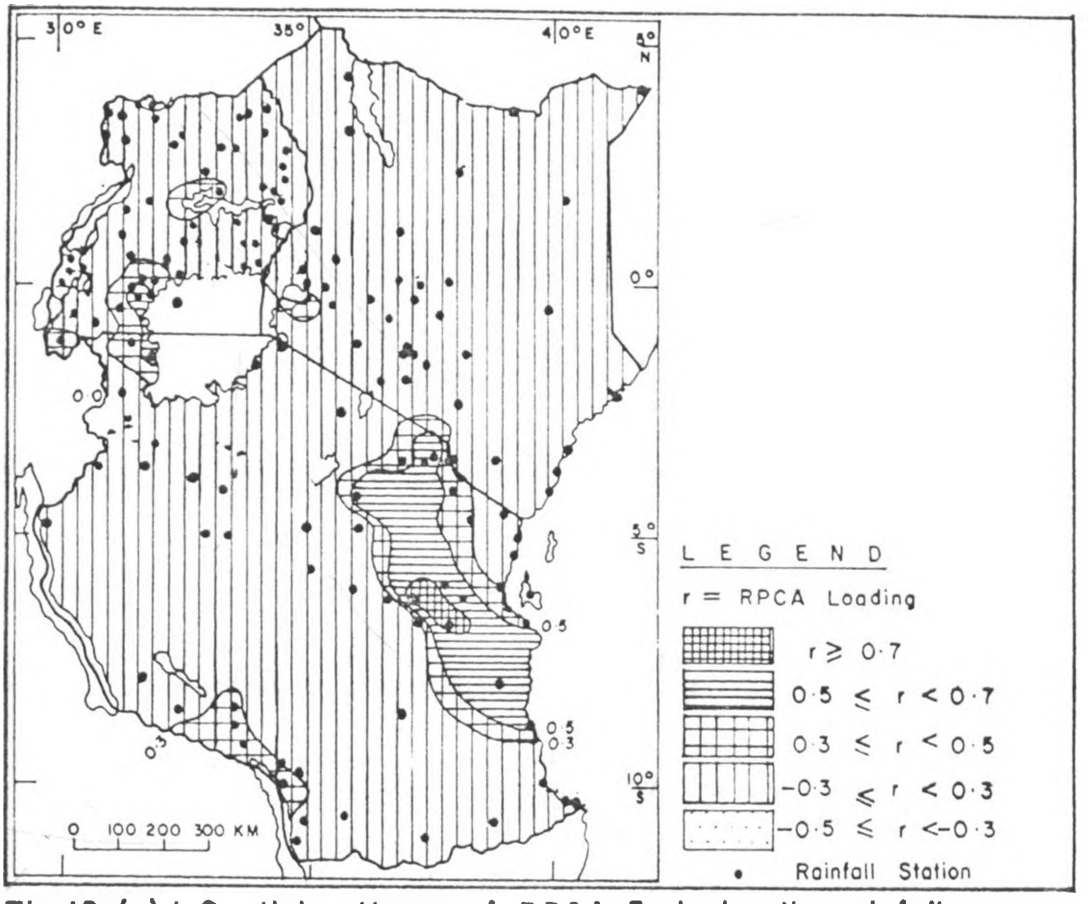

Fig. 18 (c) : Spatial patterns of RPCA 3 during the rainfall season of March — May

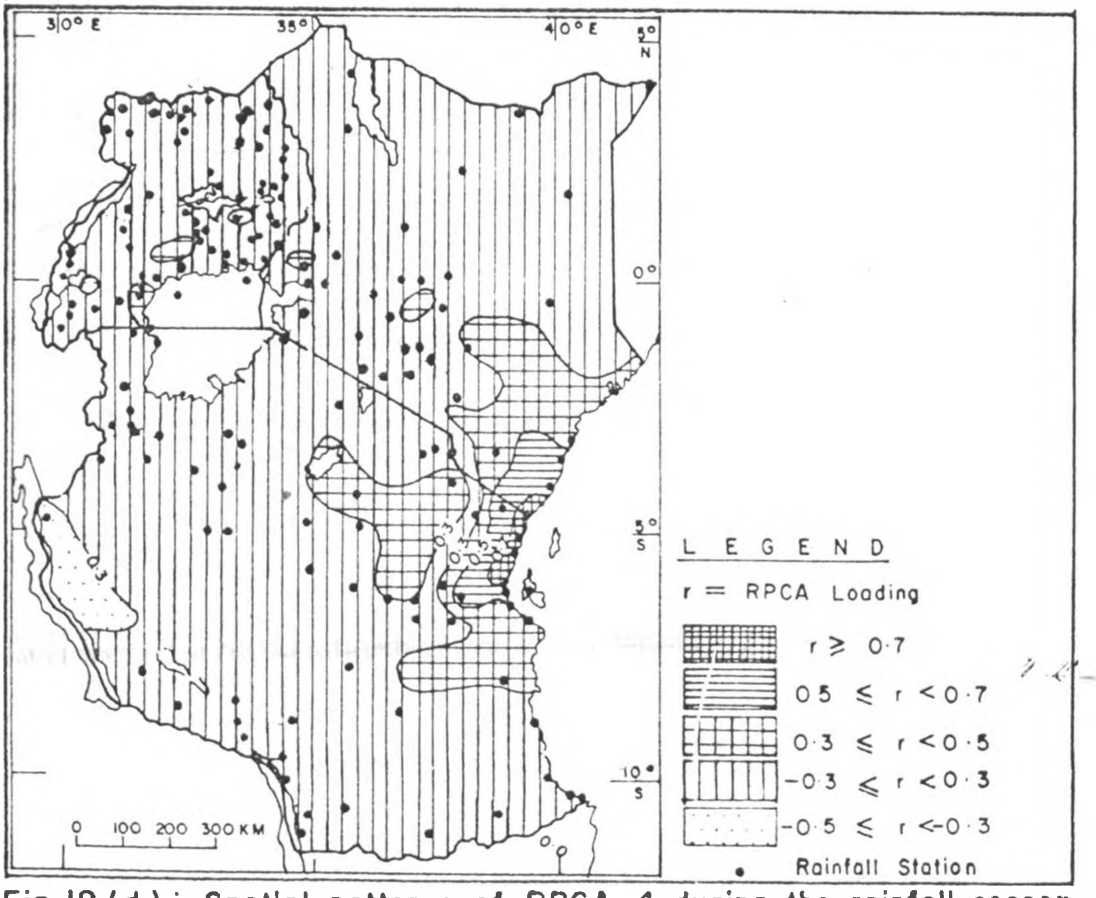

Fig. 18 (d) : Spatial patterns of RPCA 4 during the rainfall season of March — May

These accounted for about 42.6% of the seasonal total variance with the first, second, third and fourth components each accounting for 14.1%, 12.6%, 9.1% and 6.8% of total variance respectively. The spatial patterns of these components are shown in figures 19(a) to 19(d). Figure 19(a) highlights the spatial patterns of the first mode during this season. Maximum loadings were centered over the coastal strip . This seems to indicate a manifestation of the potential influence of East African low level jet during this season.

The second component indicated maximum positive loadings over northern and western Uganda as shown in Figure 19(b). Eastern Uganda and Western Kenya including some parts of the rift valley also indicated significant factor loadings during this season. The second component seems to highlight the impacts of westerly incursions into western parts during this season Anyamba (1983); Ogallo (1988) among several others.

The spatial patterns of third component are given in Figure 19(c) and maximum positive loadings were centered over the eastern rift valley in Kenya highlands. The maximum loadings in central Tanzania seem to indicate the general dry conditions during this season.

Maximum positive loadings over northwestern Tanzania and spreading to southwestern shores of lake Victoria show the spatial patterns of fourth component during this season as indicated in figure 19(d). This also seems to give a manifestation of westerly incursions into East Africa Anyamba et al. (1985) among several others.

September-November is the short rainfall season for the whole of East Africa. The first four modes during this season accounted rainfall variance of 45.7%, 7.6%, 7.3% and 5.1% respectively . The spatial patterns of some of these modes are shown in figures 20(a)-20(d).

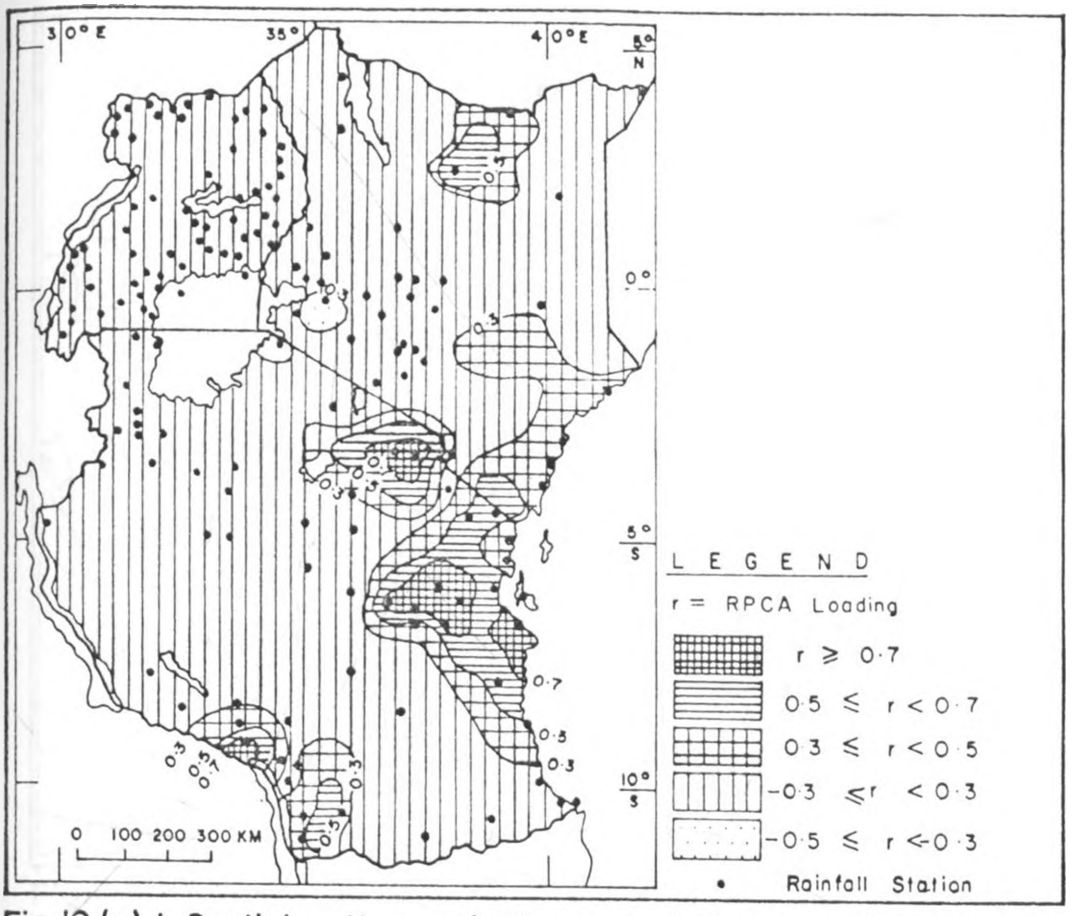

Fig.19 (a) : Spatial patterns of RPCA 1 during the rainfall season of June — August

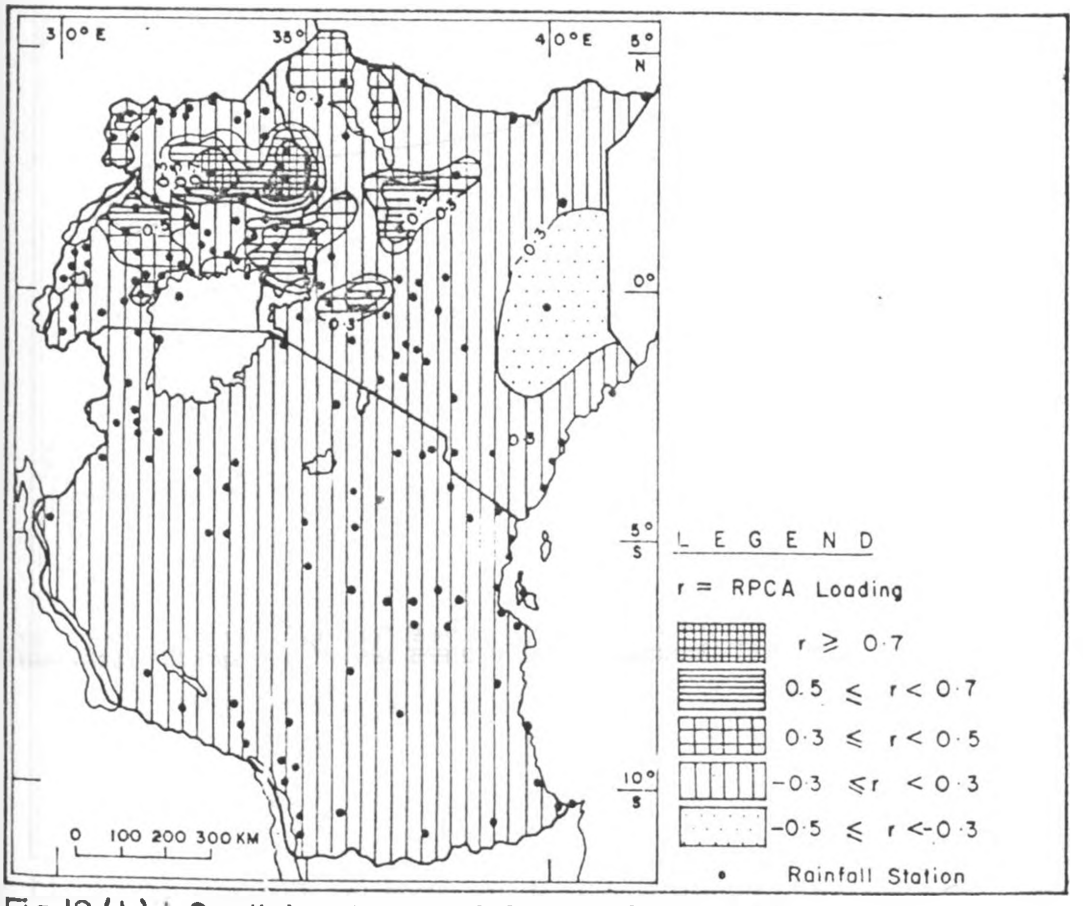

Fig.19 (b) : Spatial patterns of RPCA 2 during the rainfall season of June — August

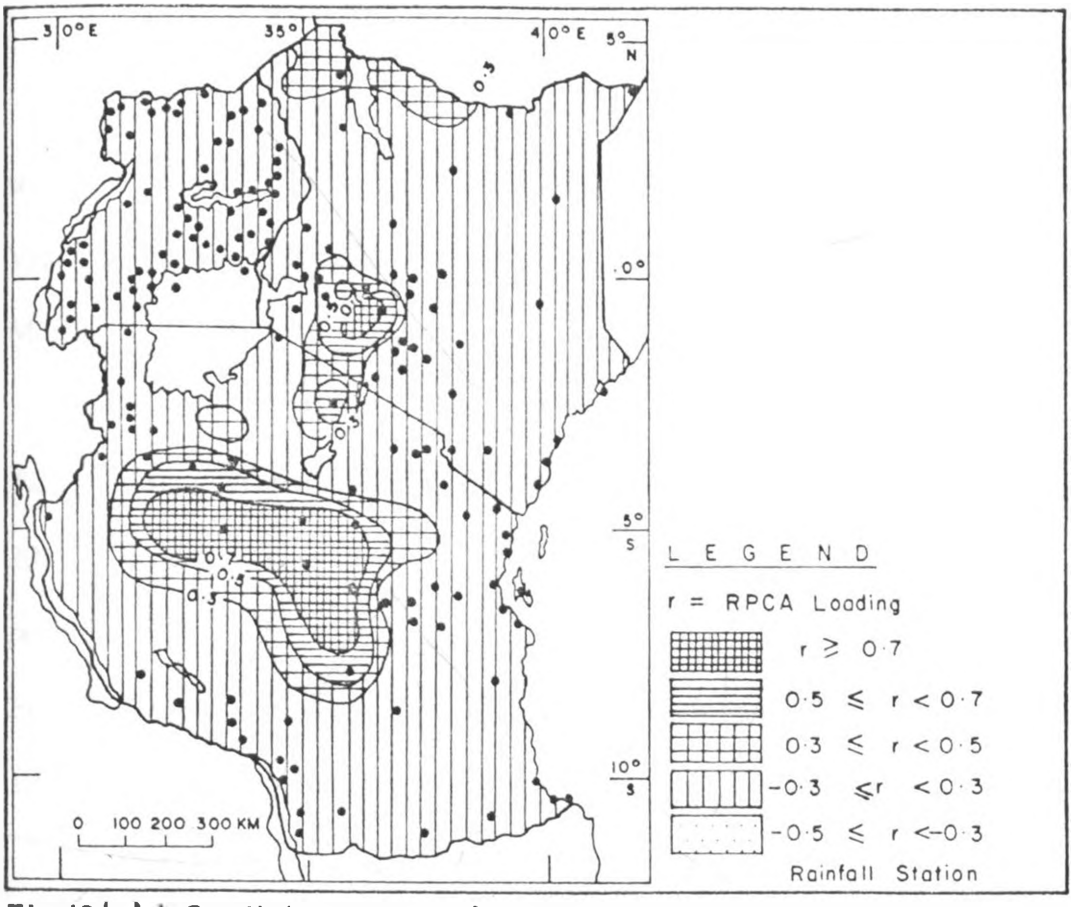

Fig.19(c) : Spatial patterns of RPCA 3 during the rainfall season of June — August

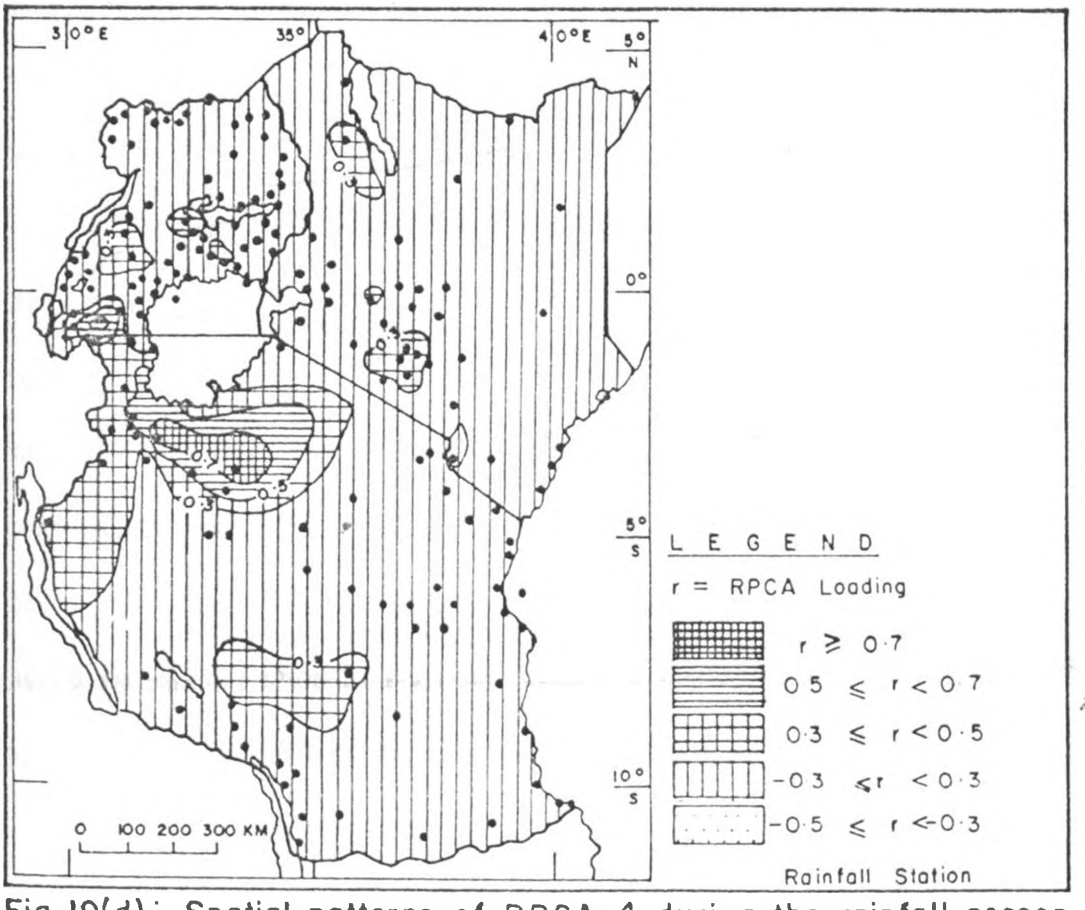

Fig.19(d) : Spatial patterns of RPCA 4 during the rainfall season of June — August

Figure 20(a) gives the spatial patterns of the first mode which is reflective of the mean seasonal rainfall pattern during the short rains which is generally concentrated over the Lake Victoria, the Indian Ocean, mountains (kilimanjaro, kenya, southern Tanzania ranges, Moroto, Ruwenzori,and Elgon) regions.

Central Uganda, western Kenya, northwestern Tanzania and highlands in southern Tanzania were covered by the spatial patterns of the second component as shown in figure 20(b). The second component seems to represent the movement of ITCZ as the zone of positive factor loadings shifts from southern Tanzania during the season of December-February, figure 21(b) and to northern Uganda during the season of June - August figure 19(b) and September-November figure 20(b).

Figure 20(c) gives the spatial patterns of the third component. Maximum loadings were centered over central Tanzania which again seems to give a manifestation of active zones of ITCZ during this season. Figure 20(d) gives the spatial patterns of the fourth component. The maximum loadings appeared over Kenyan highlands east of the rift valley while some locations indicated positive loadings in Uganda.

The season of December-February had the least number of significant factors (only 3). Apart from southern Tanzania as well as coastal strip and parts of lake region which receive rainfall during this season, the rest of East Africa experiences dry spells. The rainfall during this season is attributed to the activities of ITCZ in the southern sector and meso-scale circulations associated with land-sea interactions. These three RPCAS accounted for 52.8% of the seasonal rainfall total variance with the first, second and third accounting for 37.1%, 9.5% and 6.2% of the total variance respectively (table 7). The spatial patterns of some of the significant modes are shown in figures 21(a)-21(d).

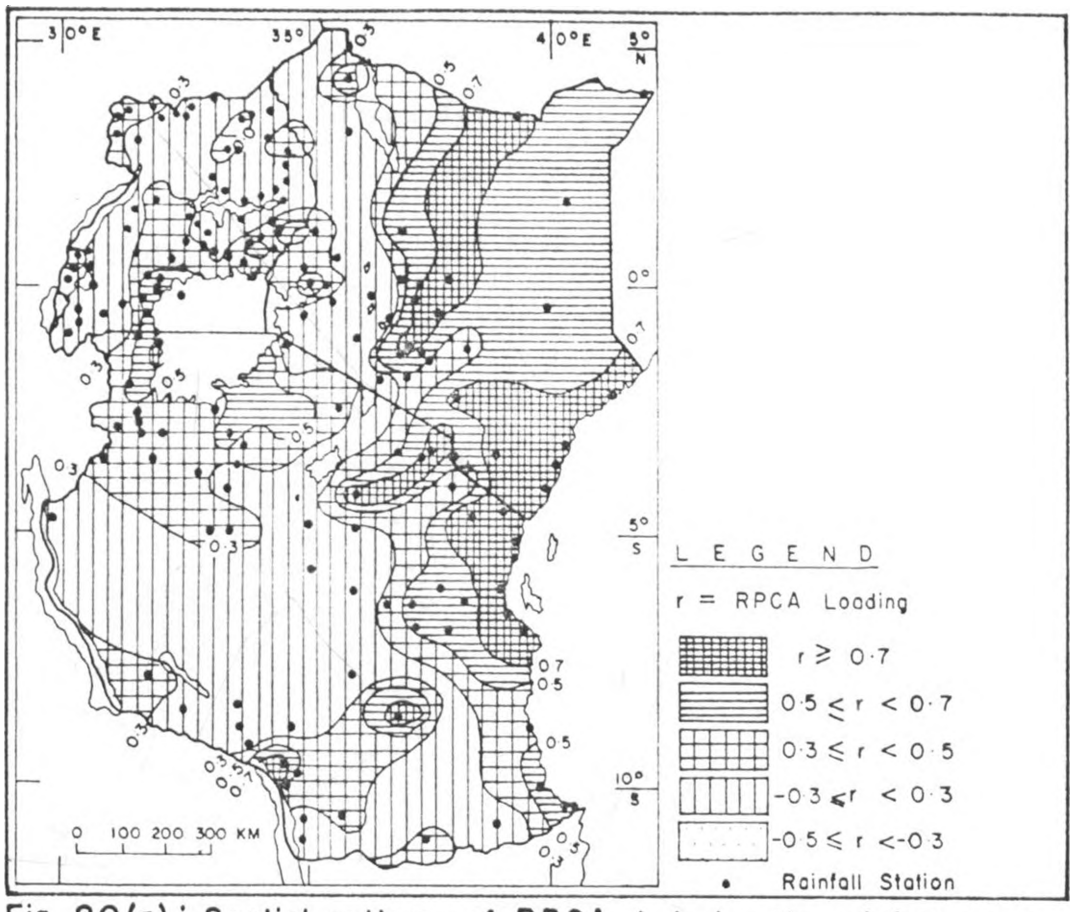

Fig. 20(a): Spatial patterns of RPCA 1 during the rainfall season of September — November

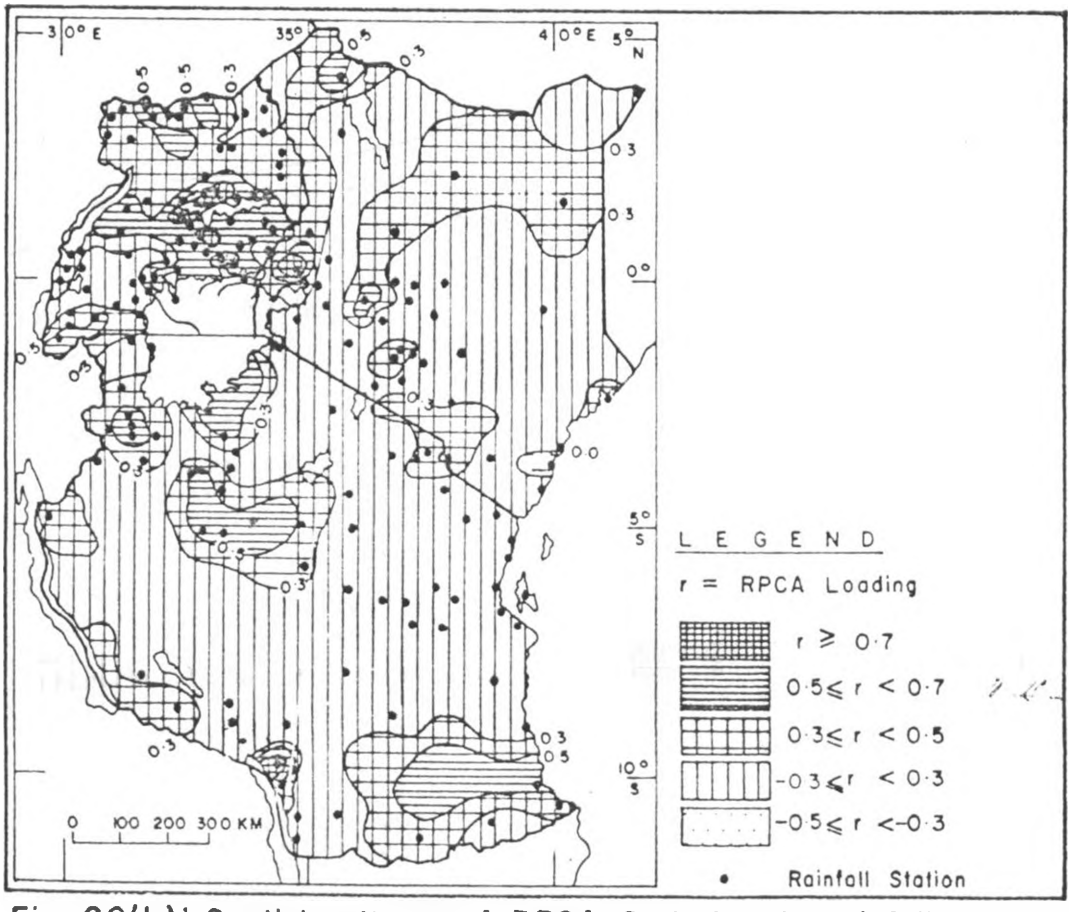

Fig. 20(b): Spatial patterns of RPCA 2 during the rainfall season of September — November

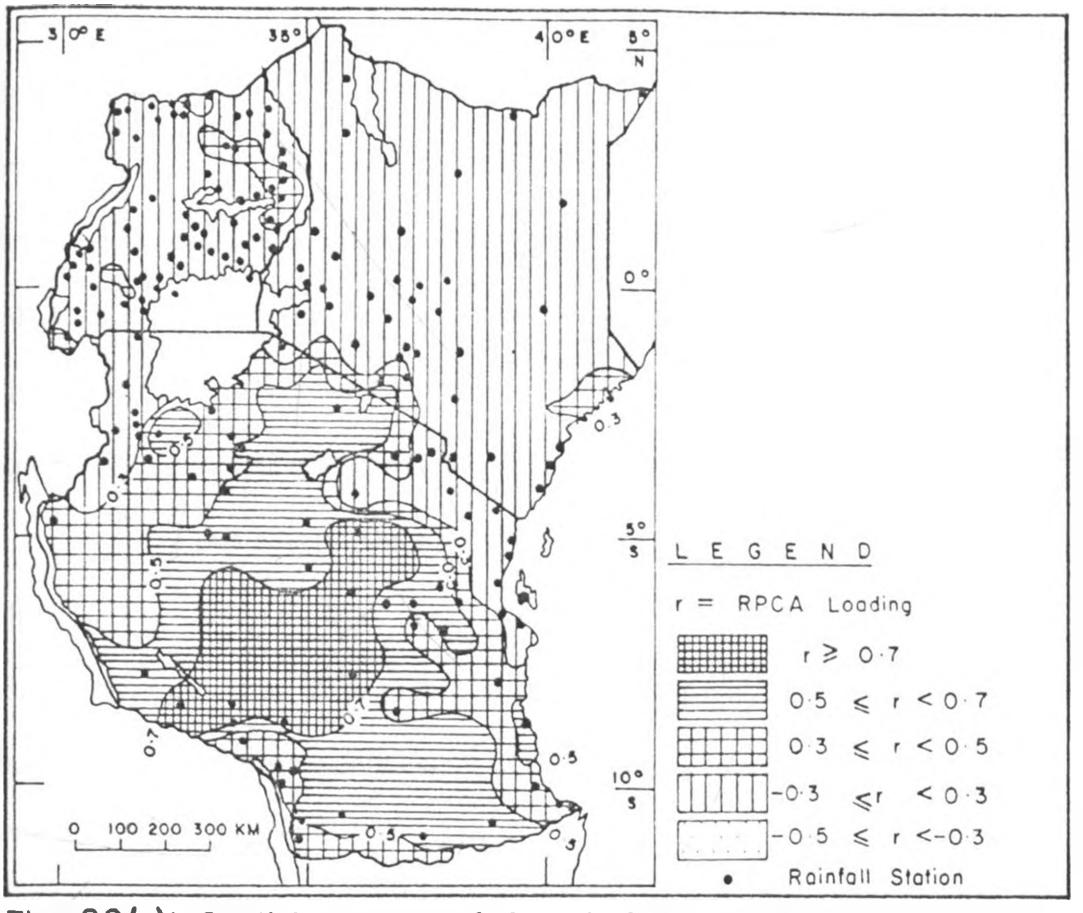

Fig. 20(c): Spatial patterns of RPCA 3 during the rainfall season of September — November

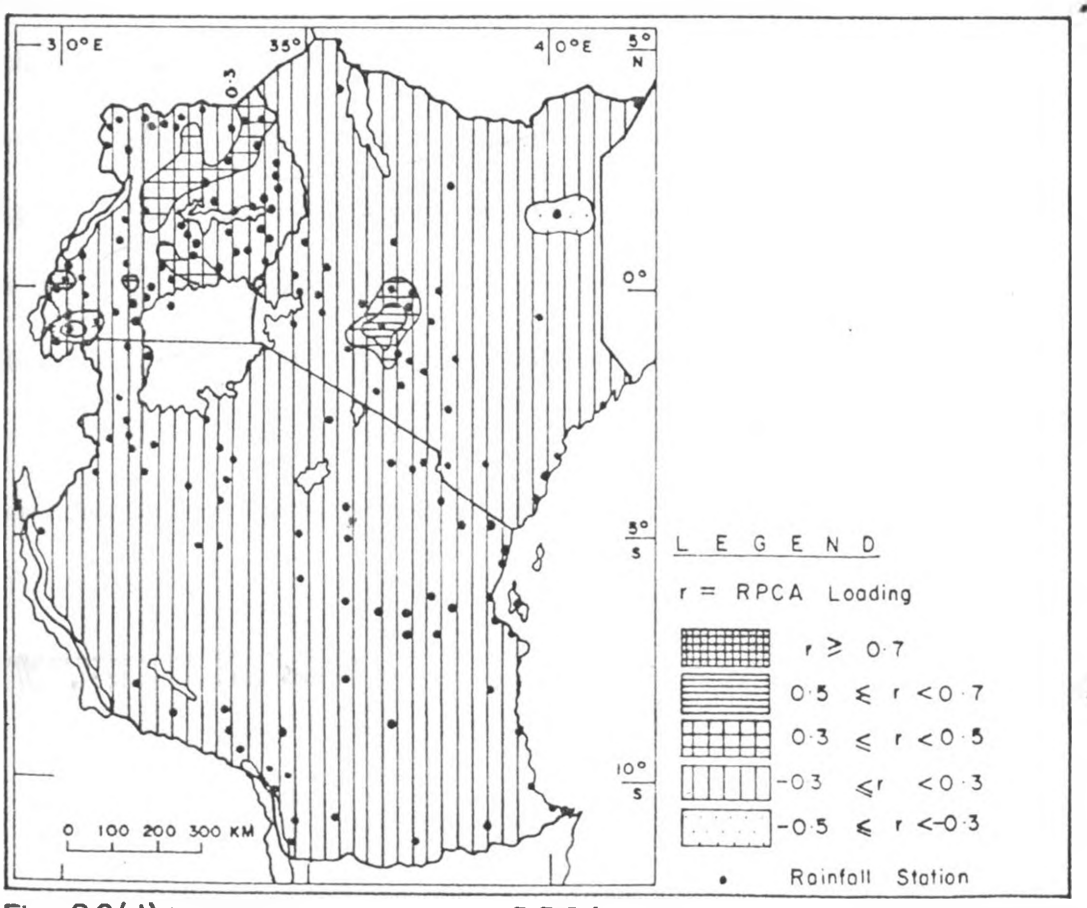

Fig. 20(d): Spatial patterns of RPCA 4 during the rainfall season of September — November

Maximum loadings of the first component over northern Uganda seem to indicate the general dry conditions while maximum loadings of the second component over southern Tanzania spreading to some parts of central Tanzania seem to indicate the general wet conditions as indicated in figures 21(a) and 21(b) respectively.

Positive loadings over western kenya and south eastern Uganda seem to indicate the general dry conditions over those locations.

During this season (December to February) spatial patterns of the third component which explains only 6.2% of the total variance were indicated over central Kenya and northern part of coastal strip. Figure 21(c) gives the spatial patterns of this component. The fourth component appears only over a small portion of the coastal strip and around mountain kilimanjaro as indicated in figure 21(d).

The spatial patterns of the dominant modes were used to delineate East Africa into similar climatological zones. Similar method was adopted by Ogallo (1987,1988) using relatively fewer network stations. Similar method have also been used by Bärring (1988); Basalirwa (1991). The homogeneous regions which were adopted in this study are given in figure 22. The stations which were clustered together in each homogeneous group are given in table 8. The derived homogeneous groups were generally close to those which were obtained by Ogallo (1988); Basalirwa (1991) among many others.

Table 9 gives the stations with highest communality values for the individual seasons and homogeneous regions. As indicated in section 2.7.2.2 the station with the highest degree of association with the rest of the stations in any specific climatological zone (communality) would represent the location.

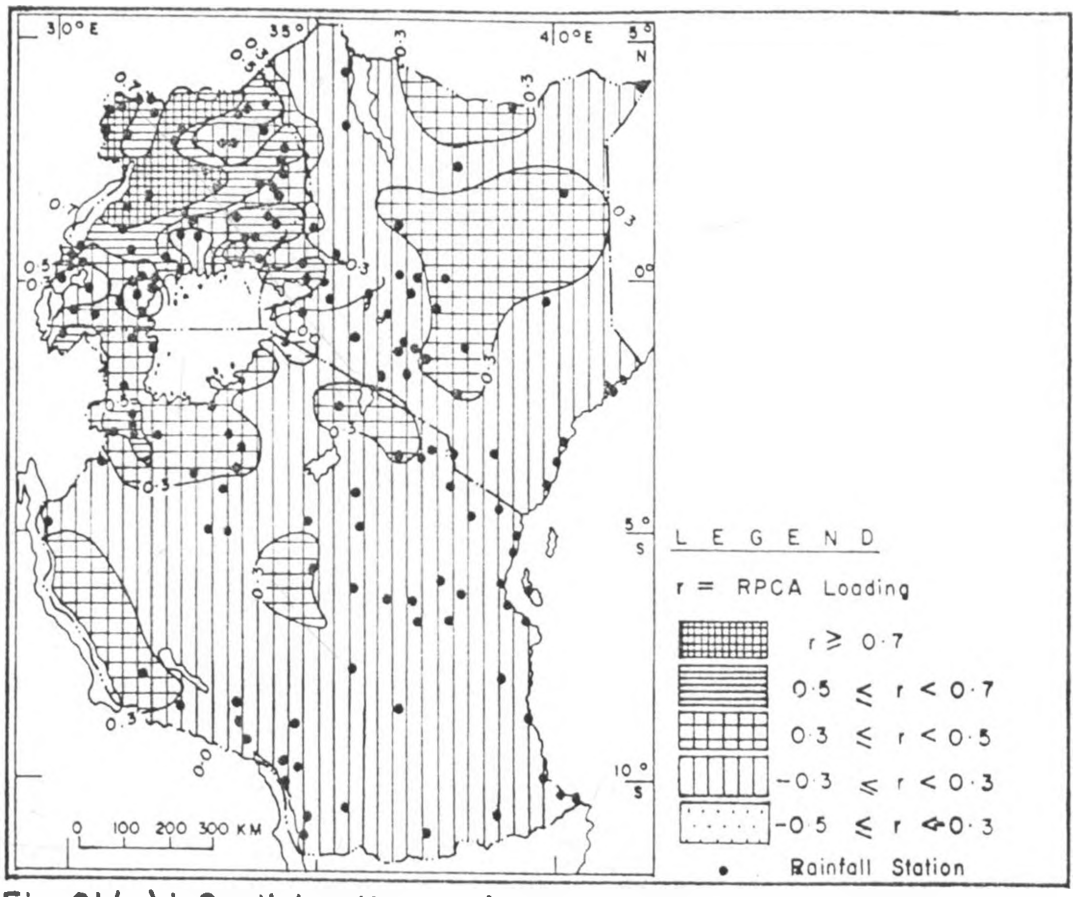

Fig. 21 (a) : Spatial patterns of RPCA 1 during the rainfall season of December — February

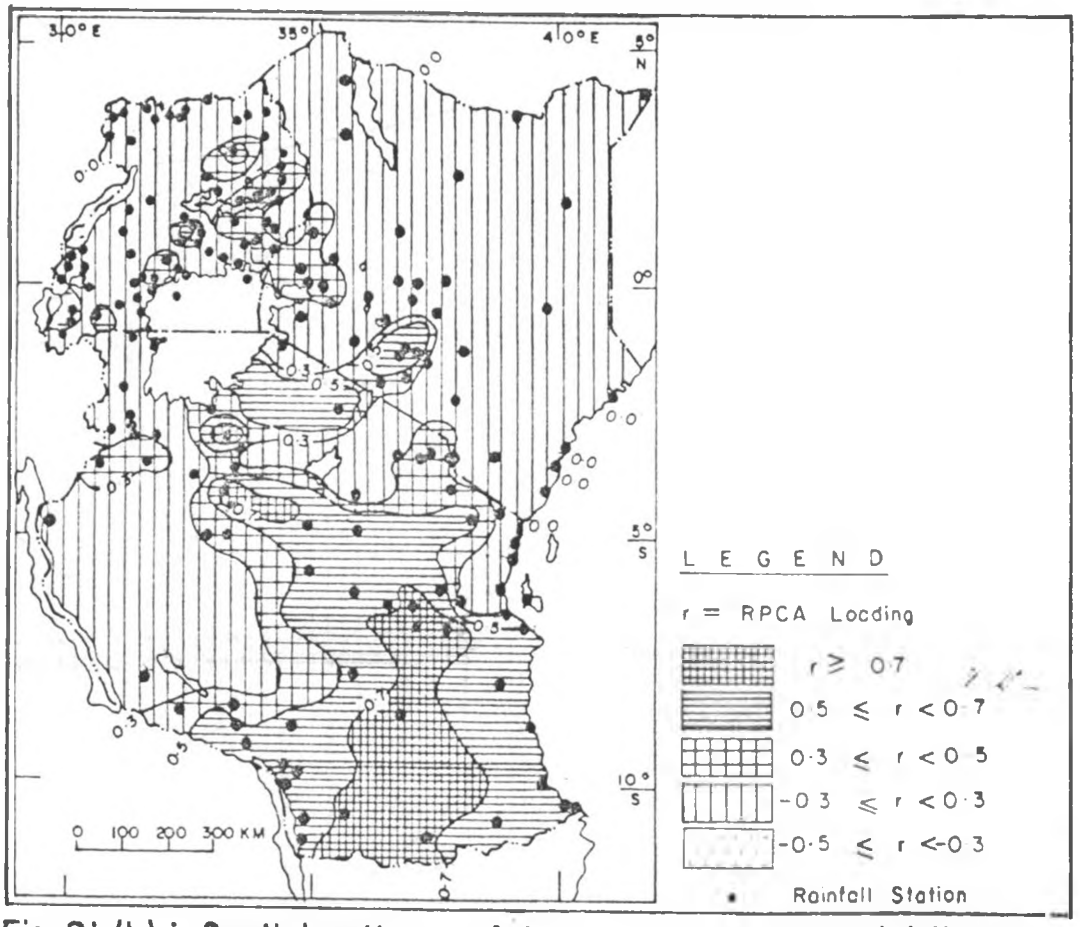

Fig. 21 (b) : Spatial patterns of RPCA 2 during the rainfall season of December — February

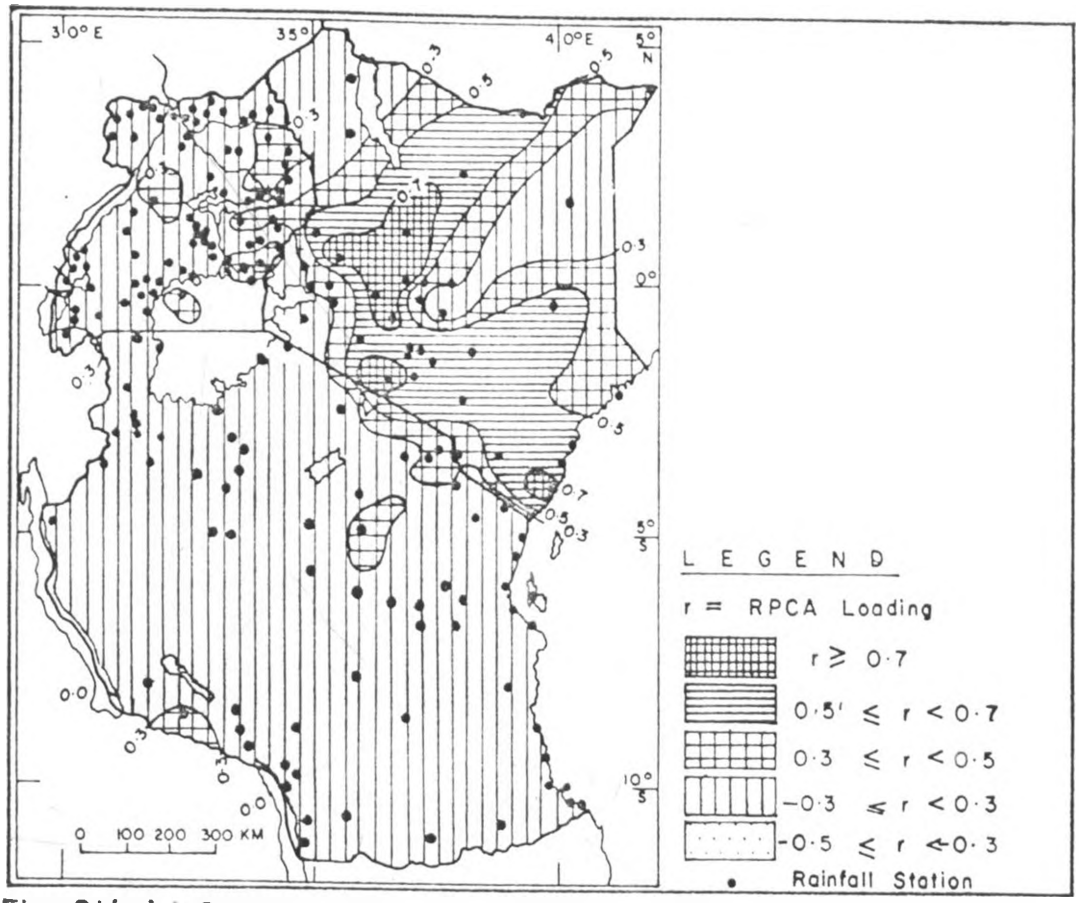

Fig. 21(c) : Spatial patterns of RPCA 3 during the rainfall season of December — February

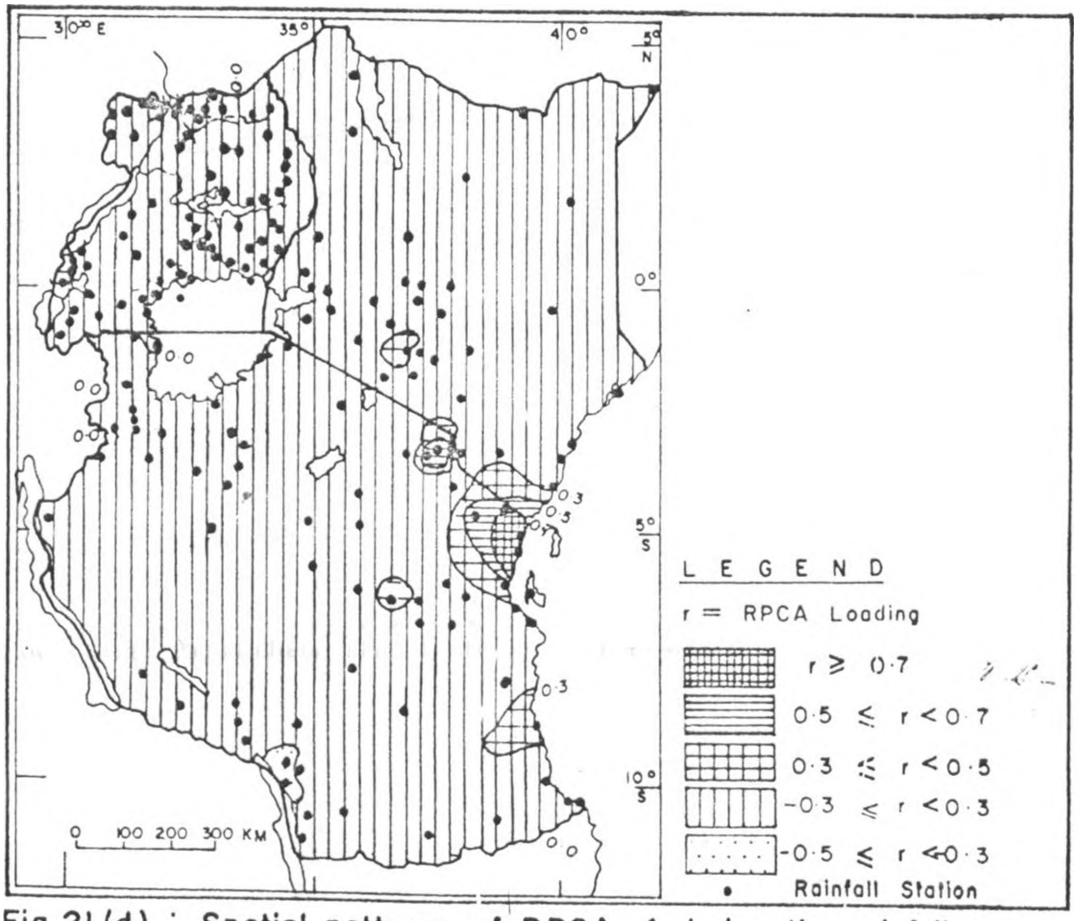

Fig. 21 (d) : Spatial patterns of RPCA 4 during the rainfall season of December — February

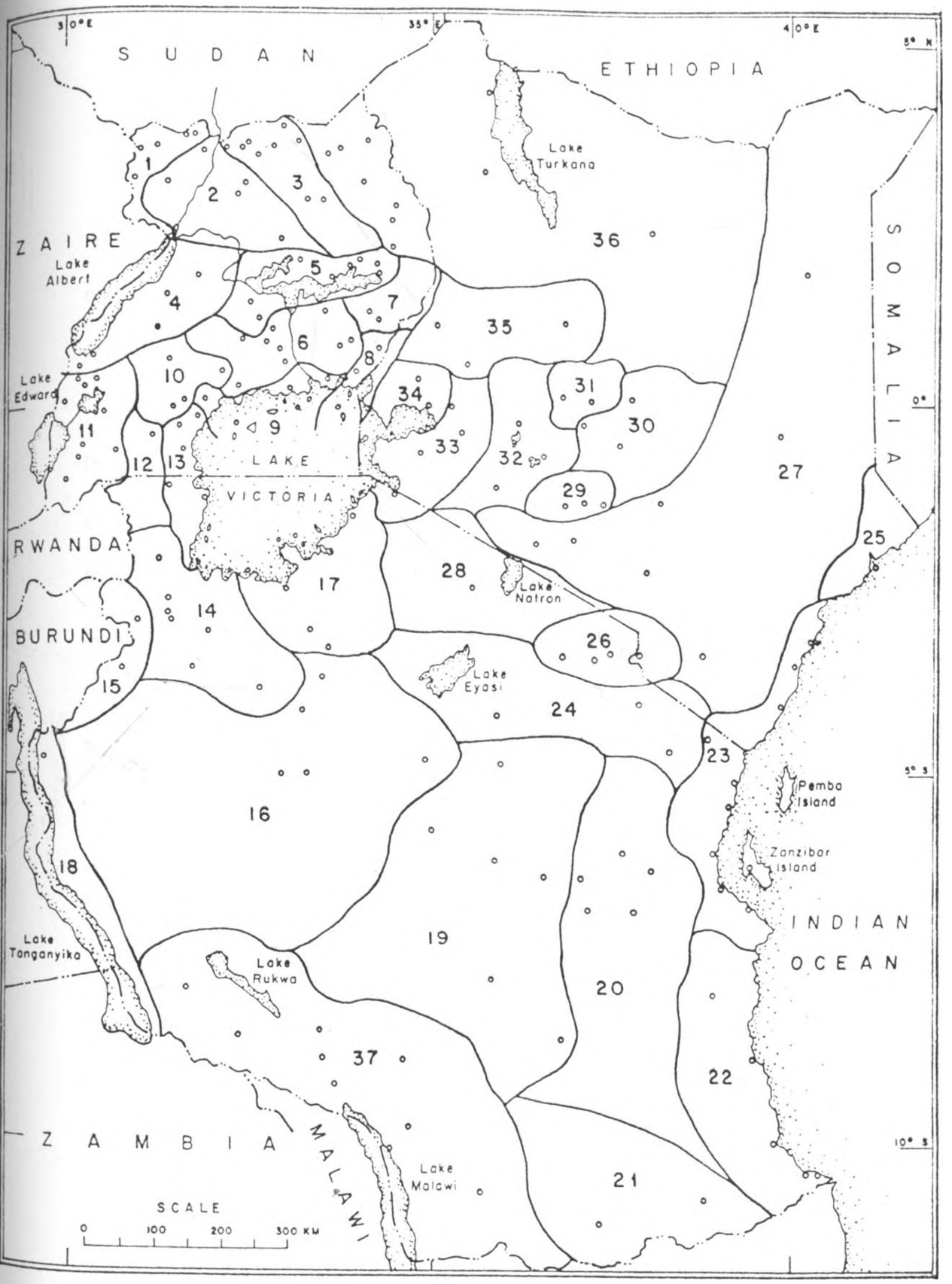

Fig. 22: Regions used in the study

Such a station may be used to represent the individual climatological zones especially when the communality values are relatively large within the zone. Such locations could be used as areal representatives of the individual homogeneous zones rather than using complex areal averaged values.

Lastly the patterns of the inter-station correlations were used to determine whether the delineated homogeneous regional subgroups were physically realistic. Under this concept stations falling under each homogeneous regional group should have the largest values of inter-station correlation. Typical examples of the inter-station correlations are shown in figures 23(a)-23(d). It can be seen from figures 20 and 23 that this was true from the results of the study. This is indicative of the physical reality of the RPCA derived climatological regions. Such maps would be very useful in planning and management of many rain-dependent activities.

3.6.1 RESULTS OBTAINED FROM CORRELATION ANALYSIS

It was noted in the last chapter that the potential predictors for seasonal rainfall were determined from the correlation between seasonal rainfall and time lagged seasonal SST values. Correlation analysis was also used to determine the prediction potential of the upper level (200 Hpa) temperatures. The results from these correlation analyses are presented in the next section.

Table 8: Regionalisation as obtained from RPCA and the stations with the highest communality in each zone are given in the third column. Word class is used in this study to indicate loading patterns of the modes.

Zone as per fig.22	Stations	Comm.	Significant RPCA Modes loading > 0.7 (dominant value; class i) 0.5 ≤ loading < 0.7 (high; Class ii) 0.3 ≤ loading < 0.5 (significant;class iii) |loading| < 0.3;class iv -0.3 ≤ loading < -0.5,class v	General Comments
1	Arua Yumbe Moyo	0.94* 0.90 0.86	modes I,II & VIII I (class iii) II (class iii) VIII (class iii)	dry sub-humid
2	Obangi Abera Gulu Lira Adilang	0.87 0.93* 0.87 0.89 0.90	mode II II (class iii)	Moist sub-humid
3	Padibe Kitgum Palabek Patonga Madi Miewini	0.84 0.84 0.85 0.86 0.95* 0 83	modes II,III & 1V II (class iii), III (class iii), 1V (class iv)	dry sub-humid
4	Masindi Bulindi Fortportal Kijura Kyembogo	0.90 0.93* 0.85 0.91 0.85	modes II & IV II (class ii) 1V (class iii)	high terrain
5	Nakasongola Bukalasa Ongino Soroti Kaberamaido Katakwi	0.93 0.97* 0.90 0.92 0.93 0.91	modes I & II I (class iii), II (class ii)	Lake shores
6	Kawanda Bakijulula Nsimbe Mpigi Moninko Vukula Nuwanzu Budumba	0.95* 0.86 0.90 0.88 0.90 0.87 0.94 0.87	mode II II (class ii)	dry sub-humid
7	Bukedea Mbale	0.92 0.92*	modes II & III II (class ii), III (class iv)	high terrain
8	Tororo Buvuma	0.94 0.95*	modes I & IV I (class iii), IV (class iii)	dry sub-humud

Table 8 continues on the next page

zones as per fig 22	stations	comm.	Significant RPCA Modes loading > 0.7 (dominant value; class i) 0.5 ≤ loading < 0 7 (high; Class ii) 0.3 ≤ loading < 0 5 (significant;class iii) |loading| < 0.3;class iv -0.3 ≤ loading < -0 5;class v	General comments
9	Jinja Mukono Bwavu Entebbe Nkozi Bumagi	0.95 0.92 0.97* 0.90 0 91 0.91	modes I & II I (class iii), II (class ii)	lake shores, moist sub-humid
10	Mubende Masaka Kabasanda Katigondo	0.87 0.91* 0.89 0.85	mode I I (class iii)	dry sub-humid
11	Bugoye Kabale Rwashamaire Mbarara	0.90 0.92 0.83 0.93*	mode II II (class iii)	high terrain, dry sub-humid
12	Lyantonde	0.83	modes I & III I (class iii), III (class iii)	semi-arid
13	Kyanamukaka Kiterede Katera Bukoba Kaisho	0.92* 0.91 0.84 0.90 0 91	mode I I (class ii)	lake shores, dry sub-humid to humid
14	Kahama Igabiro Biharamuro Ngara Mbulu Shanwa	0 91 0.92 0.87 0.87 0.97* 0.95	modes I & II I (class ii), II (class iii)	semi-arid
15	Kibondo	0.91	modes I & V I (class iii), V (class ii)	dry sub-humid
16	Shinyanga Nzenga Singida Tabora Kipalapala	0.88 0.95* 0.94 0.92 0.95	modes II & III II (class iii), III(class ii)	semi-arid
17	Mwanza Musoma Ngudu Maswa	0.93 0.96* 0.96 0.95	modes I, II , III I (class ii), II (class iii), III (class iii)	semi arid

Table 8 continues on the next page

zones as per fig.22	stations	comm.	Significant RPCA Modes loading > 0.7 (dominant value; class i) 0.5 ≤ loading < 0.7 (high; Class ii) 0.3 ≤ loading < 0.5 (significant;class iii) |loading| < 0.3;class iv -0.3 ≤ loading < -0.5;class v	General comments
18	Kigoma	0.85	mode I I (class iii) modes II, III & VII II (class iii), III (class iii), VII (class iii)	semi arid
19	Kondoa Manyoni Dodoma Iringa Lugalawa Mpwapwa Mahenge	0.94* 0.92 0.86 0.90 0.86 0.91 0.91	mode III III (class ii)	dry sub-humid to humid
20	Scutari Tungi Kilosa Morogoro Mahenge	0.96 0.96 0.84 0.96* 0.91	modes I & III I (class ii), III (class iii)	semi arid
21	Tunduru Masasi Litembo	0.94 0.94* 0.93	mode III III (class ii)	dry sub-humid
22	Utete Kilwa Lindi Mikindani	0.91 0.92 0.93 0.94*	modes I & III I (class ii), III (class iii)	semi arid

Table 8 continues on the next page

zones as per fig.22	stations	comm.	Significant RPCA Modes loading > 0.7 (dominant value; class i) 0.5 ≤ loading < 0.7 (high; Class ii) 0.3 ≤ loading < 0.5 (significant;class iii) |loading| < 0.3;class iv -0.3 ≤ loading < -0.5;class v	General comments
23	Zanzibar Malindi Kilifi Mombasa Amani Tanga Pangani Kizimbani Dar-Es-Salaam Bagamoyo	0.94 0.94 0.93 0.93 0.97 0.97 0.98* 0.94 0.95 0.94	mode I I (class ii)	dry sub-humid to moist sub-humid
24	Lushoto Same Handani	0.96 0.85 0.98*	mode I I (class ii)	semi arid
25	Lamu	0.96	modes I,II & III I (class i), II (class iii), III (class iii)	semi arid
26	Arusha Moshi Kiyungi Rombo	0.95 0.98* 0.98 0.82	modes I & II I (class ii) II (class iii)	dry sub-humid
27	Kajiado Machakos Makindu Kitui Voi Mandera Wajir Garissa	0.85 0.81 0.91 0.90 0.94* 0.89 0.91 0.85	mode I I (class ii)	arid
28	Dangobesh	0.88	modes I & III I (class iii), III (class ii)	semi arid
29	JKI Wilson Dagoretti	0.96 0.97* 0.93	modes I & II I (class ii), II (class iii)	urban semi arid

Table 8 continues on the next page

zones as per fig.22	stations		Significant RPCA Modes loading > 0.7 (dominant value; class i) 0.5 ≤ loading < 0.7 (high; Class ii) 0.3 ≤ loading < 0.5 (significant;class iii) |loading| < 0.3;class iv -0.3 ≤ loading < -0.5;class v	General comments
30	Meru Embu Nyeri	0.93 0.92 0.96*	mode I I (class i)	dry sub-humid
31	Rumuruti	0.89	modes I & X I (class iii), X (class v)	arid
32	Nakuru Naivasha	0.91* 0.88	mode III III (class i)	semi arid
33	Kericho Chemilil Kisii	0.81 0.92* 0.89	modes I & X I (class ii) X (class iii)	moist sub-humid
34	Kisumu Kakamega	0.84 0.92*	modes I & II I & II I (class iii) II (class ii)	dry sub-humid
35	Kitale Maralal Eldoret	0.76 0.89 0.89*	modes I & II I (class ii) II (class iii)	semi arid
36	Lokitaung Marsabit Moyale Moroto	0.81 0 96* 0.92 0.91	modes I & II I (class ii) II (class iii)	arid
37	Sumbuwanga Mkulwe Mbeya Tukuyu Njombe Dansland Songea Mwita	.87 .91 .84 .91 .94 .97* .87 .88	mode III III class ii	dry subhumid to moist su humid

comm. = communality. * Station which represents the region because it bears the highest communality in the zone.

Table 8 continues on the next page

Table 9: Stations with highest communality from each of the climatological regions.

Climatological zone as per fig.22	December-February.	March-May	June-August	September-November
1	Arua 0.95	Yumbe 0.85	Yumbe .89	Arua 0.94
2	Lira 0.95	Gulu 0.92	Abera 0.90	Abera 0.93
3	Palabek 0.94	Palabek 0.89	Palabek 0.88	Madi 0.95
4	Masindi 0.94	F/portal 0.90	Kijura 0.93	Bulindi 0.93
5	Kaberamaido 0.92	Bukalasa 0.89	Kaberamaido 0.92	Bukalasa 0.97
6	Vukula 0.95	Kawanda 0.89	Vukula 0.86	Kawanda 0.95
7	Bukedea 0.92	Mbale 0.84	Mbale 0.79	Mbale 0.92
8	Tororo 0.93	Tororo 0.89	Tororo 0.85	Tororo 0.94
9	Jinja 0.95	Jinja 0.87	Bumagi 0.86	Bwavu 0.97
10	Masaka 0.93	Masaka 0.87	Katigondo 0.84	Masaka 0.91
11	Mbarara 0.89	Mbarara 0.93	Mbarara 0.90	Mbarara 0.93
12	Lyantonde 0.84	Lyantonde 0.88	Lyantonde 0.74	Lyantonde 0.83
13	Kaisho 0.89	Kiterede 0.91	Kiterede 0.87	Kyanamukaka 0.92
14	Mbulu 0.91	Mbulu 0.91	Mbulu 0.95	Mbulu 0.95
15	Kibondo 0.90	Kibondo 0.90	Kibondo 0.80	Kibondo 0.91
16	Nzega 0.93	Nzega 0.90	Tabora 0.91	Nzega 0.94
17	•Ngudu 0.93	Mwanza 0.88	Ngudu 0.93	Ngudu 0.96
18	Kigoma 0.93	Kigoma 0.84	Kigoma 0.76	Kigoma 0.86
19	Njombe 0.94	Kondoa 0.92	Kondoa 0.97	Kondoa 0.94
20	Kilosa 0.96	Morogoro 0.96	Scutari 0.96	Morogoro 0.96

Table 9 continues on the next page

Climatological zone as per fig.22	December-February	March-May	June-August	September-November
21	Tunduru 0.92	Songea 0.94	Masasai 0.92	Tunduru 0.94
22	Lindi 0.90	Mikindani 0.92	Mikindani 0.95	Mikindani 0.94
23	Kizimbani 0.95	Mombasa 0.93	Mombasa 0.94	Pangani 0.98
24	Handani 0.92	Handani 0.90	Lushoto 0 91	Handani 0.98
25	Lamu 0.87	Lamu 0.91	Lamu 0.90	Lamu 0.96
26	Moshi 0.93	Moshi 0.91	Moshi 0.92	Moshi 0.98
27	Kitui 0.94	Voi 0.92	Voi 0.91	Voi 0.94
28	Dangobesh 0.91	Dangobesh 0.89	Dangobesh 0.73	Dangobesh 0.88
29	Dagoretti 0.97	Wilson 0.92	JKI 0.90	Wilson 0.97
30	Nyeri 0.94	Embu 0.88	Nyeri 0.91	Nyeri 0.96
31	Rumuruti 0.95	Rumuruti 0.86	Rumuruti 0.85	Rumuruti 0.89
32	Naivasha 0.96	Naivasha 0.95	Naivasha 0.97	Nakuru 0.91
33	Chemili 0.90	Chemili 0.90	Chemili 0.88	Chemili 0.92
34	Kakamega 0.95	Kakamega 0.89	Kakamega 0.80	Kakamega 0.92
35	Eldoret 0.95	Kitale 0.89	Eldoret 0.91	Eldoret 0.89
36	Moroto 0.93	Moyale 0.90	Moyale 0.87	Marsabit 0.96
37	Njombe 0.94	Songea 0.94	Dansland 0.95	Dansland 0.97

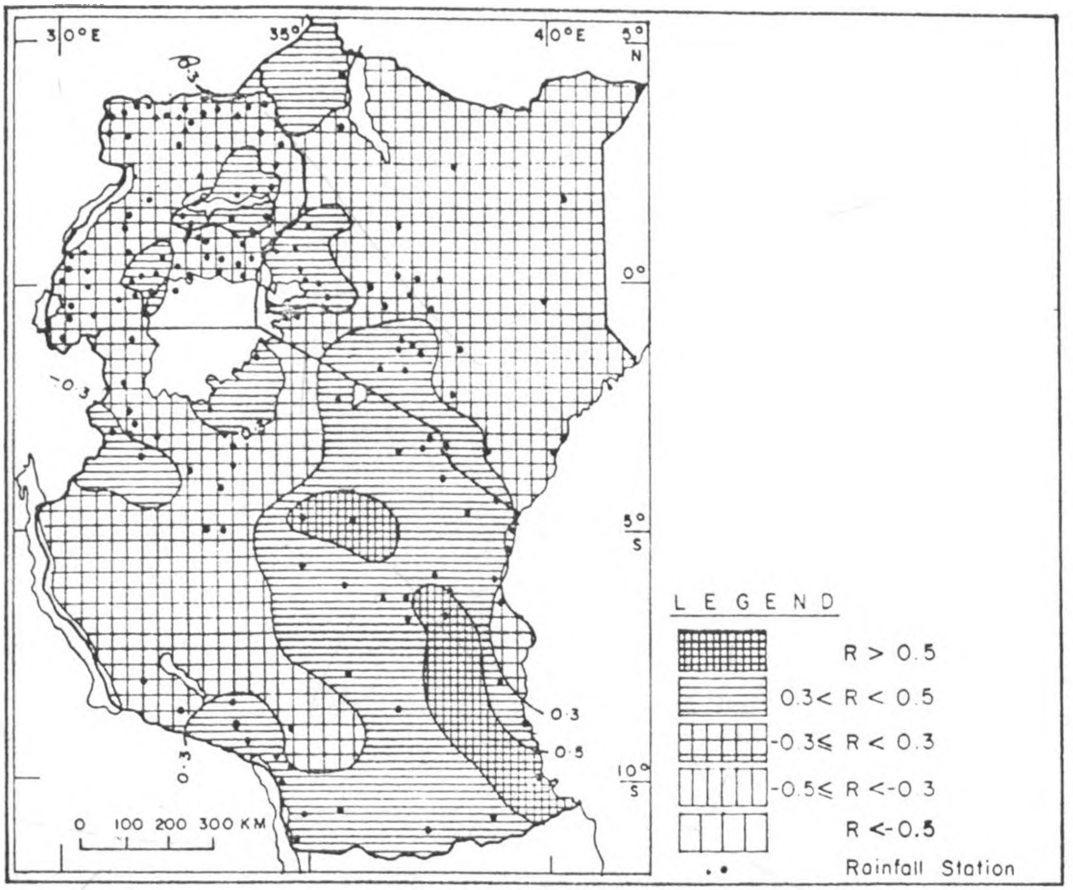

Fig. 23(a) : Correlations with Mikindani Station (No.106) during the season of December — February

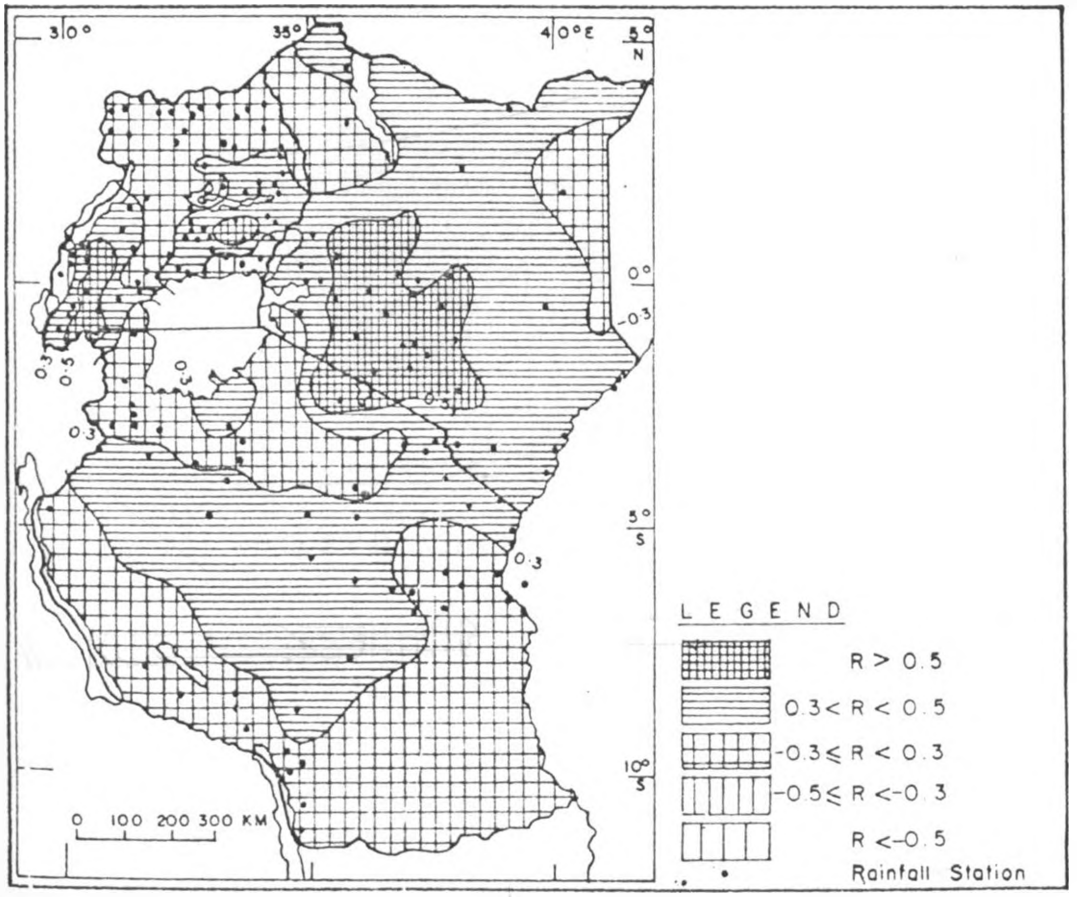

Fig. 23(b) : Correlations with Wilson Station (No.134) during the season of March — May

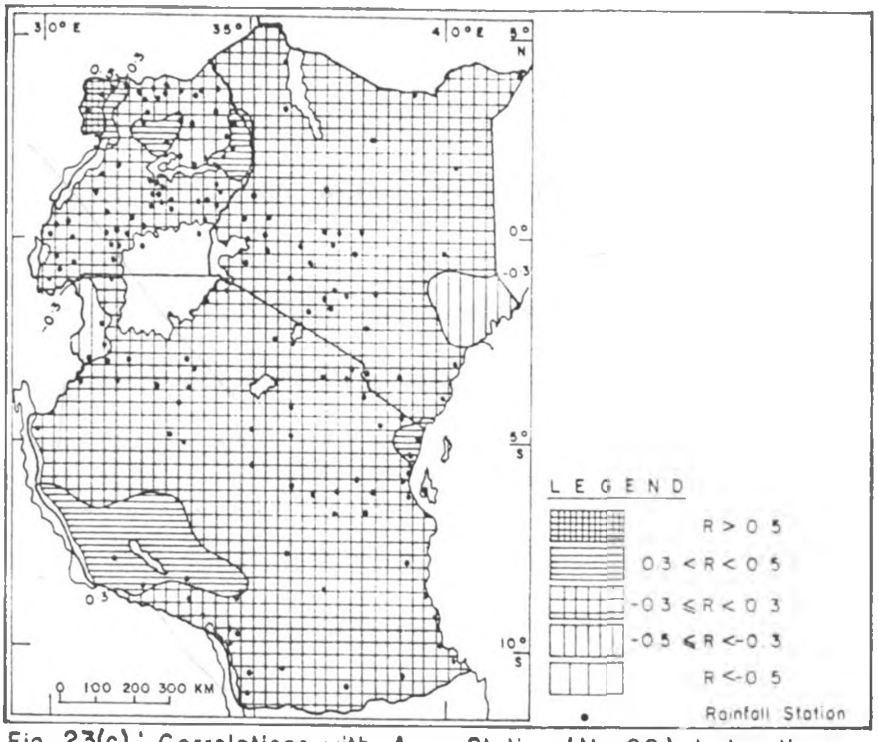

Fig. 23(c) : Correlations with Arua Station (No. 09) during the season of June — August

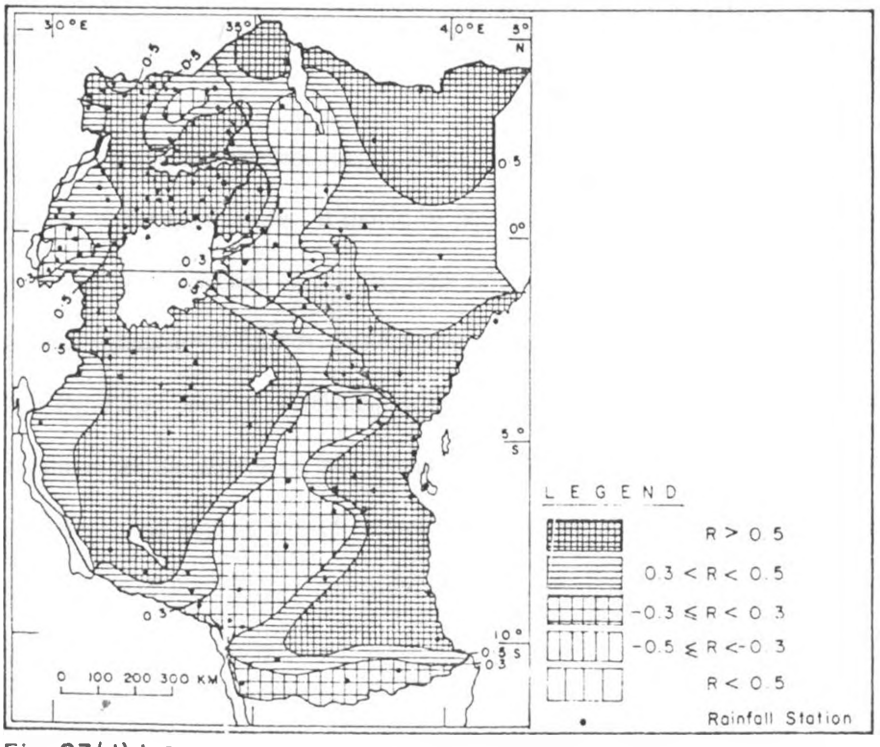

Fig. 23(d) : Correlations with Jinja Station (No. 39) during the season of September — November

3.6.2.1 CORRELATION BETWEEN SEASONAL RAINFALL AND 200 Hpa TEMPERATURE.

In this section correlation between 200 Hpa temperature over Nairobi and seasonal rainfall are discussed. One of the objectives of this study was to investigate the relationship between seasonal rainfall and anomalies in the atmospheric circulation. Atmospheric circulation over the region was quantified in this study by using 200 Hpa over Nairobi. Table 10 gives the significant correlations which were observed between areal seasonal rainfall and 200 Hpa temperature anomalies over Nairobi. At 95% confidence limit, t-distribution was used to determine significant correlation values (r). The t-test indicated that all r values greater than 0.33 were statistically significant.

Table 10 indicates that there was significant zero-time lag correlation in some of the regions. Southern Tanzania (zone 22) however indicated negative correlation during March-May season.

Central and western Kenya (zones 31 and 34) also had significant negative values during June-August season. It should be noted that these are dry periods in these regions. The negative correlation values may therefore be a reflection of the existence of many low rainfall values in the records. Results from table 10 further indicated that 22% of the zones had significant positive correlations with temperatures at 200 Hpa. These regions included locations on the shores of lake Victoria, the shores of lake Tanganyika, central Kenya highlands, and regions around mountain Kilimanjaro .These observed positive correlation values could therefore be indicative of the coupling of the meso-scale circulations with atmospheric circulations.

Table 10. Significant Correlations between seasonal rainfall at some specific regions and temperatures at 200 Hpa.

Zone as per fig.22	Season	corr.(r)	Zone	Season	corr.(r)
17	Dec.-Feb.	.37	31	Jun.-Aug.	-.28
16	Dec -Feb.	.37	34	Jun.-Aug.	-.31
21	Dec.-Feb.	.35	9	Sep.-Nov.	.43
22	Dec -Feb.	.39	13	Sep.-Nov.	.35
33	Dec.-Feb.	.48	14	Sep.-Nov.	.37
34	Dec.-Feb.	.42	18	Sep.-Nov.	-.29
22	Mar.-May	-.45	20	Sep.-Nov.	.36
25	Mar -May	.40	23	Sep.-Nov.	.34
26	Jun.-Aug.	.45	28	Sep.-Nov.	.36
27	Jun.-Aug.	.49	30	Sep.-Nov.	.35

Warmer troposphere is associated to increased convective activities (Okeyo 1987). On the other hand, an equatorial trough intensifies as it passes over the mountain terrain (Semazzi 1978). The interaction between mesoscale and large systems enhances convective activities in the convergence zones and decreases convective activities in the divergence zones (Mukabana 1992; Devies et al. 1985).

During the season of March-May relatively low correlation values were observed. December-February season however had positive correlation values over some parts of southern Tanzania. The predictive potential of the 200 Hpa temperature therefore was therefore generally low.

3.6.2.2 PROXIES

Correlation analysis between the surface temperatures and the SSTs was carried out using coastal/island stations of Lamu and Mombasa/ Aldabra and Seychelles respectively. The SST modes and some specific climatological regions which were significantly correlated at 95% confidence limit are presented in tables 11 to 14.

The tables give simple correlation coefficients between the surface temperature of the coastal/island stations and the significant respective SST grids.

The results from these tables showed that surface air temperatures for some coastal /island stations were significantly correlated with SST values over some oceans. Thus surface air temperature anomalies at some coastal/island stations can be used as proxies of SST changes over parts of the global oceans.

The following section presents results obtained from correlation analyses with SSTs.

Table 11 Significant correlations between coastal stations surface temperatures and SST during the season of December to February.

COASTAL/ISLAND STATIONS AND CORRELATED OCEAN REGIONS			
Aldabra	Lamu	Mombasa	Seychelles
10-20°S,65-70°E 0 53	10-20°N,40-50°E -.53	10-20°N,60-70°E 0 63	10-20°N,75-80°E 0 50
10-20°S,80-90°E 0 50	10-20°N;110-120°E .72	10-20°N,80-90°E 0 55	10-20°N;120-130°E 0 61
30-40°S,40-50°E -0 52	0-10°N;50-60°E 0 68	10-20°N,110-120°E 0.51	0-10°N;130-140°E 0 59
	0-10°N,60-70°E 0 61	10-20°N;120-130°E 0.66	0-10°S;50-60°E 0 52
	0-10°N;70-80°E 0.57	10-20°N,130-140°E 0 65	0-10°S,140-150°E 0 54
	0-10°N;80-90°E 0.57	0-10°N,50-60°E 0 73	
	0-10°N;90-100°E 0.64	0-10°N,60-70°E 0 60	
	0-10°N;100-110°E 0 60	0-10°N;70-80°E 0 58	
	0-10°S;40-50°E 0 53	0-10°N,80-90°E 0 56	
	0-10°S,50-60°E 0.54	0-10°N;90-100°E 0.49	
	0-10°S;60-70°E 0.65	0-10°N;100-110°E 0.55	
	0-10°S;70-80°E 0 64	0-10°N;120-135°E 0 69	
	0-10°S;80-90°E 0 61	0-10°S;40-50°E 0.78	
	0-10°S,90-100°E 0.52	0-10°S;50-60°E 0 54	
	0-10°S,100-110°E 0 63	0-10°S,60-70°E 0 50	
	0-10°S;130-140°E 0 60	0-10°S,90-100°E 0 53	
	10-20°S;50-60°E 0 51	20-30°S;30-40°E -0 54	
	10-20°S;60-70°E 0 53		
	10-20°S;70-80°E 0.68		

Table 11 continues on the next page

Aldabra	Lamu	Mombasa	Seychelles
	10-20°S,80-90°E 0.64		
	10-20°S,90-100°E 0.71		
	10-20°S,100-110°E 0 67		
	10-20°S,140-150°E 0 59		
	20-30°S,30-40°E 0 68		
	20-30°S,40-50°E -0 64		
	20-30°S,50-60°E -0 64		
	20-30°S,60-70°E -0.58		
	30-40°S;20-30°E -0.58		
	30-40°S;30-40°E -0.59		

Table 12 Significant correlations between coastal stations and SSTs during the season of March-May.

COASTAL/ISLAND STATIONS AND CORRELATED OCEAN REGIONS			
Aldabra	Lamu	Mombasa	Seychelles
0-10°N;50-60°E 0.61	10-20°S;60-70°E 0.59	0-10°N,70-80°E 0.48	0-10°N;50-60°E 0.51
0-10°N;70-80°E 0 57	10-20°S;70-80°E 0.53	0-10°N;80-90°E 0.49	0-10°N;70-80°E 0.46
0-10°N,80-90°E 0.50		0-10°S;80-90°E 0.58	0-10°N;120-130°E 0.60
0-10°N;120-130°E 0 61		0-10°S;90-100°E 0 50	0-10°N,130-140°E 0 55
0-10°N;130-140°E 0 62		0-10°S;100-110°E 0 60	0-10°N;140-150°E 0 62
0-10°N;140-150°E 0 78			0-10°N;150-160°E 0.71
0-10°N;150-160°E 0 81			0-10°N,160-170°E 0.54
0-10°N;180-190°E 0.56			0-10°N;180-190°E 0 55

Table 12 continues on the next page

Aldabra	Lamu	Mombasa	Seychelles
0-10°S,50-60°E 0.52			20-30°S;40-50°E -0 61
0-10°S;60-70°E 0.48			30-40°S;50-60°E -0 63
10-20°S,40-50°E 0.62			
10-20°S;50-60°E 0.49			
10-20°S;60-70°E 0.56			
20-30°S,40-50°E -0.52 30-40°S,40-50°E -0.49			
30-40°S;50-60°E -0.58			

Table 13 Significant correlations between coastal stations surface temperatures and SSTs during the season of June-August.

COASTAL/ISLAND STATIONS AND CORRELATED OCEAN REGIONS			
Aldabra	Lamu	Mombasa	Seychelles
10-20°N;130-140°E 0.37	10-20°N;120-130°E 0.56	10-20°N;120-130°E 0.58	10-20°N;140-150°E 0.52
10-20°N;140-150°E 0.64	10-20°N;130-140°E 0 65	10-20°N;130-140°E .74	0-10°N,90-100°E 0.89
10-20°N;160-170°E 0.67	10-20°N;140-150°E 0 54	0-10°N;80-90°E 49	0-10°N;100-110°E 0.52
0-10°N;160-170°E 0.52	10-20°S;170-160°E 0 48	0-10°N;130-140°E 0.48	0-10°N,30-140°E 0 49
0-10°N;170-180°E 0.70		0-10°N;140-150°E 0.49	0-10°S,100-110°E 0.54
0-10°S;80-90°E 0.49		0-10°S,50-60°E 0 50	
		0-10°S,80-90°E 0.50	
		0-10°S;100-110°E 0 50	
		0-10°S;140-150°E 0.55	
		0-10°S,150-160°E 0.50	

Table 13 continues on the next page

Aldabra	Lamu	Mombasa	Seychelles
		0-10°S;160-170°E 0.50	
		10-20°S;160-170°E 0.65	
		10-20°S;170-180°E 0.52	
		30-40°S;40-50°E 0.57	

Table 14 Significant correlations between coastal station temperatures and SSTs during the season of September-November

COASTAL/ISLAND STATIONS AND CORRELATED OCEAN REGIONS			
Aldabra	Lamu	Mombasa	Seychelles
10-20°N;110-120°E 0.65	10-20°N;110-120°E 0 53	0-10°N,50-60°E 0.56	10-20°N;140-150°E 0.53
10-20°N;120-130°E 0.54	10-20°N;120-130°E 0.53	0-10°N,60-70°E 0.50	0-10°N;140-150°E 0.64
0-10°N;50-60°E 0.56	0-10°S,170-180°E -0.52	0-10°N,80-90°E 0.48	
0-10°N,160-170°E -0.55	0-10°S,180-190°E -0.62	0-10°N;160-170°E -0.51	
0-10°N;170-180°E -0.53	30-40°S,40-50°E -0.54	0-10°N;170-180°E -0 51	
0-10°N;180-190°E -0.49		0-10°S;170-180°E -0.55	
0-10°S;150-160°E -0.78		0-10°S,180-190°E -0.54	
0-10°S;160-170°E -0.55		20-30°S,40-50°E -0.55	
0-10°S;170-180°E -0.72		30-40°S,40-50°E -0 48	
0-10°S;180-190°E -0.63			
10-20°S;150-160°E -0.56			
10-20°S,160-170°E -0.57			
10-20°S;170-180°E -0 63			

Table 14 continues on the next page

Aldabra	Mombasa	Seychelles	
10-20°S;180-190°E -0.65			
20-30°S,30-40°E -0 48			
20-30°S,40-50°E -0 69			
30-40°S;40-50°E -0 56			
30-40°S,50-60°E -0 55			

3.6.3 CORRELATION BETWEEN SEASONAL RAINFALL AND SST

In this section the correlations which were observed between SST and rainfall are presented independently for each of the rainfall season.

3.6.3.1. SST CORRELATION WITH DECEMBER-FEBRUARY RAINFALL SEASON

This season is generally dry apart from southern Tanzania and locations on the coastal strip. Figure 24(a) and table 15 indicate the dominant SST modes which were correlated with December-February rainfall when t-test was applied at 95% confidence level. All values $\geq$ 0.33 were declared significant from this test. The SST locations with significant correlations are indicated in tables 15-18.

The results from the table 15 generally indicated that:

(i) Indian ocean regions I1 and I2 were correlated positively with western and central Uganda, western shores of lake Victoria, western Kenya ,and northern part of Indian ocean coastline. Positive correlations over the north Indian ocean would give a manifestation of enhanced convection due to cyclonic development accompanied by increase in cloud cover and precipitation over the ocean (Hastenrath et al. 1993). The above zones would benefit from the collapse of the Arabian ridge due to the warming over the north Indian ocean and the Eastward oscillation of meridional component of ITCZ.

(ii) Atlantic Ocean regions A3 and A1 had negative/positive correlations with northeastern Tanzania, central Tanzania including southern shores of lake Victoria, coastal strip/ western Tanzania including Kigoma respectively. Negative correlations over north Atlantic ocean would give a manifestation of enhanced anticyclonic development in case of oceanic cooling.

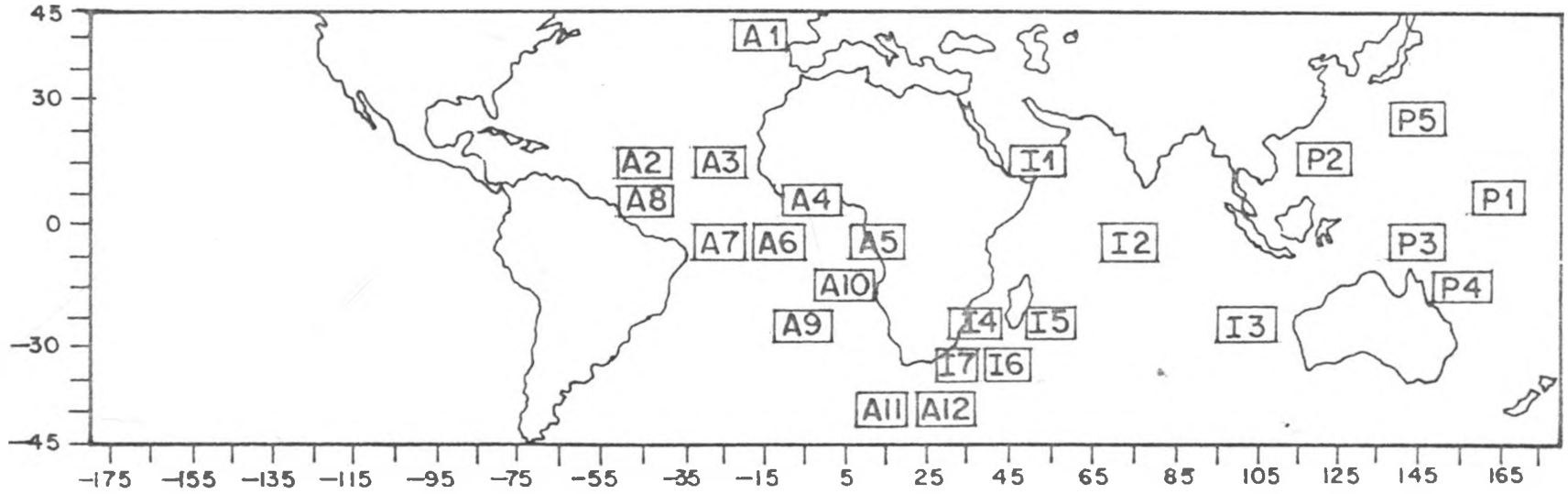

Fig. 24(a) : Significant SST modes of September — November that were used in seasonal rainfall regression model of December — February

Table 15 : Significant correlations between September-November SST modes and December to February rainfall.

Atlantic ocean modes (Ak)	Indian ocean modes (I_k)	Pacific ocean modes (Pk)
A1 (40-50°N;10-20°W)	I_1 (20-30°N,60-70°E)	P1 (0-10°N,150-160°E)
A2 (10-20°N;40-50°W)	I_2 (0-10°N,70-80°E)	P2 (10-20°N,120-130°E)
A3 (20-30°N;10-20°W)	I_3 (20-30°S,100-110°E)	P3 (0-10°N;140-150°E)
A4 (10-20°N;20-30°W)	I_4 (20-30°S,30-40°E)	P4 (10-20°N,160-170°E)
A5 (0-10°S,0-10°E)	I_5 (20-30°S,50-60°E)	
A6 (0-10°S;10-20°W)	I_6 (30-40°S,40-50°E)	
A7 (0-10°S,30-40°W)	I_7 (30-40°S,30-40°E)	
A8 (0-10°N;40-50°W)	I_8 (10-20°N;50-60°E)	
A9 (20-30°S;0-10°W)	I_9 (0-10°S;70-80°E)	
A10 (10-20°S,0-10°E)		
A11 (40-50°S;10-20°E)		
A12 (40-50°S;20-30°E)		

Note Index K represents the respective ocean grid points.

This could result in enhanced ridging from the north and increase convergence within the zones of zonal component of ITCZ. In case of warming within the North Atlantic ocean ,cyclonic development over the oceans would be enhanced (Hastenrath et al. 1993; Ogallo et al. 1988). This could lead to decreased ridging from the north and relax the convergence within the zonal component of ITCZ.

(iii) Central and western pacific regions P1 to P4 had significant correlations with many locations. Persistence at one seasonal time lead was observed in the correlation patterns. March-May results are presented in the next section.

3.6.3.2 SST CORRELATIONS DURING MARCH-MAY RAINFALL SEASON

March -May is the major rainfall period (long rainfall season) for many parts of the region. Figure 24(b) and table 16 give significant SST modes during this season. The results indicated that:

(i) North Indian ocean regions I1, I2, I8 and I11 were positively/negatively correlated with eastern Uganda, northern Kenya/southern Tanzania, Kigoma area,and coastal strip respectively,

(ii) South Indian ocean regions I6, I4, I7, I9 and I10 indicated negative correlations with shores of lake Victoria, southern low lands of Kenya and Kigoma region in Tanzania.

(iii) Equatorial Atlantic ocean regions A19, A7, A8, A9, and A10 were positively/negatively correlated with southern lowlands of Kenya, Nairobi area including eastern low lands of Kenya, central rift valley including northwestern Kenya/Kigoma region respectively.

(iv) North Atlantic ocean regions A3, A2, A4, A5 and A6 indicated negative correlations with most parts of Uganda, central and southern Tanzania, western Kenya extending up to eastern shores of lake Victoria.

(v) Northwest Atlantic ocean region A1 indicated negative/positive correlations with Kigoma area and northeastern Kenya, northeastern and central Uganda/western shores of lake Victoria respectively.

(vi) South Atlantic ocean regions A11, A12, A13, A14, A15 and A16 were positively/negatively correlated with central and northern Uganda/Kigoma region and northeastern Kenya respectively.

(vii) Southern Atlantic ocean regions A17 and A18) indicated positive correlations with central Uganda when,

(viii) Central Pacific ocean regions P1 to P4 were negatively correlated with northeastern Tanzania including southern Kenya, central rift valley, and eastern slopes of kenya highlands. The persistence of these correlations were quite evident in the patterns of the zero-time lag correlations. Results from the season of June-August are presented in the next section.

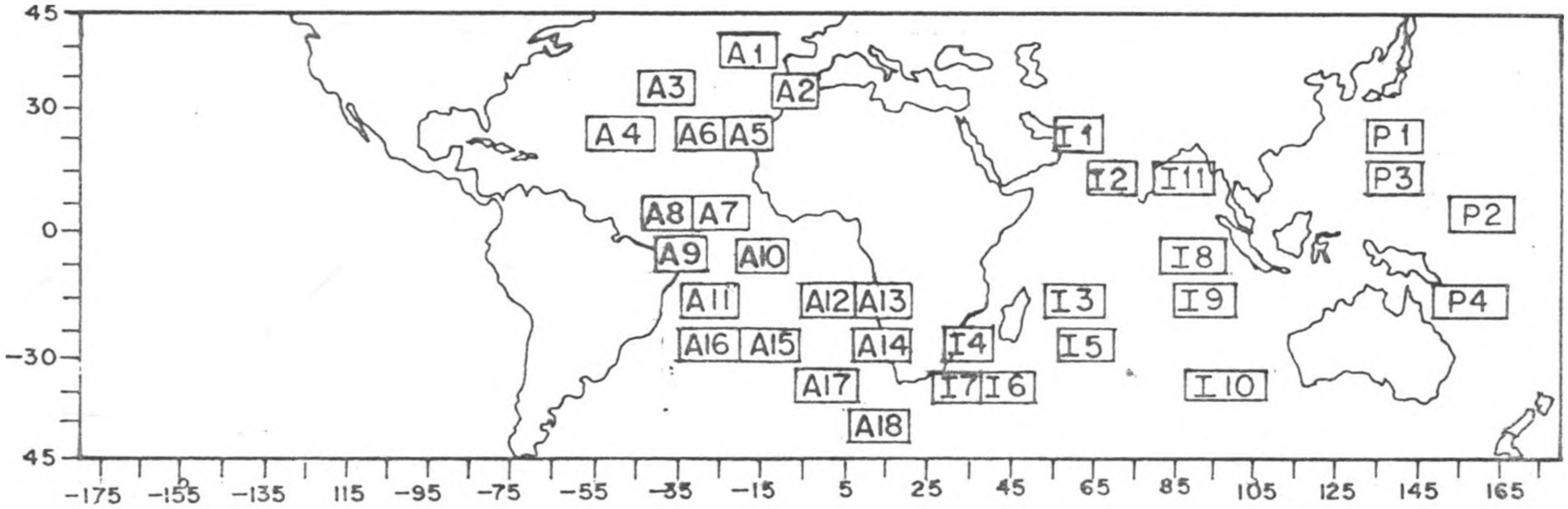

Fig. 24(b): Significant SST modes of December — February that were used in seasonal regression model of March — May

Table 16: Significant correlations between December-February SST modes and March-May rainfall season.

Atlantic ocean modes (Ak)	Indian ocean modes (I_k)	Pacific ocean modes (Pk).
A1 (40-50°N;10-20°W)	I_1 (20-30°N;50-60°E)	P1 (20-30°N;140-150°E)
A2 (30-40°N,0-10°W)	I_2 (10-20°N,50-60°E)	P2 (0-10°N,160-170°E)
A3 (30-40°N;30-40°W)	I_3 (10-20°S,60-70°E)	P3 (10-20°N;140-150°E)
A4 (20-30°N,40-50°W)	I_4 (20-30°S,30-40°E)	P4 (0-10°S;170-180°E)
A5 (20-30°N;40-50°W)	I_5 (20-30°S,60-70°E)	
A6 (20-30°N;20-30°W)	I_6 (30-40°S,50-60°E)	
A7 (0-10°N;20-30°W)	I_7 (30-40°S,30-40°E)	
A8 (0-10°N;30-40°W)	I_8 (0-10°N;90-100°E)	
A9 (0-10°S;30-40°W)	I_9 (0-10°S,90-100°E)	
A10 (0-10°S;10-20°W)	I_{10} (10-20°S;100-110°E)	
A11 (10-20°S;20-30°W)	I_{11} (20-30°N,80-90°E)	
A12 (10-20°S;0-10°E)		
A13 (10-20°S;10-20°E)		
A14 (20-30°S;10-20°E)		
A15 (20-30°S;10-20°W)		
A16 (20-30°S;30-40°W)		

Table 16 continues on the next page

Atlantic ocean (Ak)	Indian ocean (Ik)	Pacific ocean(PK)
A17 (30-40°S,0-10°E)		
A18 (40-50°S,0-10°E)		
A19 (0-10°N,0-10°E)		

Note Index K represents the respective ocean grid points.

3.6.3.3 SST CORRELATIONS DURING THE JUNE-AUGUST RAINFALL SEASON

June to August is generally dry over many parts of the region except western parts and coastal regions. Figure 24(c) and table 17 give significant SST modes during this season. Correlation results during the season of June to August showed that:

(i) Northern Indian ocean regions I1, I2, I3, I4 and I5 were negatively correlated with northern Uganda, lake Kyoga area and eastern shores of lake Victoria including western highlands of Kenya and central rift valley, central Kenya highlands. Oceanic cooling in northern Indian ocean may indicate anticyclonic development that could strengthen moisture influx in the above zones whereas oceanic warming seems to have the opposite effect.

(ii) Equatorial Atlantic ocean regions A7, A8 and A10 indicated negative correlations with northwestern Uganda,lake kyoga area, southern shores of lake Victoria including western Kenya and central rift valley. Negative correlations in Atlantic ocean during this season could be indicative of enhanced anticyclonic developments (in case of oceanic cooling) that strengthen tropospheric westerlies that influence rainfall in the above zones (section 3.7.3 which will be given later and figure 19(a) to 19(d) which were shown earlier).

(iii) South Atlantic ocean regions A13, A16 , A21, A20 and A19 indicated positive correlations with northern and eastern Uganda.

(iv) Northwest Atlantic Ocean regions A1 and A2 indicated positive correlations with Indian ocean coastal strip. Positive correlations during this season might indicate cyclonic development over the ocean and a reduction in the maritime ridging. This would reduce the negative effect of the dry north westerly winds. Oceanic cooling might have increase maritime ridging.

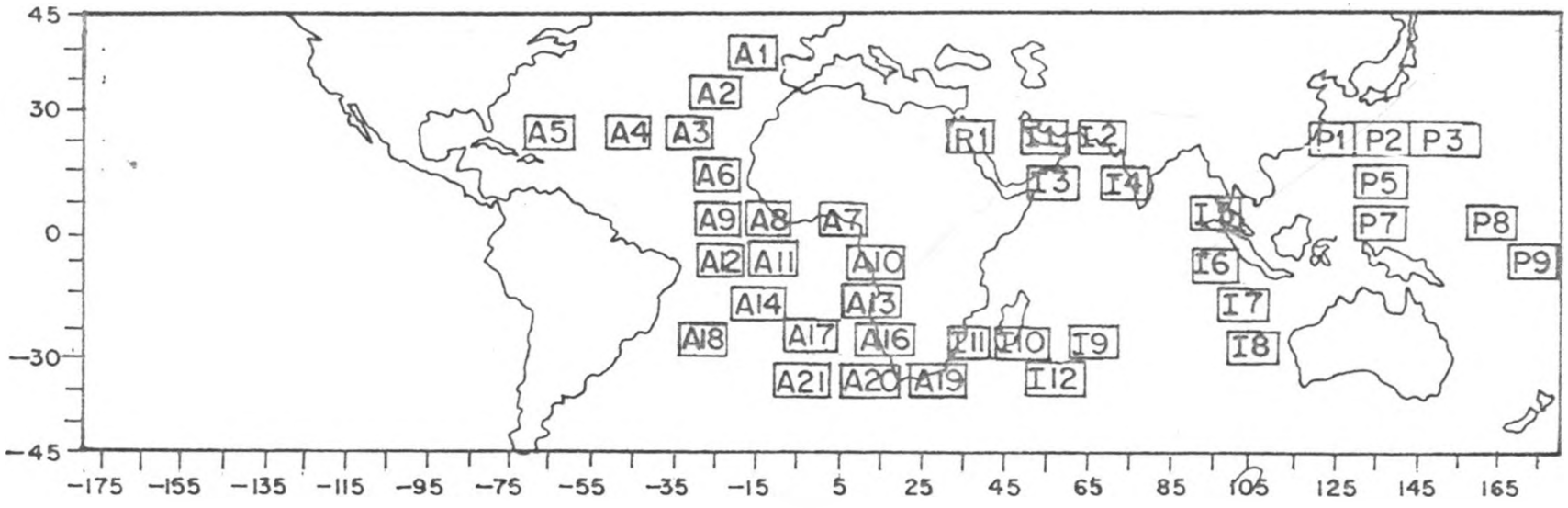

Fig. 24(c): Significant SST modes of March — May that were used in seasonal rainfall regression model of June — August

Table 17: Significant correlations between March-May SST modes and June-August rainfall.

Atlantic ocean modes (Ak)	Indian ocean modes (I_k)	Red sea modes (Rk)	Pacific ocean mode (Pk)
A1 (40-50°N;10-20°W)	I_1 (20-30°N,50-60°E)	R1 (20-30°N,30-40°E)	P1 (20-30°N;120-130°E)
A2 (30-40°N,20-30°W)	I_2 (20-30°N;60-70°E)		P2 (20-30°N;140-150°E)
A3 (20-30°N,30-40°W)	I_3 (10-20°N,50-60°E)		P3 (20-30°N;150-160°E)
A4 (20-30°N;40-50°W)	I_4 (10-20°N;70-80°E)		P4 (10-20°N,160-170°E)
A5 (20-30°N;60-70°W)	I_5 (0-10°N,90-100°E)		P5 (10-20°N;130-140°E)
A6 (10-20°N,20-30°W)	I_6 (0-10°S,90-100°E)		P7 (0-10°N;130-140°E)
A7 (0-10°N;0-10°E)	I_7 (10-20°S,100-110°E)		P8 (0-10°N;160-170°E)
A8 (0-10°N;10-20°W)	I_8 (20-30°S,100-110°E)		P9 (10-20°S,160-170°E)
A9 (0-10°N,20-30°W)	I_9 (20-30°S,60-70°E)		
A10 (0-10°S;10-20°E)	I_{10} (20-30°S;50-60°E)		
A11 (0-10°S;10-20°W)	I_{11} (20-30°S;30-40°E)		
A12 (0-10°S;20-30°W)	I_{12} (30-40°S,50-60°E)		
A13 (10-20°S;10-20°E)			
A14 (20-30°S;10-20°W)			
A15 (30-40°S,10-20°E)			
A16 (30-40°S,10-20°E)			
A17 (25-35°S;0-10°W)			

Table 17 continues on the next page

Atlantic ocean modes (Ak)	Indian ocean modes (I_K)	Red sea modes (Rk)	Pacific ocean modes (PK)
A18 (25-35°S,20-30°W)			
A19 (30-40°S,20-30°E)			
A20 (30-40°S,10-20°E)			
A21 (30-40°S,10-20°W)			

Note that Index K represents the respective ocean grid point.

(v) South Indian Ocean regions I12 , I11, I10 and I9 indicated positive correlations with central and southeastern Tanzania, central highlands including western Kenya. Oceanic cooling during this season might indicate strenghtening of pressure systems over the ocean and intensify the strength of Southeasterlies that drive the East African low level jet.

(vi) West and central Pacific ocean regions P1 to P9 indicated negative correlations with northern and western Uganda, southeastern Kenya and coastal strip. The persistence of the correlations at one seasonal time lead were observed. Results from the following season of September to November are presented in the next section.

3.6.3.4. SST CORRELATIONS DURING SEPTEMBER TO NOVEMBER RAINFALL SEASON.

September-November is the other major rainfall season (short rainfall season) for the region. Figure 24(d) and table 18 give significant SST modes during this season. The results from the table during the season of September to November indicated that: (i) Equatorial Atlantic ocean regions A5 and A6 indicated positive correlations with western shores of lake Victoria in Uganda and Tanzania, central southern Tanzania, northeastern Tanzania, Indian ocean coastal strip, eastern slopes of Kenya highlands including central northern Kenya. Positive correlations seem to indicate cyclonic development accompanied with convection and cloud development over the ocean in case of oceanic warming (Hastenrath,1993). The incursions of tropospheric moist westerlies also locally known as Congo/Zaire air mass into East Africa was observed by (Johnson et al. 1960; Ogallo et al. 1989; Basalirwa 1991; Devies et al. 1985; Anyamba et al. 1985; Griffith 1972; Ininda 1995) among several others. Schematic representation of East African equatorial low level flow during this season is

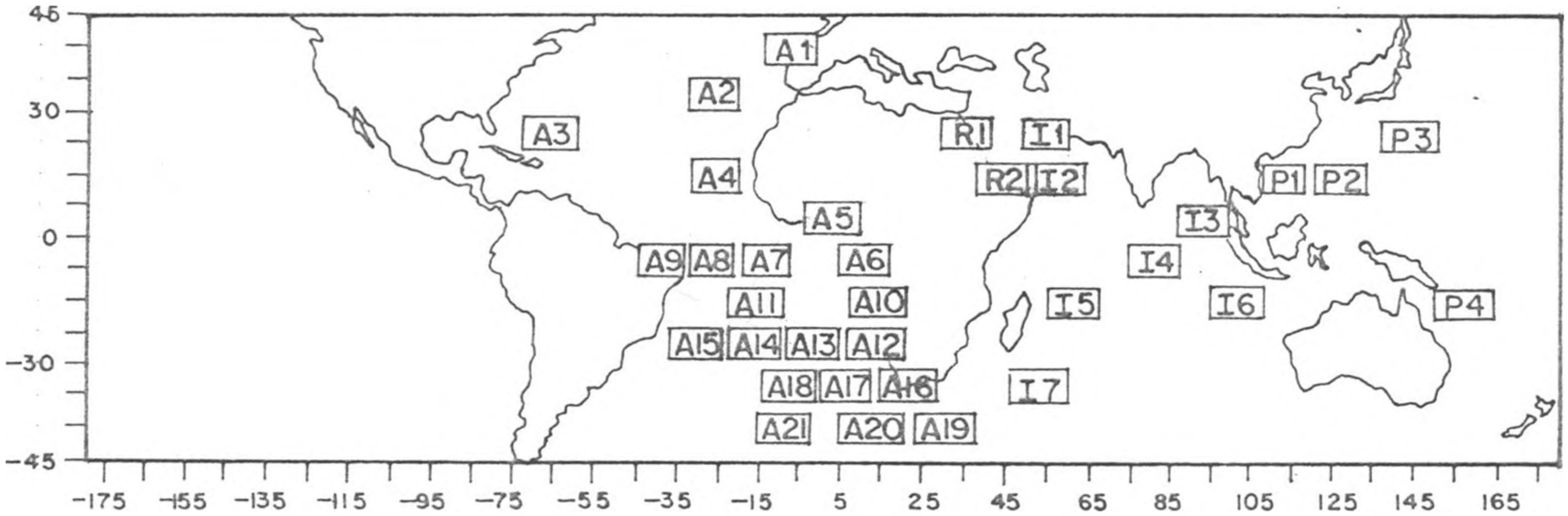

Fig. 24(d) : Significant SST modes of June — August that were used in seasonal rainfall regression model of September — November

shown in figure 25 and Walker cell circulations are shown in figure 26.

(ii) Northern Indian ocean regions I1 and I2 indicated some positive correlations with eastern shores of lake Victoria, coastal strip, northeastern Tanzania, and eastern Kenya highlands.

(iii) Northwestern Atlantic Ocean region A4 was negatively correlated with northwestern Uganda,southeastern Uganda, Kigoma area, northeastern Kenya.

(iv) South Indian Ocean regions I5, I6 and I7 indicated negative correlations with central northern Uganda, lake Kyoga area including southeastern Uganda, coastal strip, northern Tanzania. Oceanic cooling might enhance anticyclonic development and strengthen southeastrelies that seem to increase moisture fetch into the above regions.

(v) South Atlantic Ocean regions A10 to A21 was negatively correlated with central northern Uganda, northwestern and northern Tanzania, southern Tanzania, coastal strip including eastern Kenya highlands, western shores of lake Victoria, central and northern Kenya. Oceanic cooling in south Atlantic ocean might be associated with anticyclonic development which enhances moisture transport equatorward. Equatorial warming in Atlantic ocean also might enhance moist tropospheric westerlies influx as noted earlier in (i). The persistence in the correlations at one seasonal time lead was also observed during this season. Persistence and spatial patterns of correlations were also noted by Ogallo et al. (1988); Ininda (1995) among many others. The observed time lagged correlations formed the basis for the regression models which are presented in the next section.

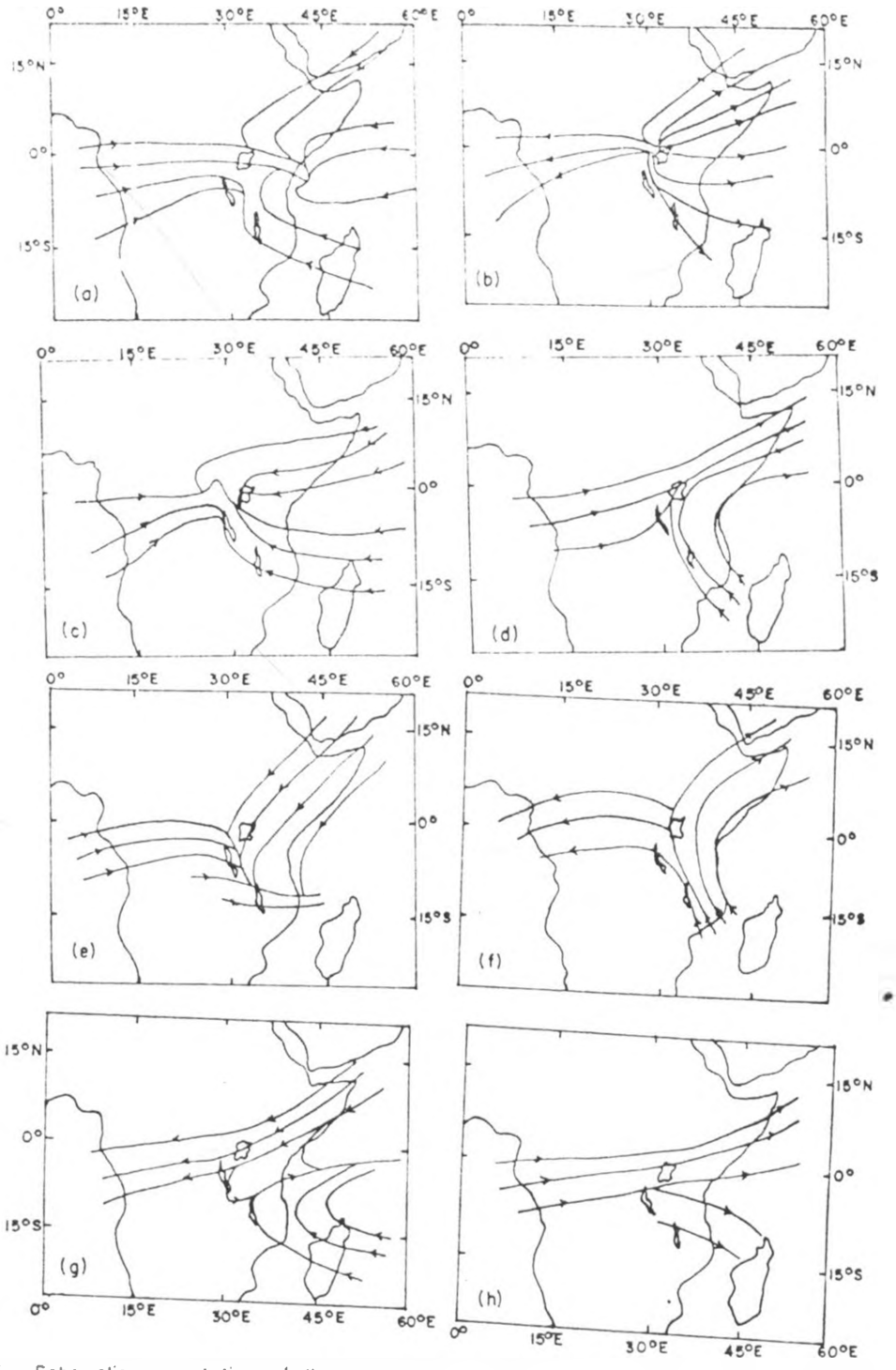

Fig 25 Schematic presentation of the anomalous low level flow corresponding to various rainfall anomaly patterns over East Africa during the Short Rains season.(a) wet over most parts of East Africa. (b) dry over most parts of East Africa. (c) wetter over the southern and western parts of East Africa and below/near normal elsewhere (d) drier over the western and southern parts of East Africa above/near normal rainfall elsewhere. (e) wetter over the western parts and drier over the southern parts of East Africa. (f) wetter over the southern and drier over the western parts of East Africa (g) wetter over the coastal areas and drier over the western parts. (h) wetter over the western parts and drier over the coastal areas.

After Inindo (1995).

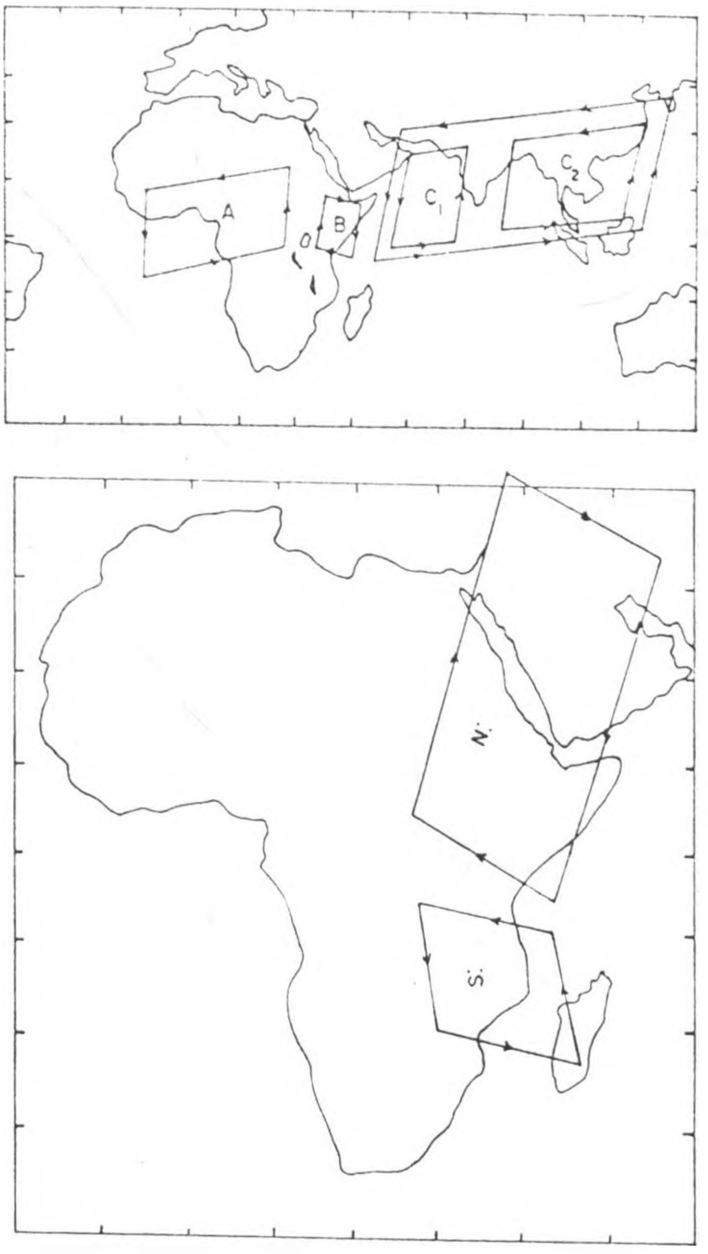

Fig. 26 : Schematic presentation of the cross-section of The divergent mass flux. The arrows indicate the direction of the flow. (a) The zonal (east-west) flow. A represent the eastern Atlantic Ocean cell; B the East Africa cell; C_1 and C_2 represent the western and eastern Indian Ocean cells respectively. (b) the meridional (north - south) flow. S is the southern local Hadley cell and N the northern local Hadley cell.

After Ininda (1995).

Table 18: Significant correlations between June-August SST modes and September-November rainfall.

Atlantic ocean modes (Ak)	Indian ocean modes (I_k)	Red sea modes (Rk)	Pacific ocean modes (Pk)
A1 (40-50°N;0-10°W)	I_1 (20-30°N,50-60°E)	R1 (20-30°N;30-40°E)	P1 (0-10°N,130-140°E)
A2 (30-40°N;10-20°W)	I_2 (10-20°N,50-60°E)	R2 (20-30°N;30-40E°)	P2 (10-20°N;130-140°E)
A3 (20-30°N;40-50°W)	I_3 (0-10°N;80-90°E)		P3 (10-20°N;110-120°E)
A4 (0-10°N;10-20°W)	I_4 (0-10°S;80-90°E)		P4 (10-20°S;140-150°E)
A5 (0-10°N;0-10°E)	I_5 (20-30°S;60-70°E)		
A6 (0-10°S,10-20°E)	I_6 (10-20°S;100-110°E)		
A7 (0-10°S;10-20°W)	I_7 (30-40°S,50-60°E)		
A8 (0-10°;20-30°W)	I_8 (20-30°S;100-110°E)		
A9 (0-10°S;40-50°W)	I_9 (20-30°S;70-80°E)		
A10 (10-20°S;10-20°E)			
A11 (10-20°S;10-20°W)			
A12 (20-30°S;10-20°E)			
A13 (20-30°S,0-10°W)			
A14 (20-30°S;10-20°W)			
A15 (20-30°S,20-30°W)			
A16 (30-40°S;20-30°E)			
A17 (30-40°S;10-20°E)			
A18 (30-40°S,0-10°W)			

Table 18 continues on the next page

Atlantic ocean modes (Ak)	Indian ocean modes (I_k)	Red sea modes (Rk)	Pacific ocean modes (Pk)
A19 (40-50°S;20-30°E)			
A20 (40-50°S,0-10°E)			
A21 (40-50°S,0-10°W)			

Note that Index k represents the respective ocean grid point.

3.7.REGRESSION MODELS

The last section identified the parts of the oceans which were significantly correlated with rainfall over specific locations and seasons of East Africa. Attempts will be made in this section to develop some regression equations which may be used to give one seasonal lead time forecasts for rainfall based on the observed rainfall-SST lagged correlations. The results are presented here on a seasonal basis using the standard seasons of the year.

3.7.1 REGRESSION MODELS FOR DECEMBER TO FEBRUARY RAINFALL SEASON

Figure 24(a) which was shown in section 3.6.3.1, gave the major September-November SST modes for the specific ocean/seas which significantly correlated with December-February rainfall for the various climatological regions of East Africa. December-February is generally dry and hot in many locations apart from some parts of southern Tanzania as it was noted earlier in section 1.3.2 & 3.5.0. It was noted in section 2.10.1.1 that step-wise regression model was adopted in this study. The step-wise regression variables were based on the SST modes which were given in figure 24(a) and table 15 (in section 3.6.3.1). The percentage variance of the seasonal rainfall which is accounted for by the regression equation and the regression coefficients at each grid point are also included in table 19. Results from the regression analysis during the December-February rainfall season indicated that maximum seasonal rainfall variance of 56.1% was accounted for at Mikindani in Southern Tanzania. Most of these variances were accounted for by the first few SST modes. The results therefore showed that 43.9% of the rainfall variance could not be explained by the SST variability.

Table 19: Stepwise regression model for December to February rainfall season for some specific regions using September-November SST modes .

Rinfall regionsnas per Fig.22	step1	step2	step3	step4	step5	step6	step7	step8	V
R20	I_7 .58	P3 .24	A12 .02	I_4 .27	I_6 -.28	A11 .07	A7 .10	P3 -.11	45.0%
R21	P4 -1.24	P3 .30	I_3 .47	I_9 .12	I_4 -.15	I_5 .52			47.9%
R22	A1 .23	A2 .33	A3 .18						23.0%
R23	A12 0.63	A10 0.15	I_7 0.02	I_6 0 33	A1 0 18	A6 -0.09	A11 -0.38	P5 0.38	56.1%
R37	I_7 0.56	I_4 0.16	A12 0.10	I_6 0.21	I_5 0.09	I_3 0.21			40.7%

V = Total of percentage of rainfall variance accounted for. Step i represents the SST mode which was used at i* stepwise regression stage. The corresponding regression constant for the respective mode is given below each mode.

Table 20: Stepwise regression model for March to May rainfall for some specific regions using December to February SST modes.

Rainfall region as per Fig.22	step1	step2	step3	step4	step5	step6	step7	step8	step9	V
R1	I_5 .10	A18 .16	P4 .08	I_3 -.05	P2 .25	A14 -.18				11.2%
R2	A4 - 22	A12 .10	A6 -.14							7.0%
R3	P4 .18	A10 .16	A18 .14	A11 -.36						9.3%
R4	P4 .36	I3 -.40								4.4%
R5	A7 .56	A8 -.25	I2 -.50							27.8%
R7	A14 14	A17 .07	A15 .01	A3 -.46	A7 .31					18.5
R8	P4 -.16	A5 .07	A8 .02	A6 -.11	A1 .35					26.6%
A9	A6 -.01	P3 .84								0.7%
R10	A10 .05	A11 .36	A7 -.10	A6 -.14	I_7 -.04	P4 -.13	I6 .11	A11 - 22		9.4%
R11	I_7 -.09	A10 .01								0.7%

Table 20 continues on the next page

Rainfall regions as per fig.22	step1	step2	step3	step4	step5	step6	step7	step8	step9	V
	A18 -.10	A17 -.26	P3 -.23	P1 .19						8.1%
R13	A12 .06	A2 .16	I_3 .11	A8 -.55	A1 .51	A7 .30				27.8%
R14	A13 .25	P1 .16								10.5%
R16	P3 -.10	A16 .11								1.8%
R17	I_5 -.51	I_2 -.01	A7 -.01	I3 -.01						36.5
R18	A11 -.02									1%
R19	P4 .13	A16 .17								4.3%
R20	A4 -.17									3.0%
R21	A6 -.35	A15 -.28	A17 -.10	I7 -.06	P1 .30	I1 .23	I2 -.31	P3 -.12		16.7%
R22	I_5 .01	I_7 .13	P4 .29	P1 -.10	I_6 .20	I_3 .03				13.6%
R23	A18 .06	P1 .35	A10 .02	P4 -.18	A17 -.18	A19 -.15	I_3 -.36	A5 -.01		41.8%
R24	I_7 -.13	P4 .24								7.5%
R26	A15 .54	A17 -.30	P3 -.14							18.9%
R27	A9 -.01									0.0%
R28	A18 -.14	A17 .15	I_2 -.09	P1	I3	P4				
R29	P1 .32	I_4 -.19	A4 .09	A6 -.66	I3 -.05					29.9%
R30	A6 .19	A18 .23	A14 -.33							14.6%
R31	I_{11} .06									0.3%
R32	A4 .16									2.4%
R33	I_3 .04	I_7 -.02	A14 -.15	A16 -.18	I_6 .08					8.4%
R34	A1 .51	A2 -.23	A4 .09	A9 -.23						23.7%

Table 20 continues on the next page

Rainfall regions as per fig.22	step1	step2	step3	step4	step5	step6	step7	step8	step9	V
R35	P3 .12	I_5 .06	A12 -.19	I_{10}- .51	P4 .50					18.1%
R36	I_5 -.18	I_7 .39	I_2 .44	A1 -.52	P4 .08	I_3 .05	A15 -.32	A17 .02	A18 .28	48.1%
R37	A6 0.35	A15 0.27	A17 -0.10	I_7 0.06	P1 0.30	I_5 0.23	I_2 -0.31	P3 -0.12	A11 0.001	16.7%
R6										
R15										

The same captions as for table 19 apply here. N.B. There were no significant correlations between seasonal SSTs and rainfall for regions 6 and 15.

The close relationships between Atlantic, Indian and Pacific oceans are evident from the table 19. Regression results for the rainfall season of March-May are presented in the next section.

3.7.2 REGRESSION MODELS FOR MARCH-MAY RAINFALL SEASON

March-May is the rainfall season for the region (locally known as the long rainfall season). December -February SST modes were used to develop step-wise regression models. Figure 24(b) and table 16 which were shown in section 3.6.3.2 give the significant SST modes for the specific oceans which significantly correlated with March-May seasonal rainfall. Table 20 presents the SST modes together with the regression coefficients for each mode. Percentage variance which may be accounted for by SST for each climatological region is given in the last column.

It is evident from the results that the maximum rainfall variance explained by all of the SST modes during this season was 48.1%. Thus 51.9% of the rainfall variance could not be explained by the SST variability. The unique characteristics of this season was also observed by Ogallo et al. (1988); Nyenzi et al. (1992); and Ininda et al. (1994) among many others. In the next section, regression model for the June-August rainfall season is presented.

3.7.3 REGRESSION MODEL FOR JUNE-AUGUST RAINFALL SEASON

June-August is generally dry and relatively cold over most parts of the region apart from western parts of the region. Few parts of the coastal region also get some rainfall due to the influence of the East African Low Level Jet and land /sea breeze . March-May SST modes were used in the step-wise regression models for the wet regions during this season. The stepwise regression variables were based on the SST modes which were given in figure 24(c) and table 17 (in section 3.6.3.3). The generated regression models are presented in

table 21.

During this season (June-August) a maximum variance of 71.6% accounted for by the SST modes occurred in Eastern Uganda in region 7 represented by Mbale. Over the northern Uganda ,western Kenya and coastal strip the SST modes explained about 67.9%, 43.9%, 34.3% of the variances respectively. Over eastern Kenya, northwestern Kenya including northeastern Uganda relatively very low percentage of variance of about 39% and 40.2% respectively were explained by the SST modes. It should be noted that some of these locations are extremely dry during this season. The high V values could be due to the influence of zero rainfall values as discuss in the correlation section. The following section gives the regression model for the season of September to November.

3.7.4 REGRESSION MODELS FOR SEPTEMBER-NOVEMBER RAINFALL SEASON

September-November is generally one of the major rainfall seasons for the region (short rainfall season). June-August SST modes were used in this case. The stepwise regression variables were based on the SST modes which were given in figure 24(d) and in table 18 (in section 3.6.3.4). Table 22 gives the stepwise regression models which were identified for the specific locations. The results from the table 22 show no significant correlations between SST and seasonal rainfall for the regions 13, 15, 18, 26 and 29.

Regression models for the season of September-November as given in table 18 also indicate the significant influence of Atlantic, Indian and equatorial Pacific oceans on regional rainfall. During this season (September-November) the SST modes generally explained higher rainfall variance at most of the locations when compared to the other seasons. The SST modes also explained high variance during the relatively dry seasons of June-August and December-February for the specific locations.

Table 21: Step-wise regression model for June-August rainfall for some specific regions using March-May SST modes

Rainfall region, as per fig.22	step1	step2	step3	step4	step5	step6	step7	step8	V
R1	A21 .06	A7 -.30	A12 -.14	I_6 -.25	I_7 .38	A20 -.24	A14 .41	A11 .27	67.9%
R2	P2 .44								19.2%
R3	I_5 -.52	A11 .46	A6 -.07	A1 -.27	P1 .13				61.3%
R4	A1 -.54	A10 .29	A7 -.04	A3 - 04	I_5 -.05	P8 -.24			46.8%
R6	P7 -.19	P4 -.25	I_5 -.03	I_6 -.14	P9 .02	A15 .28	I_3 .23		46.2%
R7	P8 -.08	P7 -.40	A7 .39	I_5 -.01	A12 -.35	I_6 - 08	P5 .46	A6 -.25	71.6%
R8	P1 -.48	A7 .1	P4 -.28	I_4 .11	A2 .26	I_{12} -.11	I_5 .36	I_7 -.47	70.6%
R18	A12 .35	A4 -.17	P5 .03	P7 -.34	P8 -.13				39.1%
R23	A6 -.18	I_4 .37	I_6 -.25						34.3%
R24	I_1 .03	I_3 .3	A4 - 22	A3 .17					27.0%
R27	I_1 .42	I_3 .15	I_2 -.12	I_4 .44	R1 .26				39.2%
R32	A20 -.34	A7 .33	A4 -.13	A3 -.14					34.8%
R33	I_8 -.32								10.5%
R34	I_6 .60	I_7 -.38	I_5 -.36	I_8 -.30	A21 .67	A20 -.24	A7 .05		43.9%
R35	I_5 -.39	I_{12} .38	A7 .23	A8 -.37					32.4%
R36	A4 .32	A3 .09	A6 .26	A1 -.23	A14 .26	I_{11} .09			40.2%

The same captions as for table 19 apply here.

Table 22: Stepwise regression model for September-November rainfall season for some regions using June- August SST modes.

Rainfall region as per fig.22	step1	step2	step3	step4	step5	step6	step7	step8	step9	V
R1	A10 -.65	A18 -.42	I_7 -.25	A15 .07	6 -.08	I_2 .16	A16 0.03	A11 .13		58.7%
R2	I_1 .21	I_2 -.37								17.6%
R3	A1 .42	A2 -.08	A15 -.48	A18 .24						44.3%
R4	A11 .28									11.2%
R5	I_4 .37									13.6%
R6	A4 .22	A12 .21	P4 .33	A11 -.08	I_2 -.2	P2 -.27				50.6%
R7	A14 -.25	A17 -.21	I_3 -.25							25.5%
R8	A18 -.21	A17 -.64	A1 .23	A16 .40	A3 .16	A2 .28	17 -0.33			58.1%
R9	I_4 -.70	I_6 -.21	P3 .09	I_3 -.35	P4 .38					33.8%
R10	I_4 .24	A3 .27	A6 .03	I_6 .27	P2 -.04	A18 -.24	P1 0.12	I_3 .08		54.8%
R11	A3 .45	A4 -.09								20.5%
R12	A2 -.29	A20 -.19	A18 -.08	P4 .25	A4 .17					40.3%
R14	A4 .07	A6 .24	A18 .01	A19 -.02	A13 -.29	A21 -.16	14 0.26	I_6 -.29		27.1%
R16	A21 -.42									17.2%
A17	I_4 .23	P4 .78	P1 .31							22.7%
R19	P4 -.31	A15 -.25	A6 .12							27.5%
R20	P4 .34	A6 -.28								23.4%
R21	A11 -.32	P4 -.21								18.5%
R22	I_3 .30	P1 -.23	I_4 .29							21.5%
R23	P4 1.5	I_4 .32	P1 -.54	A18 -.22	I_3 .02	A17 .01				43.8%
R24	A18 -.38	A19 -.11	I_4 .47	P4 -.18	I_3 -.03					32.9%

Table 22 continues on the next page

Rainfall region as per fig.22	step1	step2	step3	step4	step5	step6	step7	step8	step9	
	P3 .08	I_3 -.37	A5 .23	I_4 83	I_6 -.32	A18 - 20	A19 .07			35 0%
R27	I_4 .46	I_6 -.21	A18 -.39	A19 -.10	P3 -.01	I_3 .15	A5 -.13	A7 .16	A6 -.03	38.1%
R28	I_6 .37	I_4 .12	P1 .27	p4 .09						29 6%
R30	A21 -.34	A10 -.25	A17 -.12	A15 -.43	A4 .03	A6 .22	A19 0.27	A13 .05	A18 -.13	12.7%
R31	I_8 .34									11.6%
R32	I_2 -.41	P3 -.17	A12 .25							31.0%
R33	A18 -.48	A19 -.17	R1 .30	P3 -.10	I_3 .07	A6 -.09	I5 0.37	I_6 -.20		50.8%
R34	A3 .34	A18 -.31	A19 -.20	A21 .10	A2 .28					36.5%
R35	I_2 -.51	I_1 .17								18.0%
R36	A10 -0.40									13.1%
R37	P4 0.33									11.1%

The captions of table 19 apply here.

The variance values were largest in these seasons in some regions.

However, during the season of March-May, the SST modes explained the lowest variance in most of the locations. It should be noted that during September-November season SST modes accounted for a maximum of up to 58.7% of rainfall variability. Therefore, only 41.3% could not be accounted for by SST variability in this season. Skillful prediction of the seasonal rainfall over the region would therefore require the incorporation of other predictors. The predictive potential of September-November seasonal rainfall using SST modes was also observed by Ogallo et al. (1988); Nyenzi et al. (1992); Farmer (1987); Ininda et al. (1994), (1995); Hastenrath et al. (1993) among others. It should be however noted that the variances of rainfall which were accounted for by SSTs were generally low at most locations.

In the next section, the regression models based on the time coefficients of areal seasonal rainfall and SST modes are presented.

3.8.0 REGRESSION MODEL USING TIME COEFFICIENTS

The models presented in the previous section were derived from representative rainfall station from each of the homogeneous regions and areally averaged SST records. The rainfall station with the highest communality was used to represent the individual homogeneous rainfall zones. The problems associated with these approaches have been discussed in section 2.3.0. The number of SST modes (grid averages) used in the prediction were also relatively very many. Attempts were made in this section to use time coefficients of rainfall and SST rotated principal component analysis (RPCA) modes to represent the various rainfall and SST variables. This approach significantly reduces the complexity of the spatial dimension and the number of SST predictors. Under this method the dominant rainfall and SST RPCA

modes were determined for each region and the corresponding time coefficients calculated. These represented areal rainfall and SST records respectively for the subregions. The results from PCA indicated that an average of about four RPCA modes were significant. The rainfall time coefficients were therefore regressed with the time coefficients of the SST modes up to the fourth principal component for each of the oceans independently. Results which were obtained from the study are given in tables 23 to 26 for some specific regions. It should be noted that the regressions were done at one seasonal SST time lead.

The results from the study indicated some significant correlations between time coefficients of seasonal rainfall over several sub-regions and the first four components of Atlantic, Indian, western and central Pacific oceans. The degree of seasonal rainfall variance explained by the SST regressions however varied significantly from region to region as indicated in the tables of the results. For example during the season of December-February, the seasonal rainfall in southern Tanzania was significantly correlated with the second and third modes of Indian ocean. These ocean modes represent EL-Niño and ENSO activities (Ininda 1995). However,it is clear from table 23 that the seasonal rainfall in Southern Tanzania was also correlated with the fourth mode of Atlantic ocean. Folland et al. (1991) also found that the rotated fourth component of Atlantic ocean was one of the good predictors for the sea surface temperature anomalies. The first, second and fourth components of Pacific ocean were significantly associated with seasonal rainfall in southern Tanzania. When compared with the results obtained in section 3.7.1, time coefficient method still explained low rainfall variance. Regression equation for December to February is given in table 23. Southern sector of Tanzania/central southern accounted largest/lowest rainfall variance respectively compared to the other sectors as given in table 23.

The results obtained for the season of March to May (table 24) indicated significant

correlations between seasonal rainfall and some of the rotated SST modes for the individual oceans. The first global SST mode represents the global mean SST pattern (Ininda 1995). The results of the study indicated that over Indian and western Pacific oceans, the first mode explained low seasonal rainfall variance over most of East Africa. This again is a reflection of the low correlations between seasonal rainfall and SST during the long rains (section 3.7.2). However over Atlantic ocean, the SST first mode was correlated with several seasonal rainfall locations in East Africa. This seems to indicate that changes in SST patterns over Atlantic ocean are related with wet/dry conditions in East Africa. Rainfall over several locations were however correlated with the second mode over Atlantic and west Pacific. This seems to indicate the potential influence of the ENSO modes over western Pacific and Atlantic oceans on seasonal rainfall in East Africa. Seasonal rainfall over several locations were also correlated with the third SST modes of the Indian and Atlantic oceans. The fourth SST modes for the individual oceans were also significantly correlated with seasonal rainfall over several sub-regions of East Africa during the long rainfall season. It is evident from table 24 that most of the developed regression equations accounted for relatively low percentage of seasonal rainfall variance. Some parts of eastern Uganda including some sectors of western Kenya/coastal strip and western parts of lake Victoria accounted the largest/lowest rainfall variance respectively when compared to other sectors (table 24).

During June to August season, East Africa is generally dry. Therefore regression analysis was carried out only for some of the sub-regions which experience rainfall during this season. The regression equations for this season are given in table 25. The regression equations accounted for very low proportions of seasonal rainfall variance. The results from the table 25 indicated that the seasonal rainfall over northern Uganda and western Kenya was correlated with the first and fourth modes over Atlantic and Indian oceans. This seems to

indicate the linkage between low and medium level westerlies emanating from Atlantic ocean which might be associated with SST during this season. Warmer conditions over northwestern Indian ocean have been associated with weaker southwesterlies due to strong oceanic convection (Cadet 1985 ; Ininda 1995). Such a scenario would favour the penetration of the moist westerlies emanating from south Atlantic ocean and enhance rainfall over northern and eastern Uganda including some parts of western Kenya (Bärring 1988; Ogallo 1988; Anyamba et al. 1985; Ininda 1995 among many others). During this season west and central Pacific ocean modes were also correlated with seasonal rainfall over very few locations (table 25). Northwestern Uganda/eastern Uganda accounted for largest/lowest seasonal rainfall variance respectively when compared to the other sectors during this season (table 25).

During the short rainfall season (September to November), rainfall over several sub-regions were significantly correlated with the first rotated component over Indian and Atlantic oceans. The first mode represents the ocean SST mean patterns. The results from the study therefore indicate that inter annual variations in the mean SST patterns over the two oceans had a significant impact on the rainfall variations in East Africa. SST regression equations for this season also explained highest rainfall variance at most of the sub-regions (table 26). Some parts of central Tanzania/western Kenya accounted for largest/lowest seasonal rainfall variance respectively when compared to other sectors (table 26).

The regression models used in this study were fitted using data for the period 1940-1975. The skill of the fitted models were tested using the data for the period 1976-1990. The forecast skills of the models were tested by Root Mean Square Error (RMSE). Large values of RMSE indicated large difference between observed and predicted rainfall series while low values of RMSE indicated better skill.

Table 23. Variance accounted for at each regression step with time coefficient model for the rainfall of season of December-February and using SSTs for the season of September-November.

Regions as per fig.22	Step1	Step2	Step3	Step4	Step5	ALL AT	ALL I_N	ALL PC	ALL oceans
REG 19	I_{N2} 2.6	PC2 2.6				.7	9.9	6.1	23.8
REG 20	I_{N3} 2.9	PC4 2.8	PC1 2.7	PC2 2.6	I_{N2} 2.6	1.5	8.0	10.3	22.0
REG 22	AT1 2.9	PC2 2 8	PC4 2.8	PC1 2.8	I_{N2} 2.6	7.3	8.7	10.8	23.7
REG 21	AT2 3.0	I_{N2} 2.9	AT4 2.8			9.5	11.0	2.5	32.8

N.B. V maximum = 100. The figures indicate percentage variance explained by each SST mode. Note: REGI refers to rainfall region i as per figure 22. ATi,INi and PCi represents the i' SST mode over the Atlantic, Indian and Pacific oceans respectively. ALL AT refers to Total variance of seasonal rainfall dominant mode accounted for by the first four modes of Atlantic ocean. ALL IN refers to Total variance of seasonal rainfall dominant mode accounted for by the first four modes of Indian ocean. ALL PC refers to Total variance of seasonal rainfall dominant mode accounted for by the first four modes of Pacific ocean.

Table 24:Variance accounted for at each regression step with time coefficient model for the rainfall season of March-May and using SSTs for the season of December-February.

Region as per fig.22	Step1	Step2	Step3	Step4	Step5	Step6	ALL AT	ALL I_N	ALL PC	ALL oceans
REG1	AT1 2.9	APC4 2.8	I_{N3} 2.1				5.8	7.5	10.4	31.5
REG2	AT4 3.0	I_{N3} 2.9	PC1 1.9	PC4 1.6			3.3	9.1	9.4	31.1
REG3	PC4 2.9	I_{N2} 2.8	I_{N1} 2.8	AT1 2.7	I_{N4} 2.6	AT3 2.4	7.1	11.6	11.7	24.6
REG4	I_{N2} 3.0	AT4 3.0	I_{N1} 2.9	PC2 2.8	I_{N4} 2.7		8.0	11.0	9.2	30.2
REG5	I_{N1} 2.9	I_{N3} 2.9	AT1 1.7	AT3 1.7	PC3 1.6	PC2 1.1	4.1	9.0	10.3	26.6
REG6	PC3 2.9	I_{N3} 2.8	AT2 2.8	PC1 2.3	AT3 1.4		7.8	11.1	11.2	29.6

Table 24 continues on the next page

Region as per fig.22	step1	step2	step3	step4	step5	step6	ALL AT	ALL IN	ALL PC	ALL oceans
REG7	PC3 3.9	PC1 2.7	IN3 2.7	AT2 2.7	AT3 2.6	PC2 2.4	6.8	11.4	10.9	34.7
REG8	IN1 2.9	PC4 2.9	AT1 2.9	IN3 2.6	IN2 2.5	AT4 2.1	5.6	10.1	6.7	28.6
REG9	AT1 2.9	AT3 2.9	IN2 2.8	IN1 2.8	AT4 2.8		10.8	11.1	3.2	31.6
REG10	AT4 2.9	AT3 2.8	PC3 1.9				11.1	5.3	5.0	26.8
REG11	IN1 3.0	AT4 2.9	IN4 2.7	IN1 2.6	AT2 2.0	AT3 1.1	11.6	11.4	2.1	30.4
REG12	AT4 2.5	AT2 2.3	AT1 2.2	IN3 2.2			7.6	10.5	2.7	28.5
REG13	IN2 2.9	IN1 2.9	IN4 2.9	AT3 2.9	PC1 2.0	PC4 1.9	3.8	4.5	11.3	19.6
REG14	PC2 3.0	IN3 2.9	PC1 2.8	AT4 2.6	AT2 2.0		5.7	5.3	6.8	23.9
REG15	AT4 2.8	IN4 2.7					11.8	5.4	1.8	20.1
REG16	AT1 2.9	AT4 2.6	AT3 1.8	IN4 1.5	AT2 1.2		11.2	10.4	3.5	28.7
REG17	AT2 3.0	IN1 3.0	AT1 2.9	PC4 2.2			11.6	7.2	7.6	33.6
REG18	IN4 2.9	AT1 2.9	IN1 2.8	AT4 2.8	PC2 2.8	PC1 2.8	11.1	11.4	7.7	31.6
REG19	PC4 2.9	PC3 1.3	AT1 1.3	IN1 1.3			2.5	7.3	7.8	27.6
REG20	PC4 2.9	AT4 2.9	PC4 2.8	AT2 2.7	IN3 2.6	IN1 2.5	9.0	11.7	10.5	26.8
REG21	PC4 7.8	AT1 7.3	IN1 7.0	IN2 5.3	IN4 2.0	AT4 2.9	8.2	10.8	10.8	25.0
REG22	AT1 2.9	IN2 2.9	IN3 2.9	PC3 2.9	IN1 2.9	IN4 2.8	10.7	8.1	7.8	22.6
REG23	PC3 2.9	PC1 2.8	PC2 2.8	AT2 1.7	PC4 1.5		3.1	11.6	7.2	19.4

Table 24 continues on the next page

Regions as per fig 22.	step1	step2	step3	step4	step5	step6	ALL AT	All IN	All PC	All oceans
REG24	IN4 2.9	AT2 2.9	PC2 2.9	PC4 2.7	IN3 2.0		11.4	11.7	10.1	32.5
REG25	PC2 3.0	AT3 2.9	PC1 2.9	IN4 2.8	PC3 2.8	IN3 1.2	5.4	10.4	9.2	28.5
REG26	AT4 6.7	AT1 6.1	IN1 4.0	PC2 3.6	IN2 3.1	AT3 2.5	11.6	11.7	11.7	26.1
REG27	AT2 2.9	AT4 2.9	PC4 2.8	IN2 2.6	PC2 2.4	IN4 2.0	9.5	9.5	10.3	27.1
REG28	AT4 2.9	PC2 2.9	PC1 1.9	IN3 1.5			6.6	4.6	9.8	24.4
REG29	IN4 2.7	PC4 2.0	IN1 1.6	IN2 1.3			3.9	10.8	11.6	32.8
REG30	AT3 2.9	IN4 1.8	AT2 1.3	IN2 1.0	PC3 1.0		7.6	11.4	3.1	31.8
REG31	IN3 2.9	AT2 2.9	AT3 2.9	AT4 2.8	IN4 1.4	PC2 1.2	10.8	9.5	2.9	30.9
REG32	IN4 2.8	PC4 2.3	IN3 2.1	AT1 1.4			6.5	10.5	11.0	31.3
REG33	AT3 2.9	AT4 2.7	PC4 1.8	AT2 1.1			11.3	7.7	11.6	29.4
REG34	AT2 2.9	PC2 2.9	AT3 1.9				11.5	4.2	10.7	32.0
REG35	PC4 2.9	IN4 2.9	AT1 1.1				5.5	9.3	11.6	34.6
REG36	IN4 2.9	AT4 2.8	AT3 2.1	IN3 2.0	AT2 1.6	PC3 1.2	11.6	10.5	5.4	33.8

N.B Captions on this table are the same as in table 23.

Table 25 Variance accounted for at each regression step with time coefficient model for the rainfall season of June-August and using SSTs for the season of March-May.

Region as per fig 22	Step1	Step2	Step3	Step4	Step5	Step6	Step7	ALL AT	ALL IN	ALL PC	ALL oceans
REG1	IN2 2.9	PC1 2.9	AT4 2.8	IN3 2.8	IN1 2.7	IN4 2.7	PC2 2.7	10.0	9.1	8.0	31.1
REG2	IN4 2.8	IN1 2.8	AT1 2.5	AT3 2.1	PC2 1.6	PC3 1.0		8.3	8.9	10.0	23.6
REG3	IN4 2.7	IN1 2.7	AT3 2.7	IN3 2.6	AT2 2.6	AT1 2.5	PC4 2.0	7.4	10.7	10.4	23.9
REG7	IN2 2.8	AT2 2.7	AT1 2.7	AT4 2.7	PC2 2.7	IN1 2.6	IN3 2.5	9.5	9.1	9.5	22.2
REG23	IN4 2.9	IN3 2.8	AT2 2.7	PC4 2.2	IN1 1.7	AT4 1.5		11.4	3.6	5.0	29.5

N.B Captions are the same as in table 23.

Table 26: Variance accounted for at each regression step with Time coefficients model for the rainfall season of September-November and using SSTs for the season of June-August .

Regions as per Fig.22	Step1	Step2	Step3	Step4	Step5	Step6	ALL AT	ALL IN	ALL PC	ALL Oceans
REG1	IN4 2.8	AT3 2.8	AT1 2.5	PC4 2.0	PC3 1.3		7.4	9.9	6.9	25.6
REG2	PC4 2.8	PC3 2.8	AT4 2.8	IN4 2.6	AT2 1.0		7.2	11.1	9.6	24.6
REG3	PC3 2.8	PC4 2.7	IN4 2.6	AT4 2.4			7.5	10.4	11.0	27.3
REG4	IN4 2.8	AT2 2.8	PC3 2.7	IN1 1.2			8.3	11.4	5.5	25.7
REG5	AT1 2.9	AT2 2.9	IN1 2.9	AT4 2.8	PC3 2.8	IN2 2.8	9.5	6.3	8.9	21.6
REG6	PC3 2.6	AT2 2.6	PC1 2.1	PC2 1.9	IN1 1.7	AT1 1.2	10.3	6.6	11.3	21.7
REG7	AT1 2.8	AT4 2.6	IN1 2.1	IN2 1.7	AT2 1.4	PC3 1.2	8.4	5.3	4.3	15.3

Table 26 continues on the next page

Regions as per fig.22	step1	step2	step3	step4	step5	step6	ALL AT	ALL IN	ALL PC	ALL OCEANS
REG8	IN2 2.8	IN1 2.6	AT1 2.5	AT4 1.6	IN3 1.5	AT3 1.4	11.0	10.8	1.3	29.6
REG9	AT2 2.8	AT1 2.8	IN2 2.7	IN1 2.7	PC3 2.7	PC1 2.4	11.3	11.4	7.9	25.5
REG10	AT1 2.7	IN2 2.7	IN1 2.7	PC2 2.7	PC1 2.7	AT2 2.6	11.0	11.0	10.9	27.8
REG11	AT2 2.8	AT1 2.8	IN2 2.8	IN1 2.8	AT4 2.7	IN3 2.7	11.0	9.4	4.2	32.6
REG12	AT4 2.8	IN2 2.8	PC1 2.8	PC4 2.8	PC3 2.8	IN1 2.7	11.1	10.9	11.2	29.9
REG13	IN1 2.8	IN3 2.7	AT1 2.7	AT2 2.6	AT4 2.6	PC2 2.0	11.3	7.1	5.0	32.1
REG14	PC3 2.9	IN1 2.8	AT1 2.8	IN3 2.8	AT4 1.9	PC4 1.4	8.2	7.9	6.2	18.3
REG15	PC4 2.9	IN4 2.9	IN3 2.8	AT1 2.6	IN1 2.6	IN2 2.3	11.0	10.2	5.0	34.0
REG16	PC3 2.8	PC4 2.8	IN1 2.8	AT1 2.8	IN2 2.8	IN3 2.5	10.5	5.3	10.3	21.7
REG17	PC3 2.8	PC4 2.8	IN1 2.8	IN3 2.8	IN2 2.0	AT3 1.5	4.1	4.8	9.1	14.5
REG18	PC1 2.7	AT2 2.7	IN3 2.7	PC2 2.6			6.8	7.7	11.3	25.0
REG19	AT4 2.8	AT3 2.8	IN4 2.8	PC3 2.7	AT1 2.7	PC4 2.6	10.0	4.6	10.3	33.4
REG20	IN3 2.8	IN2 2.8	AT4 2.8	PC4 2.7	IN1 2.7	AT1 2.4	10.7	11.4	11.3	28.6
REG21	PC3 2.7	PC4 2.7	AT1 1.6				5.8	1.9	10.8	30.4
REG22	AT4 2.7	PC4 2.6	AT1 2.0	AT2 1.7			7.7	1.2	11.4	22.1
REG23	IN3 2.9	IN4 2.8	AT4 2.7	IN2 2.7	AT1 2.5	AT2 2.5	11.0	10.3	3.9	32.9
REG24	IN2 2.8	AT1 2.8	IN1 2.5	AT2 2.2			.9	10.0	10.9	32.7
REG25	IN3 2.8	IN2 2.8	AT4 2.8	AT1 2.7	IN1 2.6		11.1	9.3	1.4	19.7

Table 26 continues on the next page

Regions as per fig 22	step1	step2	step3	step4	step5	step6	ALL AT	ALL IN	All PC	All oceans
REG26	IN1 2.8	IN3 2.3	AT4 1.9				2.7	8.6	2.8	15.5
REG27	AT1 2.8	AT4 2.8	IN2 2.8	IN1 2.6			.5	11.3	1.5	19.5
REG28	IN3 2.9	AT2 2.8	PC3 2.8	IN1 2.8	PC4 2.7	PC1 2.7	10.6	8.9	10.8	27.6
REG29	IN1 2.8	AT2 1.1	IN2 1.8	PC3 1.4			1.5		4.2	21.1
REG30	AT4 2.9	AT2 2.8	IN2 2.8	IN4 2.8	IN1 2.6		11.1	9.5	3.7	30.0
REG31	AT2 2.5	AT3 2.1	IN4 1.3				10.8	1.9	6.4	26.5
REG32	IN3 2.8	AT2 2.8	PC3 1.6	AT1 1.3			6.3	11.0	3.0	28.2
REG34	PC2 2.9	IN1 2.8	AT1 2.8	PC1 2.8	IN4 1.4		3.7	10.4	4.9	20.4
REG35	IN1 2.8	AT1 2.6	AT3 1.4	IN2 1.3	PC4 1.1		4.8	7.5	2.9	11.5
REG36	AT4 2.8	IN2 2.8	AT1 2.6	IN1 2.6	IN3 2.3	PC3 1.6	11.4	9.8	4.0	23.3

N.B. Captions are the same as those in table 23.

The values of RMSE which were obtained at the specific locations for the different seasons are indicated in table 27. The forecast time series which were derived with the specific regression equations are shown in figures 27 to 30. The skill of the regression equations are generally low in many locations as can be seen for the high RMSE values. Largest RMSE values were obtained for the long rainfall season especially during the years with extremely large rainfall anomalies as can be seen in figures 28(a) to 28(j).

The results from this study also indicated that residual errors were low during the short rainfall season in most of the sub-regions. Section 3.6.3.4 indicated that highest correlations were observed between SST and rainfall during this season. Highest correlation values were concentrated over the coastal and lake Victoria regions. These climatological regions have strong meso-scale circulations associated land-sea/lake breeze circulations. Regions of high terrain also experience induced thermal circulations. The predictive potential of the June to August and short rains seemed to be attributed to the fact that SSTs explain relatively high rainfall variances during these seasons. The high predictive potential of seasonal rainfall of June to August and September to November was also observed by (Ogallo, 1988; Farmer 1985; Nyenzi, 1992; Ininda 1995 among several others).

Summary of the major results, conclusions from the study as well as recommendations for the future work as a follow up of this study will be presented in chapter four.

Table 27: Model test of skill results when root mean square error (RMSE) was applied.

Rainfall region as per figure 22	December-February season	March-May season	June-August season	September-November, season
1	1.2	0.9	1.3	1.0
2	1.0	0.9	1.1	1.1
3	0.7	1.1	0.7	0.8
4	1.1	1.5	1.2	1.2
5	N/A	1.1	N/A	1.0
6	0.9	N/A	1.4	0.9
7	1.0	0.9	1.0	1.1
8	N/A	1.0	1.7	1.4
9	N/A	1.0	1.1	0.9
10	0.9	0.9	N/A	1.4
11	1.1	0.9	1.4	1.0
12	N/A	N/A	1.3	0.8
13	1.4	1.1	1.0	1.0
14	N/A	N/A	0.9	N/A
15	1.0	1.0	N/A	1.0
16	0.9	1.0	0.8	N/A
17	0.9	1.0	1.0	N/A
18	N/A	1.2	1.2	1.1
19	1.1	1.0	N/A	1.1
20	1.3	N/A	1.1	N/A
21	1.1	1.2	1.3	1.1
22	0.9	1.0	1.1	N/A
23	1.0	1.0	1.0	1.1
24	N/A	N/A	N/A	N/A
25	N/A	1.0	1.2	0.9

Table 27 continues on the next page

Rainfall region as per figure 22.	December-February season	March-May season	June-August season	September-November. season
26	1.0	1.1	1.0	N/A
27	N/A	1.0	0.9	1.0
28	1.3	1.0	1.3	1.2
29	1.0	1.3	1.0	N/A
30	N/A	1.0	0.9	1.1
31	N/A	1.2	1.0	1.0
32	N/A	0.9	1.2	1.0
33	1.3	1.0	1.1	0.8
34	1.0	0.9	1.1	1.0
35	1.2	1.0	1.3	N/A
36	N/A	1.1	0.9	N/A

N/A means that there was no value for model validation either due to lack of data for observe series or there were no significant correlations between seasonal rainfall and seasonal SSTs.

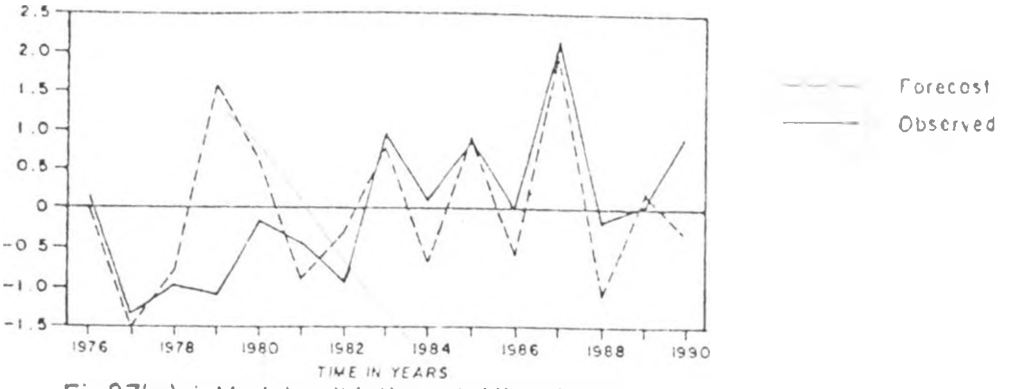

Fig 27(a) : Model validation at Mikindani during the season of December – February

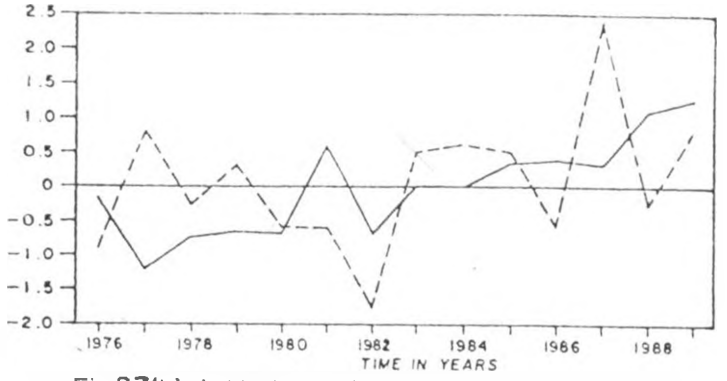

Fig 27(b) : Model validation at Kondoa during the season of December – February

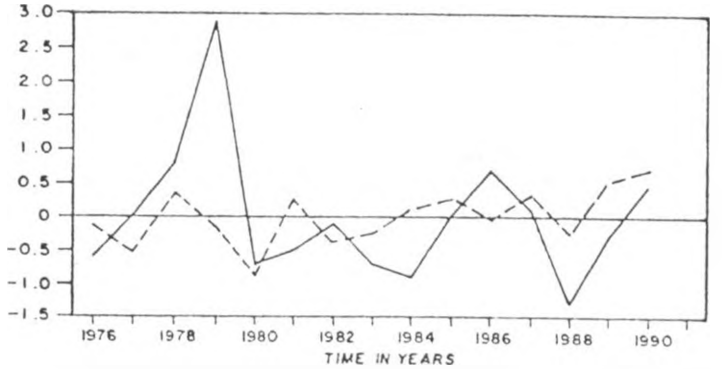

Fig 27(c) : Model validation at Mombasa during the season of December – February

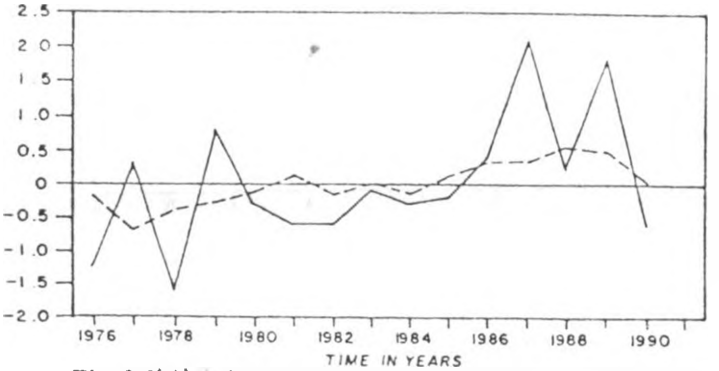

Fig. 27(d) : Model validation at Mbulu during the season of December – February

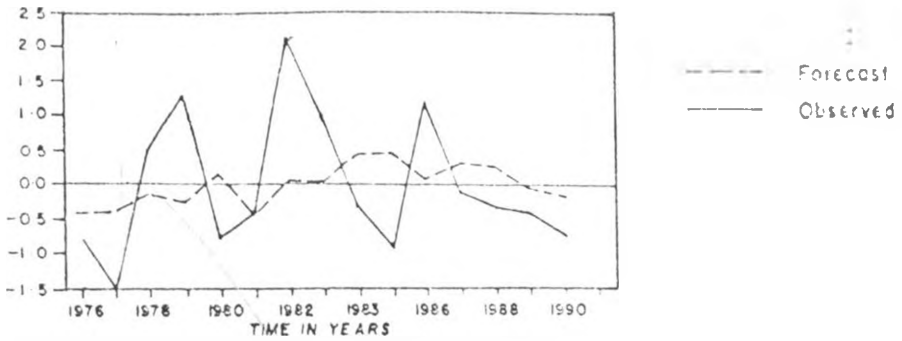

Fig.28(a) : Model validation at Mombasa during the season of March — May

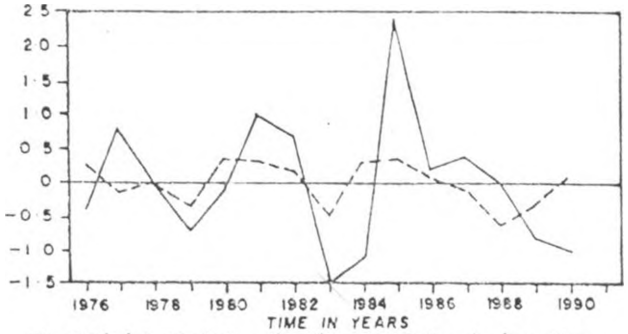

Fig.28(b) : Model validation at Gulu during the season of March — May

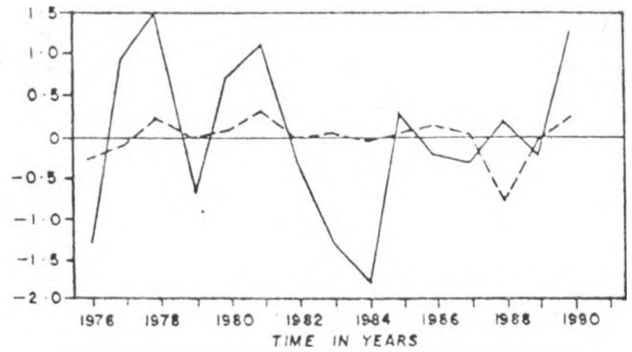

Fig.28(c) : Model validation at Naivasha during the season of March — May

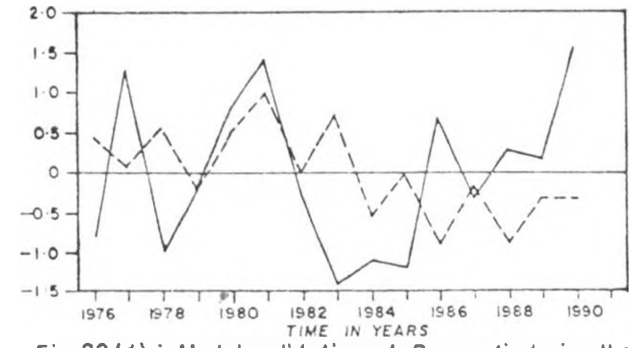

Fig.28(d) : Model validation at Rumuruti during the season of March — May

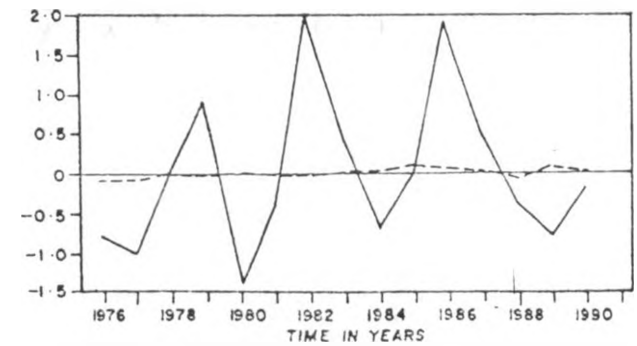

Fig.28(e) : Model validation at Lamu during the season of March — May

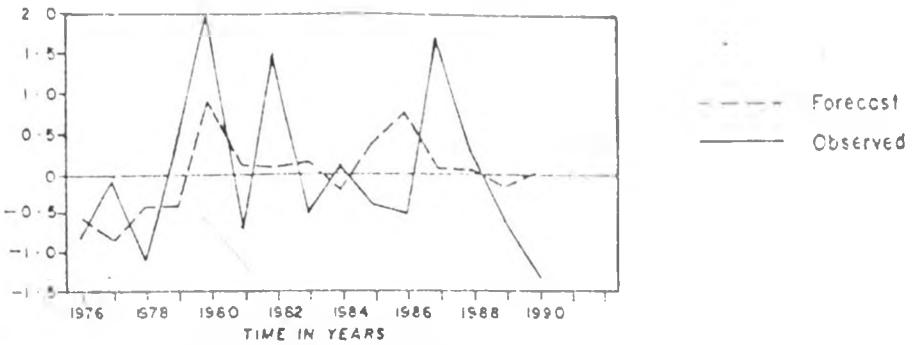

Fig. 29(a) : Model validation at Voi during the season of June — August

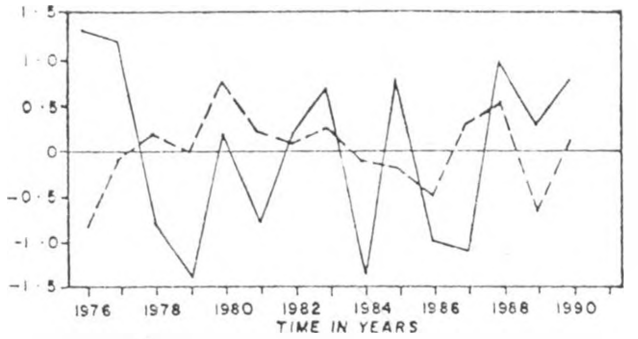

Fig 29(b) : Model validation at Gulu during the season of June — August

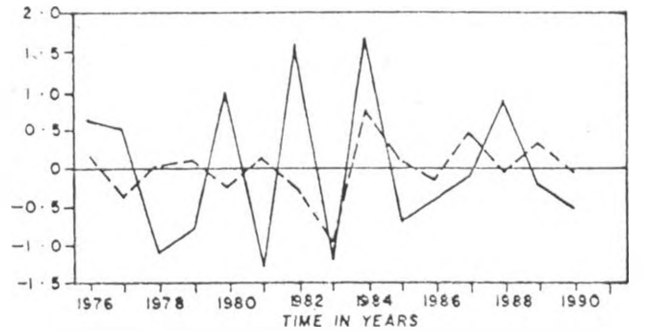

Fig. 29(c) : Model validation at Kaisho during the season of June — August

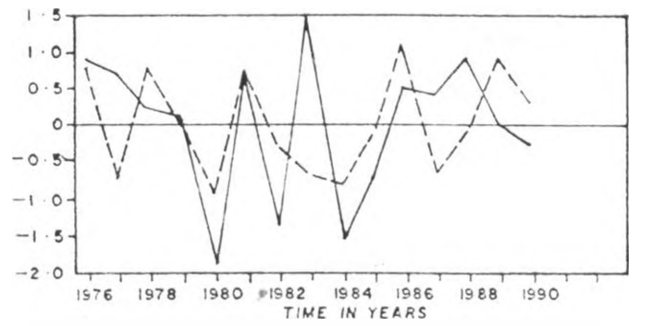

Fig. 29(d) : Model validation at Rumuruti during the season of June — August

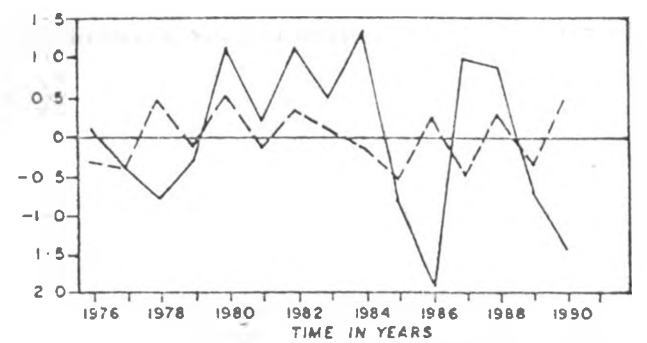

Fig. 29(e) : Model validation at Mombasa during the season of June — August

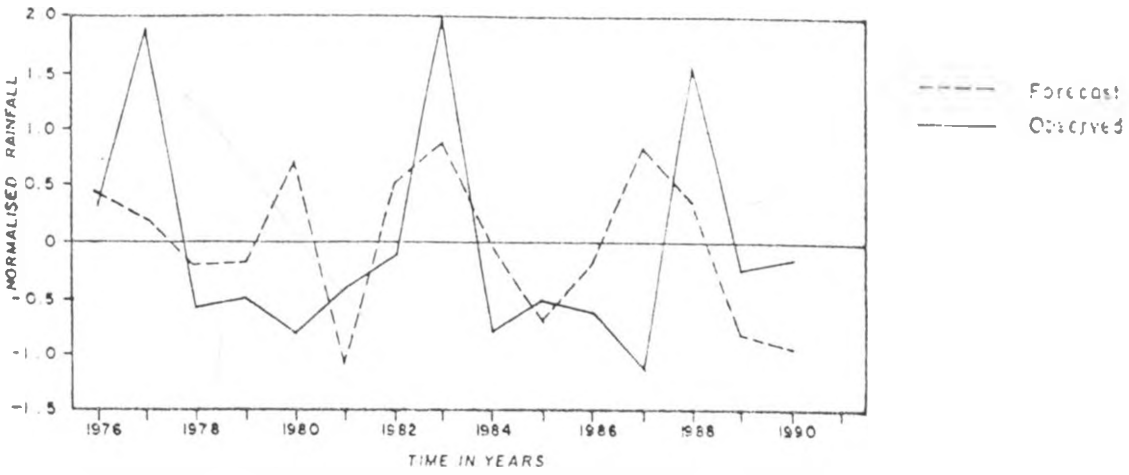

Fig. 30(a): Model validation at Mbarara during secson of September — November

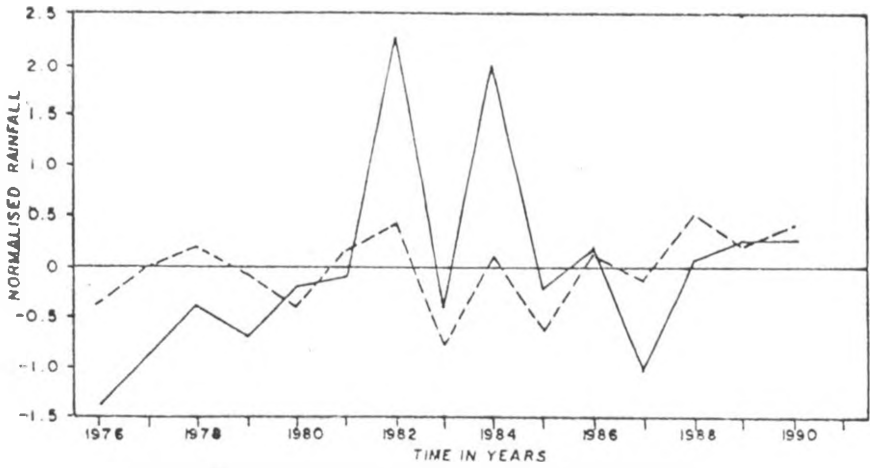

Fig. 30(b) : Model validation at Kajiado during season of September — November

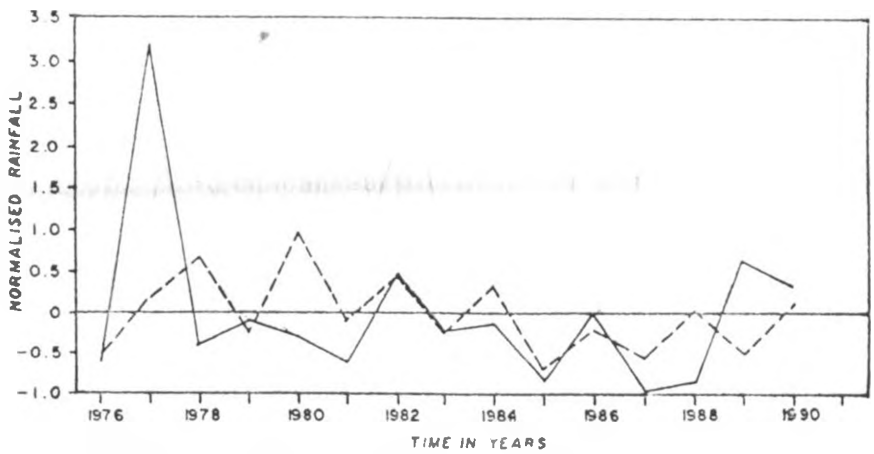

Fig. 30(c) : Model validation at Rumuruti during season of September — November

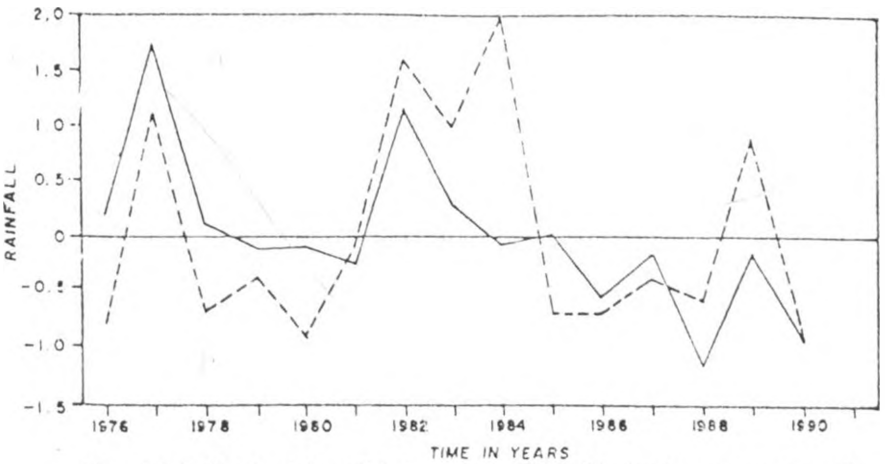

Fig. 30(d): Model validation at Chemili during season of September — November

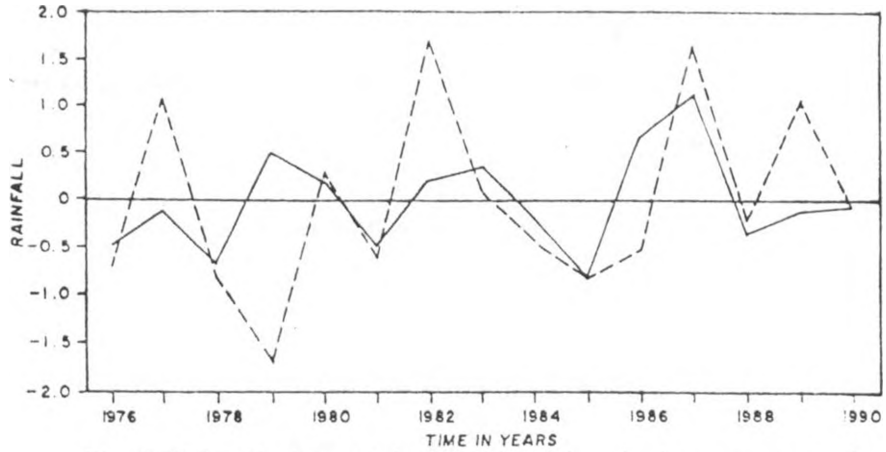

Fig. 30(e): Model validation at Jinja during season of September — November

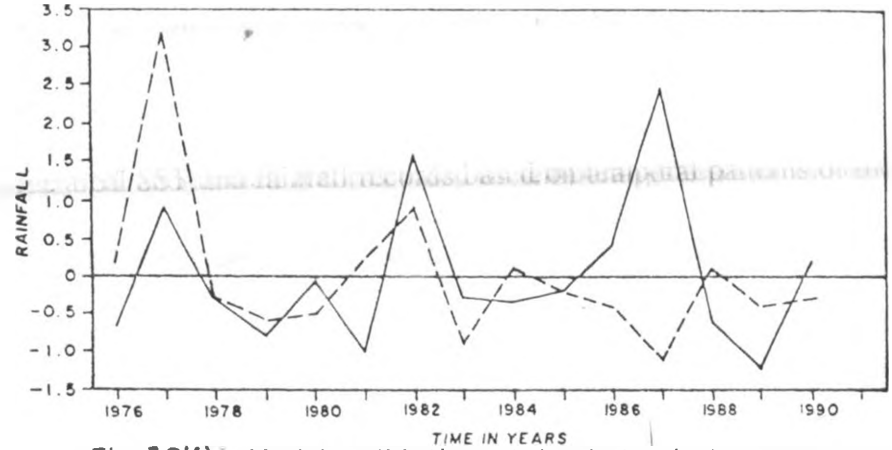

Fig. 30(f): Model validation at Lushoto during season of September — November

The quality control test indicated no heterogeneity in most of the rainfall time series. The few rainfall time series which were heterogeneous were randomly distributed in the region. No significant trends could also be detected at most of the locations. The spatial patterns of the seasonal rainfall anomalies indicated that large positive/negative values concentrated along the coastal strip,the shores of lake Victoria as well as central Tanzania during El-niño/La-nina events respectively especially during the season of September-November. It was also observed that northern Uganda and southern Tanzania experienced wet/dry anomalies during La-nina/El-niño events. The phase relationship in these regions change signs during the short rainfall (September-November).

Results from spectral analysis indicated that the 2.2-2.8 and 3.0-3.7 years spectral peaks were dominant during all the seasons and in all climatological regions. The first peak is associated with quasi-biennial oscillation while the latter is associated with El-niño and southern oscillation (ENSO). The 4.9-6.0 peak which is associated with ENSO was also observed in the rainfall as well as SST seasonal time series. The 10-12.5 years peak which many authors have associated with solar cycles was also noted in the regions of lake victoria basin as well as regions of high terrain.

Principal component analysis highlighted the influence of meso-scale circulations attributed to local factors. Furthermore, the spatial patterns of the significant loadings also highlighted the migratory nature of seasonal rainfall following the movement of ITCZ. The number of significant modes and variances accounted for by the SST modes varied significantly from season to season. Although several methods were used to extract significant modes, five and four modes were extracted from annual series and seasonal time series respectively by all the methods except the Kaiser criteria. The spatial patterns of rotated principal components were used to delineate East Africa into 37 homogeneous

The quality control test indicated no heterogeneity in most of the rainfall time series. The few rainfall time series which were heterogeneous were randomly distributed in the region. No significant trends could also be detected at most of the locations. The spatial patterns of the seasonal rainfall anomalies indicated that large positive/negative values concentrated along the coastal strip,the shores of lake Victoria as well as central Tanzania during El-niño/La-nina events respectively especially during the season of September-November. It was also observed that northern Uganda and southern Tanzania experienced wet/dry anomalies during La-nina/El-niño events. The phase relationship in these regions change signs during the short rainfall (September-November).

Results from spectral analysis indicated that the 2.2-2.8 and 3.0-3.7 years spectral peaks were dominant during all the seasons and in all climatological regions. The first peak is associated with quasi-biennial oscillation while the latter is associated with El-niño and southern oscillation (ENSO). The 4.9-6.0 peak which is associated with ENSO was also observed in the rainfall as well as SST seasonal time series. The 10-12.5 years peak which many authors have associated with solar cycles was also noted in the regions of lake victoria basin as well as regions of high terrain.

Principal component analysis highlighted the influence of meso-scale circulations attributed to local factors. Furthermore, the spatial patterns of the significant loadings also highlighted the migratory nature of seasonal rainfall following the movement of ITCZ. The number of significant modes and variances accounted for by the SST modes varied significantly from season to season. Although several methods were used to extract significant modes, five and four modes were extracted from annual series and seasonal time series respectively by all the methods except the Kaiser criteria. The spatial patterns of rotated principal components were used to delineate East Africa into 37 homogeneous

regions which were used in the analysis of the sub-regional characteristics.

Results also indicated significant correlations between seasonal rainfall and several SST modes. The correlation was observed between Equatorial Atlantic ocean SSTs and seasonal rainfall for several locations of East Africa during both long and short rainfall seasons. Correlation was also noted between northern Indian ocean SSTs and seasonal rainfall over several regions. Southeastern Atlantic and southwestern Indian oceans SSTs were negatively correlated with seasonal rainfall over most regions although the extreme southeastern Atlantic ocean SSTs were positively correlated with seasonal rainfall over some locations. Northeastern Atlantic ocean SSTs were negatively correlated with seasonal rainfall over some regions. Western and central equatorial Pacific ocean SSTs were negatively/positively correlated with seasonal rainfall over some of the regions during long rainfall season including the June-August season/ correlated with short rainfall season rainfall including December to February rainfall season respectively. The persistence of the SSTs was evident at 3 months time lead and this was used as the basis for the step-wise regression models.

The results also indicated positive correlations between seasonal rainfall and the temperatures at 200 Hpa during the season of September-November. The regions of strong meso-scale circulations (lake Victoria, coastal strip and regions of high terrain) showed strong positive correlations between temperatures at 200 Hpa and seasonal rainfall. This seemed to be a manifestation of the interactions between the meso-scale and the synoptic scale circulations.

Correlation analysis also indicated that surface temperatures of the coastal/ island stations ,Lamu & Mombasa/ Aldabra & Seychelles respectively, could be used as proxies of some of the SST anomalies.

Results from regression analysis indicated that the SST fluctuations explained maximum rainfall variances of 56.1%, 48.1%, 71.6% and 58.7% during the seasons of December-February, March-May, June- August, and September-November respectively. It was noted that SST variability indicated low predictive potential for the long rainfall season (March-May) was very low. High predictive potential for most of the locations was noted during the short rainfall season (September-November). Predictive potential for some specific regions which receive rainfall during the seasons of June-August and December-February was also good. On the other hand it was observed that when the dominant rotated principal component from each of the sub-regions was considered, time coefficients of the SST modes explained a maximum of 32.8%, 34.7%, 31.1% and 34.0% variance of the rainfall during December-February, June-August, March-May and September to November respectively. Time coefficients of SST modes and seasonal rainfall also highlighted the correlation between seasonal rainfall and SSTs over the Atlantic, Indian, western and central Pacific oceans. The second to fourth rotated ocean components explained most of the seasonal rainfall variance in comparison to the first ocean components during the long rainfall season. However, during the short rainfall season, the first and fourth ocean modes explained most of the seasonal rainfall variance.

Test of skill for the developed models showed that the season of September-November had a higher predictive potential at most of the climatological regions during the persistence of El-niño or La-nina events. The season of March-May showed poor prediction potential for most of the locations. The season of December-February showed good predictive potential in southern Tanzania while the season of June-August showed a good predictive potential in Northern including Eastern Uganda as well as the coastal strip. However, it was observed in this study that the skills of the models were relatively low for the prediction of extremely

high and low rainfall values.

In general,the results from this study indicated that SST modes could be used to give useful seasonal rainfall forecast at a time lead of 3 months. Such a prediction is vital in minimizing the severe negative socio-economic impacts arising from seasonal rainfall variations. The predictions developed in the study will go along way in improving the skill of seasonal rainfall forecast which is a vital component of early warning in the region of East Africa. Results from the study will also enhance sustainable use of rain dependant resources as well as planning agricultural activities and food security.

4.1 RECOMMENDATIONS

In order to improve on the regression models which have been built during this study, the following recommendations are deemed necessary.

(i) For operational purposes, the regression models derived from PCA time coefficients are some times difficult to apply. Simple predictors should be searched.

(ii) No good predictor was found for the March-May season which is the major rainfall season for East Africa. Diagnosis analysis of various rain generating processes must continue to be carried out and new predictors searched from the other general circulation systems.

(iii) Seasonal (3 months) time leads forecast were used in this study. SST information one month proceeding the rainfall season could give better prediction signals. The potential use of monthly SST time lead should also be investigated.

(iv) Most of the models used have assumed that the predictors and predictands were independent. Many optimal combination models are now available which could be tried in the future studies.

ACKNOWLEDGEMENT.

Glory be to God the Almighty for granting me wisdom and good health in order to accomplish this study. My deep appreciation and thanks go to my supervisor, Professor L.A. Ogallo who gave me his valuable time out of his busy schedule. He patiently but steadily gave me the opportunity to expose my ignorance after which he gave timely corrections. He also read all my manuscripts and instilled a sense of excellency in my character. I extend a word of thanks to my second supervisor, DR. M.S.Rao who helped me to focus on the subject matter through regular discussions. Although she could not stay with me up to the end of my thesis work, Dr. E.K.Anyamba was of great help to me in reading the manuscripts in the early stages of the thesis work.

My special thanks go to Dr. Ininda who was a P.HD. student whom I found very resourceful and inspiring. He contributed immensely towards the success of this study by providing the SST global data besides regular stimulating discussions that I had with him. His P.HD. results helped me to interpret the results of this study and to have confidence in the contributions of this study towards medium and long range forecasting. Iam also grateful to my fellow M.SC. students messrs Ochieng,Owili and King'uyu for their solidarity.

I am grateful to Uganda, Kenya, and Tanzania Meteorological services who provided raw rainfall data. Special thanks go to the Kenya Meteorological Department for providing the computer power and several other facilities which were laid at my disposal. I am indeed grateful to the members of the computer room especially messrs Ambenje, Njogu and Owuor who assisted with computer programming during the data analysis.In the same vein a word of thanks goes to the staff of Meteorological department of the University of Nairobi for their

support and encouragement. Iam grateful to the department for providing computer facilities for the word processing. The author is also grateful to messrs Nyakundi and Okumu for drafting the diagrams.Iam also grateful to the staff of Uganda Meteorological Department who stimulated my research zeal through discussions.

A word of thanks goes to the Government of Uganda through WMO for providing the initial scholarship and extending if for six months. A word of gratitude also goes to the top policy makers in the government of Uganda for stimulating my zeal in research after showing concern in medium and long range seasonal weather forecasting for socio-economic planning and national food security.

Lastly but not least, Iam very grateful to my beloved wife Monica who supported me by diligently handling family resources besides looking after our ageing parents and our daughters: Faith, Grace, Hope, Patience, Kukundakwe, Hannah and Joy. I am indeed indebted to the daughters for bearing with my absence and for concentrating on their studies without my guidance. The total support rendered by the family members enabled me to dedicate my time on the academic life.

REFERENCES

Agwata, J.F.M. 1992:The response of lake Victoria levels to regional and global climate changes. Master of Philosophy Thesis. Moi University .

Anderson,R.L., 1942: Distribution of the serial correlation coefficients. Annal.Math.Stat.,13 1-13.

Anderson,O.D.,1976: Moving Average Process. Statist. 25 283-297.

Anderson,O.D.,1977a,:A Box-Jenkins Analysis of the colured Fox Data from Nain.Ibid..26,51-75.

Anderson,O.D.,1977b: The interpretation of Box-Jenkins time series models.Ibid..26 127-145.

Anderson,O.D. 1977c: Time series and forecasting.Another look at the Box-Jenkins Approach. Ibid..26 285-303.

Anyamba, E. K. 1983: On the monthly mean, low-level tropospheric circulation and anomalous circulation during the 1961/62 flood in East Africa. M.sc. Thesis. Department of Meteorology University of Nairobi.

Anyamba, E.K.and P.M.R.Kiangi,1985: Mean motion fields in East Africa at the level of the EALL Jet core.Arch. Met.Geoph.Biocl., sev.B. 36, 29-41.

Anyamba,E.K. 1990: A diagnostic study of low frequency oscillations in Tropical outgoing longwave radiation. PHD Thesis University of California Davis.

Anyamba,E.K. 1993:Some properties of a 20-30 Day oscillation in Tropical convection. Journal of African Met.Soc.Vol.1.No.1.1-19.

Asnani,G.C. Matari and Ngeno,1980: Monsoon of East Africa. Asnani G .C. 1992.Tropical Meteorology Vol.2 pp 377-389.

Asnani,G.C.and J.H.Kinuthia,1979:Diurnal variation of Precipitation in East Africa.

Research Report NO.8/79.Kenya Meteorol.Dept.Nairobi pp 58.

Atwoki,K.1975: A factor analysis approach for the deliniation of the rainfall regions of Uganda. E.Afri.Geogr.Rev.,13,9-36.

Bärring,L. 1987: Spatial patterns of daily rainfall in Central Kenya: Application of principal component analysis, common factor analysis and spatial correlation. Jou.climatal. 7, 267-289.

Bärring,L.1988: Regionalisation of daily rainfall in Kenya by means of common factor analysis.Jou.Climatol.,8,371-389.

Bates,J.M. AND C.W.J. Granger,1969: The Combination Forecasts.Op.Res.Quart.,20,451-469.

Barbara,G.M.,1976:Medium term fluctuations of rainfall in Southern England. Quart.J.R.Met.Soc.,102,627-638.

Basalirwa, C.P.K. 1991: Rain gauge Network Design for Uganda. PHD Thesis. University of Nairobi.

Basalirwa,C.P.K.,L.J.Ogallo & F.M. Mutua.1993: The design of a Regional Minimum Rain gauge Network. Water Resource Department . Vol.9 NO.4. 1993.

Berlage,H.P., 1966:The southern oscillation and World weather. Medidl.Verhandel,88,Kon.ned.Meteor. Insti. pp 152

Box,G.E.P. and G.M.Jenkins,1967:Some recent advances in forecasting and control. J.Roy.Statist. Soc.,C16,91-109.

Box,G.E.P. and G.M.Jenkins,1976:Time series Analysis Forecasting and Control.(Revised ed.of 1970 Pub.).Holden-Day,575pp.

Bottomley,M.,C.K.Folland,J.Hsiung,R.E.Newell and D.E. Parker, 1990: Global ocean surface temperature.Atlas (GOSTA). A joint project of the Meteorological office and

department of Earth, Atmosphere and Planetary science, Massachusetts Institute of Technology, MIT Press, Camride,MA.

Brown, R.G., 1959: Statistical Forecasting for inventory control. McGrow Hill Book Co.

Brown,R.G. 1962: Smoothing,Forecasting and Prediction of discrete Time series. Prentice-Hill ICN., Englewood Cliffs.

Burg,J.P., 1972: The relationship between maximum entropy and maximum likelihood spectra. Geophy. 37. 375-376

Cadet, L.D.,1984: The Southern Oscillation over the Indian ocean Journal of Climatology,Vol.5,189-218 (1985).

Cadet,D.L.1985:The southern Oscillation over the Indian ocean. Journal of Clim..5. 189-212.

Castell,R.B. 1966:The Scree test for the number of Factors. Multivar. Behav.Res.. 1. 245-276.

Child,D. 1970: Factor analysis. Billing & sons LTD. Guildford and London.

Cooley,J.W.,P.A.W. Lewis, P.D. Welch, 1967: Historical notes on the Fast Fourier Transform. IEEE. 79-84.

Cornell, J.A. 1990:Experiments with mixtures, designs, models and the Analysis of Data. Second edition John Wiley and Sons Inc. pp 232-239.

Craddock,J.M.,1965:A Meteorological application of Principal Component Analysis. Staist..15.143-156.

Craddock,J.M.,C.R.Flood, 1969: Eigenvectors for forecasting the 500 mb geopotential surface over the Northern Hemisphere. Quart. J.R. Met.Soc.,95. 576-593.

Craddock,J.M.,S Flintoff, 1970: Eigenvector representation of Northern Hemispheric fields. Ibid..96. 124-129.

Davies,T.D.,C.E.Vincent and A.K.C. Beresford, 1985: July-August rainfall in West-Central Kenya. Jou.Climat.5 pp 17-33.

Deshpande,D.V. 1967:Sunspot cycle and regional rainfall.Weather.23. pp 78-79.

Farmer, G.,1987:Seasonal Forecasting of Kenya Coastal short rains, Jou. of Climatology.vol.8.489-497 (1988).

Farmer, G. 1988: Seasonal forecasting of the Kenya Coast short rains 1901-84. Journal of Climat.8, 489-497.

Findlater, J.1977: A numerical Index to monitor the Afro-Asian Monsoon during the Northern Summer hemisphere, Meteorological Magazine 106, 1977.

Fisher, R.A.: 1990 Statistical Methods,experimental Design and scientific Inferences . Oxford University Press pp 189-206.

Fleming,D.,1970: Notes on an easterly disturbance affecting East Africa 5-7 September 1969. EAMD.Techn.Memo.No.13

Folland, C.K. and A. Dickinson ,1988: Prospects for Long range Forecasting for the United Kingdom. Long Range Forecasting and Climate Research Memorandum No.21

Folland, C.,J. Owen, M.N. Ward & A. Colman,1989: Prediction of seasonal Rainfall in Sahel Region using Empirical and dynamical methods.Jou.of Clim..vol.10..21-56 (1991).

Funk,J.P. and G.J. Garnham, 1962: Australian ozone observations and suggested 24 month cycle.Tellus.14.378-382

Gichuya,S.N., 1970: Easterly disturbances in the Southeast monsoon. Proc.Symp.on Trop.Met. Honolul,Hawai.

Griffith, J.F.,1972: Climatology of Africa. World Survey of Climatology.Vol.10.

Hasternrath,S., A.Nicklis, L.Greischar,1993: Atmospheric-Hydrospheric Mechanisms of

Climate Anomalies in West Equatorial Indian ocean. Jou.Geop. Res.vol.98 No.c11 pp 20.219-20.235.

Holton,J.R.,R.S.Lindzen, 1972: An updated theory of the quasi-biennial oscillation of the tropical stratosphere. J.Atmos.Scie..29,1076-1080.

Ininda, J.M. 1987:Spatial and Temporal Characteristics of Drought in Eastern and Southern Africa. M.sc.Thesis University of Nairobi.

Ininda,J.M.,1995: Numerical simulation of the influence of the sea surface temperature anomalies on the East African seasonal rainfall. P.HD. Thesis University of Nairobi.

Johnson, D.H. and H.T. Mörth 1960: Forecasting Research in East Africa.:Bargman D.J.(ed):Tropical Meteorology in Africa.Minitalp Foundation, Nairobi PP 56-137.

Jenkins,M.G., D.G. Watts 1968: Spectral Analysis and it's applications. Holden-Day, California USA.

Johnson D.H. 1962: Rain in East Africa. Ouart.J. Roy. Meteorol. Soc.88 pp 1-19.

Kaiser,H.F., 1959:The varimax creterion for anlytic rotation in Factor analysis. Educ.Pschol Meas.. 19,413-420.

Keshvmurty,R.N.,1982:Response of the atmosphere to sea surface temperature anomalies over the equatorial Pacific and teleconnection of the Southern Oscillation J.Atmos.Sci.,39,1249-1259.

Kiangi,P.M.R., M.M. Kavishe, P.K.Patnaik, 1981: Some aspects of the mean Tropospheric motion fields in East Afica During the Long Rainfall season. Kenya J. Sci. and Techn. Ser.A2,91-103.

Klein,W.H., 1982:Statistical Weather forecasting on diffence time scales. Bull.Amer.Soc..62.No.2.170-176.

Krishnamurti,T.N., 1971: Tropical east-west circulation during the Northern

Summer.J.Atmos.Sci.28, 1343-1347.

Krishnamurti,T.N.,1979: Compendium of Meteorology.Tropical Meteorology.WMO NO. 364.PP 428.

Lamb,H.H. 1966: Climate in the 60's:changes in the World's wind circulation reflected in the prevailing temperature, rainfall patterns and the level of African lakes. The Geographical Journal. 132, 183-212.

Lau,K.M.,P.H.Chau, 1986: Aspects of the 40-50 Day oscillation during the northern Summer as inferred from outgoing Long wave radiation. Mon.Wea.Rev.,114,135-1367.

Lawrence,E.N. 1971:Recent weather extremes and sunspot cycles. Weather,26, pp 129-131.

Lumb,F.E. 1970: Topographic influence on thunderstorm activity near lake Victoria. Weather,25 pp 404-410.

Madden,R.A.,P.R. Julian,1971:Detection of a 40-50 day oscillation in the zonal wind in the Tropical Pacific. J.Atmos. Sci.,28,702-708.

Mertz, G.J. and L.A. Mysak,1983: Evidence of 40-60 Day oscillation over west Indian ocean 1976 & 1979. American Meteorological Society,1984

Minja,W.E.S. 1984: A comparative Investigation of Weather Anomalies Over Africa During the 1972 Drought and 1977-1978 wet period. M.SC. Thesis University of Nairobi.

Murakami,T.,T.Nakasawa, J.H.He,1984: On the 40-50 day during the 1979 Northern hemisphere Summer part 2: heat and moisture budget. J.Meteor.Soc, Japan,62 469-484.

Mukabana, J.R. 1992:Numerical simulation of the influence of the large scale monsoon flow on diurnal weather patterns over Kenya. P.HD.Thesis University of Nairobi.

Mukherjee,B.K.,Indira,R.S.Reddy, Ramana Murty, 1985 : Quassi-biennial oscillation in the

stratospheric zonal wind and Indian Summer monsoon. Mon.Wea.Rev.,113,1421-1424.

Newbold,P. and C.W.J. Granger, 1974: Experience with Forecasting Univariate time series and combination of Forecasts J.R.Statist.Soc.A137,131-165.

Nie,N.H.,Bent,D.H. & Hull,C.H. 1970: Statistical Package for Social Science (SPSS), compiled by Glasgow University (UK. McGraw-Hill). Rodda J.C.(1969),Hydrological Network Design. Reports on WMO/IHD Projects. Report NO.12,57pp.

Njau,L.N.,1982: Tropical wave disturbance in EastAfrica. M.SC. Thesis University of Nairobi.

North,G.R.,T.L.Bell and R.E. Cahalan, 1982: Sampling error in the estimation of empirical orthogonal fluctuations. Mon.Wea.Rev.,110,699-706.

Nyenzi,B.S.& S.E Nicholson,1990: Temporal and spatial variability of SSTs in the Tropical Atlantic and Indian oceans. Archiv. Met. Geophys. Biok. Ser. A,138-146.

Nyenzi,B.S. 1993: AN Analysis of the Inter annual variability of Rainfall over East Africa. Journal of African Met.SOc.,Vol.1.No.1,57-79.

Ogallo, L.J,1978 : Rainfall variability in Africa. Mont. Wea. Rev. Vol. 107 No.9 Sept. 1979.

Ogallo, L.J.,1980: Trend of rainfall in East Africa, Kenya Journal of Science and Technology (A) 1981 2:82-90.

Ogallo, L.J.,1979: Rainfall variability in Africa.Reprint from Mont. Wea. Rev. Vol. 107, No.9. Sept. 1979 American Meteorological Society

Ogallo, L.J.,1980: Using Time Series Analysis to Examine the Trends,Cyclical, Seasonal and random fluctuations over East Africa.P.HD. Thesis University of Nairobi.

Ogallo, L.J.,1981: The Nature of Homogeneity in Rainfall Records over East Africa. Res.

Rep. No.4/81 October 1981

Ogallo, L.J.,1983: Temporal fluctuations of seasonal Rainfall patterns in East Africa, Mausam (1984),35,2, pp 175-180

Ogallo, L.J.& W.A.Chilamba,1984 : The Characteristics of Wet spells In Tanzania,E. Afr. Agric. For J. (1982) 47(4) pp 87-95.

Ogallo, L.J., 1986: Stochastic Modelling of Regional annual Rainfall Anomalies in East Africa, Jou. of Applied Statistics,Vol.13 No.1, 1986.

Ogallo, L.J., 1987: Relationship Between Seasonal Rainfall in East Africa and Southern Oscillation, Jour.of Clima.Vol.7.1-13 (1987)

Ogallo, L. J.,1988: Long Range Forecasting. Proc. workshop on Num.Wea. Pred.Over E., Cent.and South. Afr. -Nairobi 1-12 August 1988.

Ogallo, L.J.,J.E. Janowiak and M.S. Halpert,1989: Teleconnections Between seasonal Rainfall over E. Afr. and Global SSTA. Jou.of the Met. Soc.of Japan vol.66 No.6 pp 807-821.

Ogallo, L.J. ,1989: The Temporal and Spatial Patterns of The East African seasonal Rainfall Derived from Principal Component Analysis.Jour.of Clima.Vol.9,145-167 (1989).

Ogallo,L.J., R.E. Okooola and D.W.Wanjohi 1993: Characteristics of Quasi-biennial oscillation over Kenya and their predictability potential for the seasonal rainfall. Mausam (1994),45,1,57-62.

Okeyo, A.E. ,1987: Towards The Development Of a Forecasting Numerical Model For Kenya. P.HD. Thesis University of Nairobi.

Okoola,R.E., 1989: Westward moving disturbances in the South west Indian ocean. Meteorol. Atmos.Phy.41,35-44.

Palmer.T.N.,1988: Medium and extended range predictability and stability of PNA mode.

Quart.J.R.Met.Soc.,112,639-660.

Parker,D.E.R. Greenslade and R.A. Colman,1988: Prediction of sub-Saharan seasonal rainfall. Conference on the variability of atmosphere and ocean on time scale of month to several years.8-12Sept., 1988, London.

Plumb,R.A.,1984: The quasi-biennial oscillation in the Dynamics of the middle Atmosphere edited by J.R. Holton and T.Matsuno Terra Scientic publishing Company..

Rao, C.R. 1965:Linear statistical Inference and it's applications. Second edition.John Wiley & sons. 273-279.

Rasmusson,E.M.,P.A. Akrhin,W.Y. Chen, J.B.Jalickee, 1981: Biennial varaitions in surface temperetures over the United States as revealed by singular decomposition Mon.Wea.Rev.,109.181-192.

Rasmusson,E.M.,T.H. Carpenter ,1982: Variations in Tropical sea surface temperature and surface wind fields associated with southern oscillation/EL-NIño. Mon.Wea.Rev. 110,35-384.

Rasmusson,E.M.,1984: EL-NIño:The ocean/atmosphere connection. Oceanus,27.5-12.

Rodhe, H. and H. Virji, 1976: Identification of existence of trends in the rainfall records and periodicities over East Africa. Month. Wea. Rev. Vol. 104, PP 307-315.

Ropelewski, C.F. and M.S. Halpert, 1987: Global and Regional Scale precipitation patterns associated with El-Niño/Southern Oscillation. Mon..Wea.Rev..115.1606-1626.

Rowell, D.P.,J.M. Ininda,M.N.Ward ,1994: The impact of Global sea-surface temperature patterns on seasonal rainfall in East Africa. Proc.Int. Conf. on monsoon variability and prediction.Trieste.Italy. 9-13 May 1994.

Semazzi, F.M.,1978: Numerical Experiments on the Dynamic-Orographyic Influence in the Tropics. M.SC. Thesis University of Nairobi.

Semazzi, F.H.M., Neng-Huei lin, Beverly Burns and Jae-Kyung Schemm,1992: A Diagnostic Study of Teleconnections Between the Continental rainfall of Africa and Global Sea-Surface Temperature Anomalies. In print Jou.of Climate Semazzi, F.H.M.,H.M. Bervely Burns & Neng-Huei Lin & Jae-Kyung,1992 : A GCM Investigation of the Teleconnections Between the Continental Climate of Africa and Global Sea-Surface Temperature and prediction Temperature Anomalies. In print J.of Climate

Semazzi, F.H.M.,Neng-Huei Lin and Filippo Giorgi,1992: A CCM1-MM4 Nested Model Study of the influence of temperature Anomalies on the Sahelian Climate. In print Jou.of Climate.

Thaphiyal,V., 1982: Stochastic dynamic model for long range prediction on monsoon rainfall in Peninsular India.Mansam.33,339-404.

Thompson, B.W. 1966: The mean annual rainfall of Mount Kenya.Weather 21 pp 48-49

Tomsett, J.E. 1969: Average Monthly and annual rainfall maps of East Africa. Tech.Memo NO.14. Kenya Meteorol.Dept. Nairobi pp 20.

Trewartha,G.T. 1961: The Earth's problem Climate,Univ. of Wisconsin press,Madison pp 334.

Tyson, P.D. 1993: Modelling Climatic Change in Southern Africa. Reprint from the South African Jou. of Science,86, 1990, pp 318-330.

Tyson, P.D. 1993: Recent Developments in the Modelling of the future Climate of South Africa. Reprint from the Sou.Afr.Jou.of Sc.,89,in press.

Willet,H.C. 1965: Solar-Climatic relationship in the light of standardized data. Jou.Atmos. Sci..22,120-136.

Ward, M.N. and C.K. Folland,1989:Prediction of seasonal rainfall in the north Nordeste of

Brazil using eigenvectors of sea surface temperatures. Inter.Jou.of Clima., vol.11,711-743 (1991).

Weickmann.K.M.,G.R.Lussky,J.E.Kutzhach, 1985: Intraseasonal (30-60 day) fluctuations of outgoing Long wave radiation and 250 mb stream function during northern Winter.Mon.Wea.Rev.,113,941-961.

World Meteorological Organisation,1966:Climate Change. Technical Note No.79. WMO NO.195 TP100.

World Meteorological Organisation,1986: Guidelines on the Quality Control of Surface Climatological Data, WCP-85.WMO/TD NO.111.PP 56.

Yasunari,T., 1980:A quasi-stationary appearance of 30-40 Day period in cloudiness fluctuations during the Summer monsoon over India. J.Meteorol.Soc.,Japan,58,225-229.

Yevjevich,V. 1972: Probability Statistics in Hydrology (Fort Collins,CO,Water Resources Publication),302 pp.